https://doi.org/10.25923/44n2-7964

NOAA Technical Memorandum NMFS

JULY 2021

DISTRIBUTION PATTERNS OF FISH AND INVERTEBRATES FROM SUMMER SALMON SURVEYS IN THE CENTRAL CALIFORNIA CURRENT SYSTEM 2010–2015

Jeffrey Harding[1], Edward Dick[1], Nathan Mantua[1],
Brian Wells[1], Arnold Ammann[1], and Sean Hayes[2]

[1] NOAA Southwest Fisheries Science Center
Fisheries Ecology Division
110 McAllister Way, Santa Cruz, CA 95060

[2] NOAA Northeast Fisheries Science Center
Protected Species Branch
166 Water Street, Woods Hole, MA 02543

NOAA-TM-NMFS-SWFSC-645

U.S. DEPARTMENT OF COMMERCE
National Oceanic and Atmospheric Administration
National Marine Fisheries Service
Southwest Fisheries Science Center

About the NOAA Technical Memorandum series

The National Oceanic and Atmospheric Administration (NOAA), organized in 1970, has evolved into an agency which establishes national policies and manages and conserves our oceanic, coastal, and atmospheric resources. An organizational element within NOAA, the Office of Fisheries is responsible for fisheries policy and the direction of the National Marine Fisheries Service (NMFS).

In addition to its formal publications, the NMFS uses the NOAA Technical Memorandum series to issue informal scientific and technical publications when complete formal review and editorial processing are not appropriate or feasible. Documents within this series, however, reflect sound professional work and may be referenced in the formal scientific and technical literature.

SWFSC Technical Memorandums are available online at the following websites:

SWFSC: https://swfsc-publications.fisheries.noaa.gov/

NOAA Repository: https://repository.library.noaa.gov/

Accessibility information

NOAA Fisheries Southwest Fisheries Science Center (SWFSC) is committed to making our publications and supporting electronic documents accessible to individuals of all abilities. The complexity of some of SWFSC's publications, information, data, and products may make access difficult for some. If you encounter material in this document that you cannot access or use, please contact us so that we may assist you.
Phone: 858-546-7000

Recommended citation

Harding, Jeffrey, Edward Dick, Nathan Mantua, Brian Wells, Arnold Ammann, and Sean Hayes. 2021. Distribution patterns of fish and invertebrates from summer salmon surveys in the central California Current System 2010–2015. U.S. Department of Commerce, NOAA Technical Memorandum NMFS-SWFSC-645.
https://doi.org/10.25923/44n2-7964

DISTRIBUTION PATTERNS OF FISH AND INVERTEBRATES FROM SUMMER SALMON SURVEYS IN THE CENTRAL CALIFORNIA CURRENT SYSTEM 2010–15

Jeffrey Harding[1], Edward Dick[1], Nathan Mantua[1], Brian Wells[1],
Arnold Ammann[1], and Sean Hayes[2]

[1]Fisheries Ecology Division, Southwest Fisheries Science Center, National Marine Fisheries Service, 110 McAllister Way, Santa Cruz, CA 95060

[2]Protected Species Branch, Northeast Fisheries Science Center, National Marine Fisheries Service, 166 Water Street, Woods Hole, MA 02543

ABSTRACT

We describe spatial and temporal patterns of abundance among salmonids and other fish and invertebrate species co-occurring in coastal (~30m depth to shelf break) surface waters in the central California Current System (CCS) during six summer surveys 2010–15. We caught a total of 63 fish and 18 invertebrate species during 366 surface trawls at predetermined stations. Chinook salmon (*Oncorhynchus tshawytscha)*, coho salmon (*O. kisutch*), and steelhead (*O. mykiss*) were present in all surveys but varied in abundance spatially. Salmon catch was consistently high between the Klamath River and Cape Mendocino for all three species, and low or nonexistent in southern Oregon and south of Mendocino, except for juvenile Chinook which remained abundant on southern lines including those within the Gulf of the Farallones (GF) where migrating California Central Valley juveniles enter the sea. Epipelagic nekton community structure varied with latitude and was most distinct in the GF, where trawl catch on four southern lines formed a coherent group with similar average communities in nMDS plots. Principal coordinates analysis supported this interpretation of a measurably different GF biota with a higher abundance of characteristic fish and invertebrate species associated with warmer, saltier GF summer water. Community structure also differed significantly among years but no single year in the 6-year time series stood out as exceptional, even during the unusual 2014–15 marine heat wave. Ordination and cluster analysis showed a gradual progressive shift in catch composition over time, with significant effects of both year and shelf position on community structure. Shelf position affected species richness and abundance, but not evenness and diversity. Using a matrix-matching model, variation in full community structure was best described by a subset of local spatial and environmental variables that included bottom depth, water transmissivity, and water temperature. Using a negative binomial regression model, variation in juvenile Chinook salmon abundance was best described by bottom depth, transmissivity, and latitude. This survey provides useful data for exploring fisheries ecosystem structure in a hydrographically complex but less often studied region in the core of the CCS.

INTRODUCTION

The Fisheries Ecology Division of NOAA's Southwest Fisheries Science Center conducted its first juvenile salmon ocean survey in 1995 off central California. The initial goals of the study were limited to obtaining samples of sub-yearling California Central Valley (CCV) fall-run Chinook salmon (*Oncorhynchus tshawytscha*) from the San Francisco estuary and nearby coastal ocean in order to compare estuarine and ocean diet, growth, and physiological ecology (MacFarlane and Norton 2002). The survey was repeated annually until 2007, with one missing year (2006).

The primary objective of the study at that time was to measure the physiological condition of first-year ocean salmon relative to local (e.g. temperature, salinity, chlorophyll, upwelling) and larger scale (e.g. El Niño / La Niña, Pacific Decadal Oscillation) variation in ocean conditions. Fish lipids were extracted and used to predict energy reserves and growth capacity during early ocean residence near the point of ocean entry at the Golden Gate in May and June, and compared to samples taken from older juveniles in summer and fall after a period of growth at sea (MacFarlane et al. 2005, MacFarlane 2010). The survey operated mostly within the Gulf of the Farallones (GF) over the continental shelf, in a radius of about 65 km from the Golden Gate. A secondary objective of the survey was to record and describe the assemblage of pelagic nekton co-occurring with juvenile salmon. Consistent record-keeping of trawl bycatch at the species level started around 2000 for fin fishes, and around 2004 for invertebrates. Regional, seasonal, and annual patterns of community structure for fishes taken by trawl from 2000–05 in the Gulf of the Farallones and adjacent waters are described in Harding et al. 2011.

Beginning in 2010 we expanded the scope and range of our existing program through partnership with NOAA's Northwest Fisheries Science Center to develop a unified annual coast-wide (northern Washington to central California) summer survey of salmon and their ocean habitat. NOAA and Oregon State University initially partnered to study juvenile salmon off the coast of Oregon and Washington in the late 1970's and over the next two decades expanded their objectives to include assessing the effects of ecological interactions and oceanography on juvenile salmon growth and survival at sea (Pearcy and McKinnell 2007). Beginning in 1998, the Bonneville Power Administration funded NOAA and other agencies through the Ocean Survival of Juvenile Salmonids Study to address concerns about the status of threatened and endangered Columbia River stocks. Their primary mandate was "to determine the physical, biological and ecological mechanisms that control survival of salmon during their early marine life". The NWFSC now conducts one or two surveys annually under the name Juvenile Salmon Ocean Ecosystem Survey (JSOES) in the Columbia River plume and coastal pelagic waters off Oregon and Washington with a comprehensive approach for studying salmon and their associated nekton and ocean environment (Jacobson et al. 2012(a), Morgan et al. 2019).

In keeping with this broader approach the SWFSC salmon survey began to place more emphasis on sampling the full epipelagic coastal community. This shift was also consistent with a NOAA science objective for fisheries surveys to move in the direction of integrated ecosystem studies (Fluharty and Cyr 2001, Francis et al. 2007) and provide data relevant to ecosystem-based fishery management planning. In 2010 we increased the number of stations, extended transects beyond the shelf break, added standardized seabird counts to our daily plan, recorded continuous hydroacoustic profiles to measure the abundance of krill and other forage organisms, and extended our study further north to close the gap in sampling between the regions formerly covered by the separate Southwest and Northwest Center surveys. JSOES and SWFSC salmon surveys from 2010–15 were conducted at slightly different times of the year and usually on different ships, but with identical trawl and plankton nets.

With extended coverage the survey incorporated an ecologically important and hydrographically complex but less often studied region in the core of the California Current System (CCS) from Point Arena to Cape Blanco (39°–43°N latitude), where coastal wind forcing and seasonal upwelling are most intense and mesoscale water current instabilities are most frequent (Huyer 1983, Checkley and Barth 2009). Mean wind stress and wind-driven coastal upwelling in June and July reach their maximum values in the CCS in the vicinity of Cape Mendocino (Nelson 1977). The expanded coverage also notably included the waters off the Klamath and Rogue Rivers, home to populations of salmonids whose ecology, conservation status, and recovery have long been high priority concerns for fishery managers, especially after the widely-publicized 2002 mass mortality of adult Chinook salmon in the lower Klamath River (National Research Council 2004) and the ensuing curtailment of the commercial salmon fishery in California and Oregon in 2006 due to very low forecasted abundance (Pacific Fishery Management Council 2006).

This report summarizes a portion of the data and samples collected at sea during the annual summer salmon surveys in the north-central CCS from 2010 to 2015 by the Fisheries Ecology Division of NOAA's Southwest Fisheries Science Center. The objectives of this report are to: 1) provide a complete record of locations and types of samples collected; 2) document trawl catch and ocean conditions during each survey; 3) describe spatial and temporal patterns of abundance among salmonids and other selected species taken by trawl; 4) describe spatial and temporal patterns of abundance among the full community of pelagic nekton taken by trawl; and 5) examine the relationship between trawl catch, sample location, and a suite of water properties measured in-situ at the time of each net collection.

METHODS

Frequency and spatial plan:

Beginning in 2010 we adopted a more uniform and symmetrical sampling grid with extended latitudinal and shelf coverage spanning the coast from southern Oregon to the Gulf of the Farallones in California. A summer survey was conducted annually in June or July from 2010 to 2015, and a fall survey was conducted in 2011, 2013, and 2015 (Table 1). Only the results of the six summer surveys are reported here.

The study area for 2010–15 SWFSC salmon surveys was a strip of coastal ocean between Heceta Head, Oregon (44°00' N) and Pigeon Point, California (37°10' N), a distance of about 750 km north to south. The sampling grid consisted of 16 east-west transect lines (Fig. 1a) each spanning the continental shelf from near shore to beyond the shelf break. Transects were spaced about 50 km apart, although line spacing was not chosen to be uniform. The locations of transects were selected for proximity to coastal geographic features that could potentially influence salmon distribution (e.g. rivers) or affect coastal currents and upwelling (e.g. headlands and bays). Five fixed stations were located on each transect line. Station positions were chosen using criteria for bottom depth targets and distance from shore, or usually some compromise between these two criteria due to variation in the width and slope of the shelf. The median water depth for shelf positions 1–5 was 30, 55, 83, 122, and 370m. The shelf-break usually occurred between positions 4 and 5, or between positions 3 and 4 in a few locations with a narrow shelf or submarine canyon. The median distance from shore (due west) was 3, 7, 14, 23, and 32km for positions 1–5 respectively. The same fixed locations were used throughout the

study (Table 2), except for one line (BF) where potential interference with commercial crab-fishing gear forced us to move the location of the line several times.

On most days we were able to complete sampling at all five stations, usually starting inshore at position 1 shortly after sunrise and working shallow to deep. In 2015, unlike previous years, sampling was attempted at only the three shoreward stations (positions 1–3) on each transect line. In that year alone we tried to complete three sequential trawls at one of these three stations each day, plus a single trawl at each of the two remaining stations.

Trawling methods:

To collect salmon and associated fish and invertebrates residing in near-surface water, we used a 264 Nordic Rope Trawl (264 NRT; NET Systems, Bainbridge Island, WA) with 3m^2 foam-filled pelagic doors, each fitted with additional 200lb weight shoes. Net dimensions while fishing were approximately 22m wide x 18m high at the mouth and 200m total length with a 16mm stretched mesh knotless liner in the codend. The net was rigged with 70m bridles and fished with 140m of warp. Six large floats (Polyform, size A5) held the headrope within 0.5m of the surface continuously during tows. Footrope depth was ~16–22m (average 18m) during tows, and a few meters deeper (average 32m) during layout and haulback. Depth recorders (Reefnet Sensus Ultra dive data recorders) attached to the headrope and footrope verified deployment depths. A mechanical flowmeter (General Oceanics, Miami, FL) was towed alongside the boat for the duration of each tow to measure distance traveled through water. Sets were 30 minutes in duration, except where jellyfish were very abundant, in which case tow time was reduced according to jellyfish density. Tow speed (calculated from flowmeter distance) ranged from 3.0–3.8 knots through water (average 3.5kn), and tow distance averaged 3.2km for completed 30 minute tows. Wind and seas permitting, the tow path roughly followed the depth contour and intersected the station coordinates near the midpoint of the tow. Thus, tows usually ran parallel to shore, toward the south or southeast with the prevailing seas.

Active measures were taken to reduce the possibility of capturing marine mammals. During the approach to each station a lookout was maintained, and if any protected animal was observed within 1.0 nautical mile of the intended point of deployment, the boat moved on to a new location at least 1.0nm away. If animals were sighted after net deployment the Cruise Leader determined the best strategy to avoid potential takes. In some situations, the decision was made to immediately retrieve the net and move away from the area. At other times the tow was continued until the animal(s) were clear of the area and away from potential contact with gear during haulback, when the risk of entanglement is believed to be highest.

In addition to active avoidance, starting in fall 2011 the net was equipped with a Mammal Excluder Device (MED) to expel any large animals (e.g. mammals, sharks, turtles) that were unintentionally captured. The MED consisted of a rigid aluminum grate affixed at a 45^o angle in the intermediate section ahead of the codend. In theory, large animals are deflected by the bars of the grate and expelled from the net through a hole in the webbing, while smaller organisms pass through the grate and are retained in the codend. Initially the MED escape hole was oriented facing up, but in 2014 and 2015 we flipped the orientation to a downward-facing hole which was thought to reduce the unintended loss of target species (Wainwright et al. 2019). Finally, two acoustic pingers (Future Oceans 70 kHz Dolphin Pingers) were attached to the net. These devices emit a 145 decibel signal every 4 seconds for 300 m/s and are believed to repel dolphins and possibly other marine mammals. Video cameras mounted inside the net near the MED recorded passage of organisms through the escape opening and the grate.

We identified and counted invertebrates and non-salmonid fishes in each tow, and measured the length of 30 randomly drawn individuals of each species. Very large hauls were subsampled by volume, and total species abundance estimated from the composition of subsamples. All salmonids were identified and measured to fork length (FL). Juvenile salmon (80–250mm FL) were individually frozen for transport back to shore. Dorsal scales for ageing and growth analysis, a small piece of caudal fin tissue for genotype analysis, and in some cases blood plasma samples for IGF1 growth hormone assay were taken from each juvenile salmon before freezing. Subadult salmon (>250mm FL) were either kept or released, depending on their condition after capture and degree of recovery in aerated seawater holding tanks. A majority (>60%) of subadults resumed active swimming and were released. Scales and fin clips were also taken from subadults whenever possible.

Additional biological samples were routinely collected but those results are not presented here. They included plankton sampling with a 300µm bongo net and 200µm vertical hoop net, continuous hydroacoustic sampling using a multi-frequency echosounder (SIMRAD EK60), and daily visual counts of seabirds along measured transects (Table 1).

Water Properties:

We used a Sea-Bird SEACAT 19+ CTD (conductivity, temperature, and depth) profiler with added sensors for hydrographic sampling conducted immediately before or after trawling at each station. The CTD and carousel unit was held underwater briefly to equilibrate, then lowered at a constant rate of 30m/min to a depth of 5m above the bottom, or to a maximum depth of 200m. Water temperature and salinity measurements were also recorded throughout the survey with a Sea-Bird thermosalinometer (TSG) receiving seawater continuously from the ship's intake at 3m.

Five in-situ water properties were measured during CTD casts: water temperature (Temp), salinity (Sal), photosynthetically active radiation (PAR), transmissivity (Trans), and fluorescence. Chlorophyll-*a* concentration (Chl) was derived from fluorescence after calibration using filtered water samples collected at reference points from a subset of casts. For each of the variables, all values recorded between 3–20m of water depth were averaged for each cast, producing a single value that covered about the same range as the vertical opening of the trawl net. In addition, surface water temperature was measured at every station with a bucket and mercury thermometer (BucTemp), and surface water clarity was measured with a Secchi disk (Secchi) (Table 3).

The variables Secchi, PAR, and Chl had skewed distributions that were improved by square-root or logarithmic transformation prior to plotting and statistical testing. The remaining variables Trans, Temp, BucTemp, and Sal did not require transformation. Three variables describing the spatial location of samples were used in analysis: latitude (Lat), bottom depth (Dep), and distance from shore (Dis). Dep and Dis were log transformed to improve normality.

Trawl catch and species data:

Very small organisms that easily passed through the mesh of the NRT liner (e.g. euphausiids, ctenophores) were occasionally captured but were not included in the analyses. Other small organisms including several taxa of young-of-year (YOY) and postlarval fish (rockfish—

Scorpaenidae, flatfish—Bothidae and Pleuronectidae, and osmerids—Osmeridae) were retained often and in sufficient numbers to justify inclusion in the analysis, although their true abundance was underestimated by our equipment. Despite this, the presence and relative abundance of common postlarval and YOY fish taxa in the catch remains informative and their inclusion here is consistent with our analytical approach. A 264 NRT equipped with a fine (3mm stretched mesh) liner was successfully used to quantify invertebrates and larval fish as small as 2cm length (Phillips et al. 2009). Larval fish are common prey items for juvenile Chinook and coho salmon at sea (Brodeur and Pearcy 1990, MacFarlane and Norton 2002, Daly et al. 2009) and measures of their relative abundance are useful indicators of juvenile salmon distribution, growth and survival.

Most organisms were identified at the species level. Some taxa were more broadly classified, for example certain speciose groups such as flatfish and rockfish whose postlarval forms can be difficult to identify to species. Conversely, salmonids in this study were differentiated by species *and* size class as either "juvenile" (≤250mm FL) or "subadult" (>250mm FL) individuals. The length-frequency distribution of Chinook salmon collected in our survey from 2010–12 showed a clear break at around 250mm FL, separating fish in their first ocean year from older cohorts (Hassrick et al. 2016). Similar distinctions have been used in previous community studies to account for differences in marine habitat use and migration of juvenile versus older and larger salmon (Brodeur et al. 2005). Hereafter, the term "species" is used broadly to include these groups. We also use the term "nekton" loosely to include large medusae, heteropods, salps, and pyrosomes, all of which are members of the gelatinous zooplankton.

To account for differences in tow distance and duration, abundance was standardized to a volume of $10^6 m^3$ for all hauls. This catch per unit effort (CPUE) standard is approximately equal to a 30-minute tow at a speed of 5.6 km/h (3.0 knots), therefore CPUE is usually close to or slightly less than the actual count of organisms captured in a typical completed tow.

Abundance patterns—species level:

We examined patterns of abundance of salmonids and several other fish and invertebrate bycatch species. For Chinook salmon, coho salmon, and steelhead, we plotted CPUE or a related variable as a function of latitude, shelf position, year, and station. For other selected fish and invertebrates, we plotted CPUE by year and by station.

Juvenile Chinook salmon were the primary target of our survey and the most abundant salmonid group in the catch. For this species and age category, we modeled fish density as a function of several in-situ measurements of water properties while controlling for location (latitude and depth). Specifically, we fit counts of juvenile Chinook using a negative binomial regression model with an offset term to account for differences in tow length. Use of the offset term is equivalent to modeling fish density, and we standardized the distance units (assuming a constant net opening of 380 m^2) to estimate the number of fish per million cubic meters of water. The data were filtered to exclude observations from lines PI and PP due to anomalous catch on those two lines in a single year of very high Sacramento River discharge, under conditions thought to be unrepresentative of the survey in general.

To allow for differences in density by latitude, we defined a categorical covariate with 1-degree latitude bins ranging from 37–44° latitude. Depth was treated as a continuous covariate and log-transformed. Temperature, salinity, transmissivity, and chlorophyll (log-transformed) were also included in the set of candidate models, along with 2-way interactions. Due to correlations

between transmissivity and chlorophyll concentration in the data, we did not include both terms in a single model but evaluated them separately. We modeled interannual variability in abundance using a categorical variable for year, also considering an interaction between year and latitude treated as a random effect.

Model parameters were estimated in R (R Core Team, 2019) using the function “stan_glm.nb” from the “rstanarm” package (Goodrich et al. 2018). We selected a ‘best-fit’ model based on the leave-one-out cross-validation (LOO) criterion, implemented with the “loo_compare” function in the “loo” package (Vehtari et al. 2017). Performance of the best-fit model was evaluated using posterior predictive checks.

Abundance patterns—community level:

Beyond a species-level approach, analytical methods that utilize the full community can be advantageous because they simultaneously incorporate *everything* in the sample collectively, without arbitrary choices and omissions. In particular, multivariate ordination and related methods dampen the uncorrelated noise of individual species counts and environmental measurements, and may reveal broad, biologically important patterns generated by whole suites of species responding together (Mackas and Beaugrand 2010).

We define “community” in this report as the set of fish and invertebrate taxa sharing the upper 20m of the water column during daylight hours and caught by the rope trawl. These animals co-occur in space and time and some of them no doubt interact, although we did not define community membership by interaction or behavior but only by common presence in the defined habitat sampled by our net. We used two complimentary approaches to examine community structure. First, we measured four univariate metrics which highlight certain key properties of biotic structure, such as species richness and evenness. Second, we used multivariate ordination to visualize in two dimensions the complex multidimensional structure of biotic samples containing dozens of species. For each of these two approaches, we grouped the basic sampling units (individual trawl hauls) in specific ways—by station, transect line, shelf position, and year—to form broader aggregate samples that could then be compared to visualize and test for spatial and temporal community patterns. We looked for spatial pattern in two directions: latitude and shelf position. We looked for temporal pattern among years.

Univariate analysis:

We examined richness, abundance, evenness, and diversity. Species richness, *S*, is simply the number of species present in a sample. Abundance, *N*, is the total number of individuals present in a sample. The Shannon diversity index, *H’*, is a frequently used statistic in community studies that considers both species richness and evenness at the same time:

$$H' = -\sum_i p_i \log(p_i)$$

where p_i is the proportion of the total count arising from the *i*th species. The value of *H’* increases with both the number of species present, and the degree to which individuals are evenly distributed among those species, their equitability. A closely related statistic, Pielou’s evenness index, *J’*, more explicitly measures the equitability component of structure:

$$J' = H' / \log(S)$$

Because their values are sensitive to sample size, area, and effort, we calculated diversity measures directly from individual hauls in all cases, before any aggregation of hauls was made. Each of these four variables describes in a single number a different characteristic of the full community; together, they offer a reasonably good description of a community in simple univariate terms and provide a useful complement to the more complex multivariate picture. Biodiversity metrics have been used to describe the response of midwater forage assemblages to variable ocean conditions and ocean climate cycles in some of the same shelf waters as the present study (Santora et al. 2017).

We used linear regression to test the hypotheses that *S, N, H',* and *J'* vary with location along the coast (transect line order), and 1-way ANOVA to test for differences among shelf positions and among years. Simple normalizing transformations were used to improve the shape of the variable distributions: a square-root transformation for *S, H'* and *J'*, and a logarithmic transformation for *N*. Four empty hauls were excluded because diversity is nonexistent in this case, and 11 hauls with only one species where excluded because *J'* cannot be calculated and *H'* is meaningless. This filter resulted in 351 hauls with at least two taxa, for which all four diversity variables could be obtained.

Multivariate analysis:

The second approach—multivariate ordination and related statistical tests—required cumulating samples in several ways. Individual hauls were often low in taxonomic richness, sometimes containing only one or two species. By themselves, samples such as these contain too little information to produce meaningful ordinations or run multivariate statistical tests. For this reason, it was necessary to combine hauls into larger sample groupings before proceeding with the analyses. Because sampling effort was not equal among stations, transect lines, positions, or years, averaging the CPUE of each species (rather than pooling) was the appropriate method to cumulate hauls into larger groups that could then be plotted and compared.

For latitudinal comparisons (i.e. to examine spatial patterns among transect lines), individual hauls from each line were averaged across all six years and all five shelf positions to obtain a single aggregate biotic sample for each line. For comparison among shelf positions and among years of the survey, individual hauls were averaged by shelf position, but separately for each year. The year 2015 was excluded from some of the subsequent ordinations and tests based on this layout because shelf positions 4 and 5 were not sampled in 2015.

To visualize biotic differences among stations, hauls were averaged by station across all available years and subjected to a filter to include only those stations where trawling occurred three or more times in the six-year study period, again due to problems associated with plotting overly sparse samples. Sixty-two of the 80 stations passed this filter. This arrangement and filtering of data was also used prior to a matrix-matching procedure (BIO-ENV).

The analytical methods we used are robust to the inclusion of rare species and unaffected by zero values in the community matrix. For all multivariate procedures in this report, CPUE values were fourth-root transformed (before subsequent averaging) to reduce the disproportionately large influence of highly abundant species, and biotic similarity matrices were created with Bray-Curtis resemblance values. PRIMER analytical software (v.6.1.6, PRIMER-E Ltd, Plymouth, U.K.) with PERMANOVA+ (Anderson et al. 2008) was used for all multivariate routines.

We used non-metric multidimensional scaling (nMDS) as the primary ordination technique for visualizing community patterns. nMDS is an unconstrained nonparametric method commonly used to show relationships among samples containing numerous species. It is considered the most flexible and robust ordination technique available for visualizing complex community patterns in a small number of dimensions (Anderson et al. 2008), however because it is based on the rank order of values in the resemblance matrix rather than the similarity or distance values directly, scaling of nMDS axes is arbitrary and a true partitioning of sample variance in the final plot is not possible.

We used principal coordinates analysis (PCO) to show the relationship of selected individual variables to the community pattern. PCO is an unconstrained ordination whose primary utility relative to nMDS is that the points in a PCO plot are direct projections onto axes, so unlike nMDS the scales of PCO axes can be interpreted in the units of the resemblance measure used to create the plot, and each axis explains a true percentage of the total variation in the full multidimensional data set (Anderson et al. 2008). This feature allows the use of vectors to display simple linear relationships between individual variables measured among the samples (e.g. water properties, abundance of key species) and the ordination axes themselves.

The environmental variables measured in this study fall into two categories: those that describe the location and year of collection (spatiotemporal variables) and those that describe water properties. The former may explain some of the variability in the latter, and both types may explain variability in biotic structure, so it is of interest to examine this chain of interaction and test for relationships among sets of variables at different points along the chain. We used a distance-based linear model, DISTLM, to test for a relationship between the location and year of sample collection and a set of six water properties. We also used DISTLM to test for change in community structure with latitude. The test functions in a manner analogous to a multivariate multiple regression but allows for use of any resemblance measure for the response variables (e.g. Bray-Curtis for biotic, Euclidean distance for environmental), is largely free from assumptions about normality, and generates *p*-values by permutation.

We tested for differences in community structure among shelf positions and years using PERMANOVA, a semiparametric test for differences among categorical groups in multivariate samples. Like the other multivariate routines employed here, it operates without explicit assumptions about the distribution of the original variables (e.g. normality) and generates *p*-values by permutation. PERMANOVA calculates a pseudo-*F* statistic for each term in the model and partitions sample variance among factors and interaction terms.

Lastly, the degree of similarity between corresponding trawl and environmental samples was measured using a matrix-matching permutation test (BIO-ENV). This protocol compares biotic and abiotic samples from matching locations (62 stations in this case, using the filter described above) and finds a subset of environmental variables which maximizes the correlation to the full community pattern (Clarke and Warwick 2001). A set of nine environmental variables (three spatial and six water properties) was taken as the starting point for the test. The variable “year” was not available because samples in this arrangement were averaged by station across years.

RESULTS

Water properties:

Maps of hydrographic properties measured at trawl stations provide moving snapshots of the conditions present at the time of sampling (supplement, Fig. S1). Water temperature at the surface (BucTemp, not shown) and temperature averaged over 3–20m in the water column (Fig. S1 – CTD Temperature) showed similar patterns including a warm zone offshore to the north of Cape Blanco (43°–44°N) in about half of the years surveyed, a mostly colder central zone from Point Arena to Cape Blanco (39°–43°N), and a consistently warm to very warm zone south of Point Reyes (38°N) which was especially pronounced in 2014. Bucket temperature in 2014 was 2°C higher, on average, than any other year in the series.

Average salinity at 3–20m was lowest offshore to the north of Cape Blanco in most years, especially 2011–12, and intermediate south of Cape Blanco (Fig. S1 – CTD Salinity). The low salinity zone north of Cape Blanco likely derived from Columbia River plume water carried south by prevailing summer surface currents through a region (43°–46°N) that is largely uninterrupted by headlands and offshore-flowing jets. Salinity measurements in 2011 also revealed a plume of fresh water entering the Gulf of the Farallones from the Sacramento River, and in 2014 the coastal zone was unusually salty throughout the study area and especially in the south, where salinity exceeded 35 psu in the GF.

Transmissivity (Fig. S1 – CTD Transmissivity), Secchi depth (not shown), and chlorophyll (Fig. S1 – CTD Chlorophyll) appeared patchier and showed more local variation and more onshore/offshore structure than the corresponding temperature and salinity maps. Water clarity generally increased with increasing distance from shore. Shared local features among these variables can be identified in some years and locations (e.g. the low Trans/high Chl feature near 40°N in 2011, and a similar feature near 38°N in 2012). Concordance among turbidity variables was not always consistent, however (e.g. coast-wide Chl was lowest in 2012 and highest in 2014 and maps of Chl from these two years appear very different, whereas Trans maps from these two years do not appear very different).

Figure 2 shows pairwise relationships among hydrographic variables. There was a strong positive correlation between surface temperature (BucTemp) and mean temperature at 3–20m (Temp). Mean 3–20m salinity (Sal) was weakly correlated with BucTemp, but not significantly correlated with Temp. All pairwise correlations among the remaining variables (Trans, Secchi, PAR, and Chl) were significant, affirming that these constitute a family of related measurements describing aspects of water clarity. For example, Trans was positively correlated with Secchi and PAR, and negatively correlated with Chl.

We tested for effect of location and year on water property variation using DISTLM. This procedure measured and ranked the extent to which the four space/time variables explained the overall structure (response) of water properties over the six years. In marginal tests, each of the predictor variables taken separately was significant. By itself, year explained 24.5% of the overall variation in water properties, latitude explained 8.8%, bottom depth explained 5.3%, and distance from shore explained 2.8%. In sequential tests using a step-wise selection procedure all four variables were included in the best linear model (adjusted R^2=0.38, p=0.001, Table 4). The order of variable selection was consistent with the marginal test: year was the most important predictor of water properties, followed by latitude, bottom depth, and lastly distance from shore.

Annual differences in water structure are apparent in a scatterplot of Temp vs Sal for the six-year study period (Fig. 3). For example, 2014 was especially warm and salty, 2012 cool and fresh, 2011 fresh, and 2010, 2013, and 2015 intermediate for both variables. Temperature and salinity variation may be used to identify the origins and define the boundaries of different water masses, and may also help to identify groups of species with shared habitat affinities and provide evidence of collective transport from a common source location elsewhere (e.g. boreal and subtropical copepods off central Oregon; Peterson and Miller 1977). We plotted the scaled abundance of several common taxa onto the Temp-Sal domain (supplement, Fig. S2) to examine species distributions relative to potential habitat. Plots of this kind are useful aids to predicting conditions and locations under which species are more or less likely to co-occur and potentially interact within a larger area.

Trawl catch—overview:

We caught a total of 63 fish and 18 invertebrate species during 366 surface trawls on six summer surveys, and like most studies of this kind our catch was dominated in abundance and frequency of occurrence by only a handful of species. Scientific and common names with details of annual catch (total CPUE and frequency of occurrence, FO) are presented for 42 species and broader taxa observed on more than a single haul during the six-year period (Table 5). The most abundant organisms numerically were invertebrates: market squid (*Doryteuthis opalescens*), sea nettle jellyfish (*Chrysaora fuscescens*), and crystal jellyfish (*Aequorea* sp). The species rounding out the top-ten overall most abundant list were YOY rockfish (*Sebastes* spp.), whitebait smelt (*Allosmerus elongatus*), unidentified smelt (Osmeridae) larvae, juvenile Chinook salmon (*Oncorhynchus tshawytscha*), jacksmelt (*Atherinopsis californiensis*), Pacific butterfish (*Peprilus simillimus*), and Pacific herring (*Clupea pallasii*). Ranked by frequency of occurrence, the top-10 species were market squid, crystal jellyfish, juvenile Chinook salmon, subadult Chinook salmon, sea nettle jellyfish, moon jellyfish (*Aurelia labiata*), rockfish YOY, flatfish larvae, fried-egg jellyfish (*Phacellophora camtschatica*), and juvenile wolf-eel (*Anarrhichthys ocellatus*).

As is typical for trawl data such as these, both abundance and frequency of occurrence varied dramatically among species. For example, the most abundant species in the catch, market squid, had a six-year total CPUE of over 670,000 individuals and was present in 70% of hauls, whereas the fifth most abundant species, whitebait smelt, had a six-year total CPUE of 8754 individuals but was present in just 6.7% of hauls. One of the most ubiquitous and evenly distributed species, wolf-eel, was present 28% of the time but only 153 fish were taken in six years, most often singly. Most hauls were sparse. The majority of species were seen in fewer than 10% of hauls, and average species richness (S) was just 6.3. Richness ranged from zero (four “water hauls”) to a maximum of 17 (two hauls).

Salmonids:

Three species of Salmonidae, Chinook salmon, coho salmon (*Oncorhynchus kisutch*), and steelhead (*O. mykiss*), are common in our study area and were captured in all years of the SWFSC survey. Two other species, chum salmon *(O. keta)* and pink salmon (*O. gorbuscha*), were rarely caught (total of 16 and 6 fish, respectively). The salmonid catch in Washington and Oregon surveys was typically more diverse. In addition to Chinook, coho, and steelhead, our NWFSC colleagues regularly caught chum and sockeye salmon (*O. nerka*) (Morgan et al. 2015 Cruise Report).

The latitudinal distribution of salmonids from line 1 at Heceta Head to line 16 at Pigeon Point (Fig. 4) was not uniform. For all three species, the largest portion of the cumulative six-year CPUE was located on four adjacent transect lines north of Cape Mendocino: Klamath River (KR), Mussel Point (MP), Trinidad Head (TD), and Eel River (ER). Steelhead of all sizes and juvenile coho salmon CPUE peaked at MP, and catch of larger coho peaked on the adjacent line KR. Steelhead and coho salmon were rarely caught south of Cape Mendocino in our survey, and both species were taken primarily from stations occupying a narrower temperature and salinity range than Chinook (Fig. S2).

CPUE of subadult Chinook salmon was highest on the ER line and very low north of KR and south of Fort Ross (FR). Juvenile Chinook catch was lowest on the four northernmost lines, highest in the region between the Klamath River and Cape Mendocino, and high again in the south. Genetic stock identification of fish collected in this survey from 2010 to 2012 showed that the majority of juvenile Chinook (>90%) taken in the central region (SR to BF) were of Klamath basin origin, and southern (FR to PI) Chinook were almost entirely California Central Valley origin (Hassrick et al. 2016). Juvenile Chinook were caught on all southern lines proximate to the point of ocean entry for CCV stocks at the Golden Gate. A surprising 24.5% of the total juvenile Chinook catch was made on the two southernmost lines, Pillar Point (PP) and Pigeon Point (PI), both located south of the Golden Gate. This figure is based on three very unusual large hauls on PP and PI in 2011, of 369, 69, and 63 fish. In all other years of the study combined, only 18 juvenile Chinook were taken on these two lines, consistent with the observation that juvenile CCV Chinook migration usually follows a northern path after ocean entry (R.B. MacFarlane, personal communication).

Salmonid distribution was also not uniform across the shelf. Catch was typically highest at shallow stations located closer to shore (Fig. 5). Juvenile Chinook salmon were encountered in about half of all hauls at each of the inner three shelf positions, but encounter rate dropped to 2% at position five, furthest from shore. The distribution of larger Chinook was shifted a bit further offshore than juveniles, with encounter rates between 32–44% at positions 1–4, dropping to 12% at position five. Juvenile coho salmon were present in about 25% of hauls at positions one and two, and their presence dropped off gradually with increasing distance from shore to about 2% at position five. Larger coho were encountered further from shore than juveniles, with a peak probability of capture of about 32% at shelf position three. Steelhead of all sizes were distributed further offshore than the other two salmonid species. Juvenile steelhead capture probability was highest at position three (13%), but almost zero at positions one and five. Subadult steelhead were most likely to be caught farthest from shore at position five (20% of hauls), and least likely at position one (zero hauls).

Salmon CPUE also varied widely among years (Fig. 6), but the high variability of catch among sites within years makes it difficult to assess interannual trends. Without inferring statistical significance, CPUE of coho salmon, steelhead, and subadult Chinook was lowest in 2010. In that year, only juvenile Chinook were caught in numbers consistent with subsequent survey years. Mean annual CPUE increased across species and size categories in the 2011 survey, followed by decreasing catch of juvenile coho, juvenile steelhead, and subadult Chinook after 2011 or 2012. By 2015 CPUE of all species and sizes but juvenile Chinook had reached low levels similar to those of 2010.

In the final data set that was used to model juvenile Chinook CPUE, sampling intensity varied both spatially and temporally. The number of samples per year and latitude bin ranged from zero to 20 tows, averaging 7.3 hauls per year/latitude stratum and totaling 308 tows from 2010–

2015 (Table 6). Three year/latitude strata contained no samples, specifically between 42° and 43° N. latitude in 2013 and 2014, and between 39° and 40° in 2012.

We selected a best-fit model from a candidate set of 32 negative binomial regression models (Table 7). Pairwise differences in expected log pointwise predictive densities (ELPD) supported a model with latitude, log depth, transmissivity (all fixed effects), plus a random effect for the interaction between latitude bin and year. Although this model was the best descriptor of the mean response, several other models had similar predictive ability as indicated by a large ratio of the pairwise difference to its standard error. We consider models for which this ratio is less than 2 (last column in Table 7) as having similar support from the available data.

Given the correlation between transmissivity and chlorophyll, it is not surprising that substituting Chl for Trans in the best model produced similar results (compare rows 1 and 4 in Table 7). Depth appears to be an important predictor, as indicated by a difference of 13 in ELPD (SE = 5.6) when removed. Models that ignored latitudinal differences had poor performance overall, and the best models consistently included both fixed effects for latitude and a hierarchical structure for the interaction between latitude and year (e.g. a “random effect”).

The best-fit model predicts a sharp decline in CPUE between 50–200m depth, as well as a sharp decline north of the California-Oregon border, i.e. 42° N (Fig. 7a,b). Although the total number of samples between 42°–43° was small (15 tows across all years), only one positive tow was observed in this area during the study (Table 6). Although CPUE declined with increasing Trans (Fig. 7c), predictions from the best fit model are highly variable below roughly 65–70% Trans. This is due in part to fewer samples in the range of 50–65% Trans. Data sets generated by the best-fit model contained between 50–70% zeros, compared to 61% in the observed data set (Fig. 7d).

Non-salmonids:

As with salmon, catch of other species varied widely both among and within years (Fig. 8), with little apparent synchrony in temporal patterns of abundance among the commonly encountered species. Mean annual CPUE varied by an order of magnitude among years for some taxa (e.g. crystal jellyfish, Pacific butterfish, YOY rockfish), and several species were notable for a single year of relatively high abundance and almost complete absence from the catch at other times. These included whitebait smelt in 2010, twin-sailed salp (*Thetys vagina*)—locally known as bunny salp—in 2013, ocean sunfish (*Mola mola*) in 2014, and fried-egg jellyfish and larval northern anchovy (*Engraulis mordax*) in 2015. Northern anchovy and Pacific herring, two common schooling pelagic species known to occur at times within the study area in very high local densities, were consistently rare or absent from our catch. These two species and several others undergo diel vertical migration in the water column, rising to the surface at night and returning to depths below the reach of our net (i.e. >20m) during daylight hours (Krutzikowsky and Emmett 2005). Because we sampled surface waters during daylight, it is very likely that our survey underestimated the true abundance of these and other diel vertical migrators including whitebait smelt, Pacific sardine, and Pacific hake.

Some species (e.g. jacksmelt and surf smelt) were limited in their use of temperature-salinity habitat, while others (e.g. wolf-eel and herring) were found across a wide range of thermal conditions. Among larval fish taxa commonly eaten by juvenile salmon and observed in our catch, osmerid smelts were captured almost exclusively in the coldest water sampled, while rockfish and flatfish larvae were taken across a much wider temperature range. Among the

common invertebrate bycatch, sea nettles were ubiquitous but more abundant in warmer saltier water, crystal jellies more abundant in cooler fresher water, and market squid abundant in all conditions (Fig. S2).

Sea nettles appeared to vanish from our survey in 2015 after more than 15 years of predictably high abundance. On previous surveys, high densities of sea nettles, especially in southern nearshore stations in the GF, often made trawling impossible or damaged the net, and the biomass of this species in the catch sometimes exceeded 10,000kg in a single haul. The sudden disappearance of sea nettles in 2015 coincided with record high abundance of another large scyphozoan, the fried-egg jellyfish.

Full community—alongshore pattern:

Three univariate diversity metrics were significantly correlated to the spatial order of samples along the coast, based on tests with linear regression (Fig. 9; Table 8). The strength of the relationships of *N, H',* and *J'* with transect line order was driven almost entirely by the difference between the four southernmost lines adjacent to the Gulf of the Farallones (TB, GF, PP, and PI), versus all the remaining lines to the north.

Species richness, *S*, (Fig. 9a) was not correlated to line order, with or without the inclusion of the four southern lines. Total abundance of organisms, *N*, (Fig. 9b) was significantly correlated to line order. N was about ten times greater, on average, in hauls on the four southern lines than elsewhere. The Shannon index, *H'*, (Fig. 9c) considers both richness and evenness and was also significantly correlated to line order: *H'* was lowest on the four southern lines, reaching its lowest value of 0.37 at PI. *H'* was highest (0.96) near the center of the study zone at TD. Pielou's evenness index, *J'* (Fig. 9d), closely matched the pattern of Shannon diversity and was also lowest in the south. Excluding the four southern transects, there was no significant relationship of abundance, diversity, or evenness to the position of the remaining lines HH to FR.

Ordination by nMDS offers a more detailed look at community structure associated with the spatial order of transects. For this, hauls were grouped by line and the average CPUE of each species calculated across years and stations for each group. The resulting plot of transects in species space (Fig. 10) reveals an obvious but imperfect north-south gradient in catch composition. The four southern lines form a tight group with similar average communities. Lines in the central study area (FR to ER) fell centrally on the plot, and lines to the north (TD to SR) are more dispersed as the gradient weakens. The three northern lines in Oregon (RR to HH) fold back toward the center, with the northernmost line HH equally similar in species composition to its nearest actual neighbor FM and to the more distant line GP. A reference line connecting the transects in true order from north to south only crosses itself once, indicating that most transects are more similar to their nearest neighbors than to more distant places along the coast, and that community structure changes gradually and progressively with latitude.

A test of the null hypothesis of no change in structure/composition with latitude was significant and H_o was rejected at p=0.001 (DISTLM: R^2=0.34, pseudo-F=6.72). In keeping with the general dissipation of the latitudinal pattern among the northern lines in the nMDS plot, only 34% of the variation in community structure present in this layout was explained by latitude alone in DISTLM.

Full community—cross-shelf and interannual patterns:

The other spatial dimension examined was east-west across the continental shelf, roughly perpendicular to the coastline. Among the univariate metrics, richness (*S*) and abundance (*N*) varied significantly among the five shelf positions, with both decreasing as depth and distance from shore increased (Fig. 11; Table 9). For both *S* and *N*, shelf positions 1–3 each differed from shelf positions 4–5, based on pairwise comparisons. There was no difference in *S* or *N* among the inner three nor among the outer two positions, indicating that richness and abundance declined most rapidly from position 3 to 4, near the midpoint of each transect line between 83m and 122m water depth. Evenness (*J'*) and diversity (*H'*) were not significantly different among positions. Evenness remained stable (*J'* actually increased with increasing distance from shore, but not significantly so). *H'* incorporates evenness and was also not significantly different among shelf positions.

For temporal pattern there were significant differences among years for all variables except total abundance *N*, but no consistent pattern among the five years tested and no single year during the period 2010–14 that stood apart as a consistent outlier (Fig. 12; Table 9). Richness, *S*, was significantly higher in 2013 by about 1.6 species per haul, on average, than in the two preceding years 2011–12. Diversity, *H'*, was lowest in 2014, significantly more so than in the preceding four years. Evenness, *J'*, was also lowest in 2014, but significantly more so than only 2011 and 2012 based on pairwise comparisons. 2015 was not examined because full transects were not sampled in that year.

Following the rationale for latitudinal pattern, ordination by nMDS offers a more holistic look at cross-shelf and yearly variation. The resulting plot, with factors arranged in a crossed two-way layout (Fig. 13) showed a clear gradient in community structure from nearshore (right) to offshore (left) which was surprisingly consistent among years. Distance from shore and depth of water beneath the net altered community structure in a consistent way among years, and cross-shelf variation was magnified furthest from shore—in three of five years, the fifth position was most strongly different from the others. In addition, each year formed a non-overlapping group in the plot (demonstrating interannual difference), and there was evidence of a temporal gradient seen in the ordered stacking of years in their actual temporal sequence from 2010 at top to 2014 at bottom.

The crossed layout allowed simultaneous testing of the null hypothesis of no position or year effects on trawl catch. A two-way PERMANOVA confirmed differences in community structure associated with both main effects (*position:* pseudo-$F_{4, 24}$=5.79, p=0.0001; *year:* pseudo-$F_{4, 24}$=6.10, p=0.0001). Testing for position-year interaction was not possible due to the lack of replication in this data arrangement.

A single linkage cluster plot (Fig. 14) with years as endpoints offers an alternative way to visualize interannual biotic pattern. To include year 2015 and still maintain consistency among years, only shelf positions 1–3 are included here. The first branch in the dendrogram occurred at 60% Bray-Curtis similarity, the point at which the most dissimilar year 2010 joined the remaining years. The next most dissimilar year was 2015, followed in order of branching by 2011, 2012, and finally the two most similar years 2013 and 2014 joining at 75% similarity. In support of the ordination in Fig. 13, the sequence of branching in the cluster plot also suggests gradual progressive change in catch composition over the course of the study, at least during the period 2011–14 when the branching pattern followed the temporal sequence of surveys.

Full community—relationship to environment:

A final graph of biotic structure, here using PCO on station-averaged catch (Fig. 15) provides a complimentary look at community pattern and its relationship to location, water properties, and frequently encountered fish and invertebrates. The placement of 62 stations in the ordination is based entirely on their species similarity, and vectors show the magnitude of correlation between selected variables and the first two PCO axes.

Stations located on the four southernmost transect lines (PI to TB) form a loose cluster that occupies the lower left quadrant of the graph, shaded orange in Fig. 15a. Southern stations had similar communities, different from central and northern stations, shaded blue, which fell elsewhere on the plot with only one exception (station FR03). Among the central and northern (FR to HH) group, offshore stations (shelf positions 4–5) mostly occupy the lower right quadrant of the graph, while nearshore stations (shelf positions 1–3) mostly occupy the upper right quadrant (positive values of axis 2).

Vectors representing location and water properties clarify the relationship between biotic and environmental structure (Fig. 15b). Lat increased to the upper right, thus stations with high scores on both axes were mostly northern stations and those with low scores on both axes mostly southern stations. Sal and Temp had higher values overall in the south, and lower values in the north. Dep and Dis increased to the lower right, consistent with the location of stations populated by offshore species. Three related variables—Trans, Secchi, and PAR—also point in this direction and indicate that water clarity increased with increasing station depth and distance from shore. Conversely, Chl was generally higher at shallow nearshore stations.

Vector overlays of several frequently caught species show where they were most often found and with what other species. The suite of fish most strongly associated with northern stations included surf smelt (*Hypomesus pretiosus*), unidentified larval smelt, juvenile and subadult coho salmon, subadult Chinook salmon, and juvenile steelhead (Fig. 15c). The abundance of these fish increased with increasing scores on both axes and so too with increasing latitude. Conversely, jacksmelt and Pacific butterfish were most strongly associated with southern stations and the Gulf of the Farallones. Among the common invertebrates, bunny salp were more abundant at northern stations while market squid and all large scyphomedusae jellyfish species (excluding the smaller crystal jelly, a hydromedusa) were more often encountered in the south (Fig. 15d).

Fish species most strongly associated with shallow and nearshore stations included juvenile Chinook salmon, wolf-eel, Pacific herring, whitebait smelt, surf smelt and medusafish (*Icichthys lockingtoni*). Fish species more strongly associated with offshore stations included flatfish larvae, king-of-the-salmon (*Trachipterus altivelis*), YOY rockfish, jack mackerel (*Trachurus symmetricus*), and subadult steelhead. Common nearshore invertebrates included crystal jellyfish and sea nettles, while glassy nautilus heteropods (*Carinaria cristata*) were more frequently taken in offshore water. Evidence of the commensal relationship of young medusafish and sea nettles can be seen by the nearly identical position and length of the two species' vectors, signifying that they were frequently captured together at nearshore southern stations.

These associations with latitude, distance, depth, and water properties are generalizations. The vector overlays are useful exploratory visual aids to show where the most abundant and frequently encountered species were more likely to be found relative to the spatial arrangement of trawl stations, and relative to each other. Overall, the first two PCO axes captured only 39%

of the full multidimensional variability, so the 2-dimensional picture is in this case only an approximation of the true relationship among stations.

We used the routine BIO-ENV to further examine and formally test the relationship between a station's biotic structure and its water properties and location. The test identified a 3-variable best solution to the matrix match between environment and biota (Table 10). The subset that maximized the Spearman rank correlation ρ_s between the two resemblance matrices was a combination of one spatial and two water property variables: Dep, Temp, and Trans (ρ_s=0.578, p=0.001 with 999 random permutations). This reduced subset outperformed all other combinations of variables including the full 9-variable starting point, which also produced a significant but slightly weaker match to biotic structure (ρ_s=0.538, p=0.001). Bottom depth and transmissivity mostly described east-west, cross-shelf variation in community structure, while water temperature mostly described north-south alongshore variation. Latitude was included in the second-best solution (ρ_s=0.573), along with the three variables from the best solution.

DISCUSSION

Summary of main results:

Water properties differed among years and regions of the survey. 2014 was warmer and saltier on average than the other 5 years surveyed, especially in the south, whereas 2011 and 2012 were fresher, especially in the north. Ship-based sampling revealed a warm fresh zone at the northern offshore end of the study area that appears to derive from the southward-flowing Columbia River plume in summer, a broad and consistent warm salty zone in the south near Pt. Reyes and the GF, and a mostly colder central zone coinciding with the region of historically strongest winds and upwelling in the CCS. Retention and warming of coastally trapped water appeared to be negligible in this cool central zone but was evident in the GF during our surveys. A set of correlated variables describing water clarity showed more numerous local, cape-and-bay scale features and more cross-shelf structure than did maps of temperature and salinity. Water clarity increased with increasing distance from shore.

Community structure also differed significantly among years but no single year in the 6-year time series stood out as exceptional, even during the 2014–15 marine heat wave. The 2010 community was most dissimilar in cluster analysis, and diversity (H') was significantly lower in 2014 than the other years. Ordination by nMDS suggested a gradual and progressive change over time, with significant effects of both year and shelf position (by PERMANOVA test) on community structure. Shelf position also affected species richness and abundance.

Salmon catch was highest between the Klamath River and Cape Mendocino for all three species, and dropped rapidly south of Mendocino for coho and steelhead. Juvenile Chinook had a second peak of abundance in the GF region where CCV populations enter the sea, and were found unusually far to the south in 2011, a year of high freshwater runoff followed by several years of drought. Models fit to juvenile Chinook CPUE supported a negative correlation with depth and transmissivity, and a sharp decline in CPUE north of the California-Oregon border. Latitudinal differences in CPUE varied by year, but highest estimated CPUE within California generally occurred in the Klamath region, i.e. within 1 degree latitude south of the border.

Latitudinal differences within the full epipelagic community were also present: metrics of biodiversity were significantly related to line order, nMDS produced an arrangement of samples that closely matched their true spatial order along the coast, and DISTLM confirmed the

statistical significance of a latitude-community gradient. North-south biotic differences were driven mostly by the greater dissimilarity of the four southernmost transects proximal to the Gulf of the Farallones; this broad embayment appears to be a unique biological zone whose influence in summer extends north around Point Reyes to the TB line and possibly beyond. Principal Coordinates Analysis supported this interpretation of a measurably different gulf biota with a higher abundance of characteristic fish and invertebrate species associated with warmer, higher salinity gulf water in summer. Scyphozoan jellyfish, market squid, and a few common fish species (e.g. Pacific butterfish, jacksmelt) were typical of this region, while crystal jellyfish, osmerid smelts and salmon were representative of more northerly stations. Lastly, a subset of three local environmental variables—bottom depth, water temperature, and transmissivity—generated the best (highest correlation and most parsimonious) overall match to the community pattern measured among stations, although a four-variable solution including latitude and the previous three variables did about equally well. Cross-shelf variation in water properties and community structure occurred across shorter distances than alongshore variation.

Spatial pattern in the California Current System:

Coastal pelagic organisms in the CCS are not randomly or uniformly distributed throughout their range. This is hardly surprising, but why is it so? Studies that set out to describe space and time patterns of plankton and nekton often focus on the role of a geographic feature, oceanographic event, or climactic anomaly of some kind as a driving agent of variability. Geographic features such as headlands, bays, submarine canyons, and banks interrupt the uniformity of the coastline and shelf, and rivers send plumes of fresh water, nutrients, and sediment into coastal habitats. These irregular features are known to introduce spatial variability to pelagic communities in the CCS, primarily through their influence on local upwelling, their ability to alter the strength and direction of currents, and in the case of rivers the formation of density and turbidity fronts.

The properties of an array of whimsically named and ubiquitous features of coastal currents (e.g. filaments, jets, squirts, and meanders) are well described in reviews of CCS oceanography (Hickey 1998, Checkley and Barth 2009). Headlands and capes strongly influence small-scale hydrodynamics. They interrupt the flow of prevailing southerly coastal currents and cause the formation of localized plumes and jets that divert nearshore upwelled water far offshore (Kelly 1985, Keister et al. 2009) and affect biological patterns. Some headlands are known to trap water in locally retentive cyclonic eddies close to shore on their down-current sides, for example south of Point Año Nuevo in Monterey Bay (Paduan and Rosenfeld 1996, Graham and Largier 1997) and south of Cape Mendocino (Hayward and Mantyla 1990). Residence time for pelagic larvae and other plankton increases in these retention zones, promoting the development of different communities north versus south of headlands. This “upwelling shadow” phenomenon appears to be common in coastal upwelling zones worldwide (Largier 2004).

Planktonic larvae of coastal benthic invertebrates begin and end their journey in shallow water and if not advected and lost offshore, they have been found to settle in higher abundance (Mace and Morgan 2006) and more consistently over time (Ebert and Russell 1988) in the shadows of even small headlands. Latitudinal differences in community structure associated with specific headlands have been seen for copepods north and south of Cape Blanco (Peterson and Keister 2002), and zooplankton species richness in neuston samples was highest in a patch just south of Cape Blanco (Reese et al. 2005). Among larger pelagic nekton in the CCS, the effect of headlands and their upwelling shadows is largely unknown. Brodeur et al. (2004) found a weak latitudinal gradient in fish assemblage structure across central and southern Oregon with a

break in abundance near Cape Blanco, possibly associated with currents and shelf circulation magnified by the cape.

Peterson et al. (2010) hypothesize that submarine canyons may act as conduits for krill transport onto shallow shelf waters, thus contributing to the observed latitudinal differences in abundance of yearling salmon captured off Washington (high) versus Oregon (low). Reese and Brodeur (2006) mapped two discrete zones in the northern CCS with consistently high nekton biomass and species richness. One of these was located above the Heceta Bank, an offshore extension of the shelf which appears to influence the local biota, perhaps through interaction with the Columbia River plume and increased proximity of shelf habitat to warmer offshore water. A study located within the Columbia River plume itself (Emmett et al. 2006) found inshore versus offshore differences in the abundance of common pelagic predator and forage fish species which appeared to be related to the strength of the river discharge (inshore water was colder, less saline, and more turbid than offshore water farther from the river mouth). The authors proposed that the increased turbidity of plume water may hide forage fish and juvenile salmon from their predators. Using an expanded data set from the same survey, Litz et al. (2014) compared nekton community structure within versus outside the plume and identified unique sets of indicator species associated with different water types, for example juvenile Chinook salmon, Pacific herring, surf smelt, and whitebait smelt were representative of both the “fresh” group and the “inshore” group.

Using an arbitrary dividing line near the center of his survey area, Auth (2008) found significant differences in ichthyoplankton community structure between northern and southern stations in a region spanning about 944 km of coastline from southern Washington to northern California (i.e. the northern and central CCS). At even larger spatial scales (~1550 km along the coast), Thompson et al. (2014) found different ichthyoplankton communities in central Oregon versus southern California but no evidence of synchrony in annual variation of abundance of taxa between the two regions, presumably because a strong biotic response to local environmental variation masks the signal from broad indices affecting the entire CCS. At even larger scales, Hertz et al. (2015) found numerous regional differences in the stomach contents of juvenile Chinook salmon across the northeast Pacific basin from California to Alaska, indicating the prey communities of larval fish and zooplankton eaten by salmon were also highly variable among regions.

Cross-shelf patterns:

Cross-shelf variation in plankton and nekton assemblages in the northern CCS typically form stronger gradients across shorter distances than alongshore patterns (Jacobson et al. 2012(b), Brodeur et al. 2005) and are more frequently described in the literature. Cross-shelf biotic structure is primarily the result of wind-driven coastal upwelling and associated temperature and salinity fronts that advance and retreat across the shelf. For example, Graham et al. (1992) found different zooplankton communities at a spatial scale of <10km residing in two distinct water masses that formed a front extending into Monterey Bay during upwelling season, and Papastephanou et al. (2006) found a sharp change in abundance of several copepod taxa between adjacent nearshore stations during relaxation after upwelling near Bodega Head. Off the Oregon coast where upwelling is less intense, copepod community structure changed significantly along a gradient from shore to beyond the shelf, with the most rapid change occurring near the shelf break and coincident primarily with cross-shelf changes in temperature and salinity (Morgan et al. 2003). Advective filaments spinning out from Cape Blanco shifted

cold-water coastal copepods much further offshore and had a leveling effect on copepod diversity and biomass longitudinally (Keister et al. 2009).

Ichthyoplankton samples from Oregon and northern California formed a clear east-west gradient in nMDS ordinations, with partial separation of three groups classified by station depth as either coastal, shelf, or offshore types (Auth 2008). Near Point Sur in central California, larval rockfish densities differed widely across small spatial scales (a few km horizontally, and a few meters vertically) in close association with upwelling fronts (Bjorkstedt et al. 2002). In a study of micronekton (2–10cm organisms) captured in fine-mesh trawls off Oregon and Washington, Phillips et al. (2009) found strong and persistent cross-shelf assemblage structure, with distance from shore and sea-floor depth correlated more strongly to ordination axes than all other environmental variables measured, including water temperature, salinity, fluorescence, turbidity, and latitude.

Analyses of larger nekton in the NCC also consistently found cross-shelf patterns of assemblage structure. Groups identified by cluster and ordination clearly separated on east-west axes defined by local environmental variables including temperature, salinity, bottom depth, and distance from shore (Brodeur et al. 2004, 2005, Reese and Brodeur 2006, Litz et al. 2014), with suites of typical inshore and offshore species (e.g. *inshore:* juvenile Chinook and coho salmon, herring, anchovy, smelts, and squid; *offshore:* YOY flatfish and rockfish, Pacific mackerel, sardine, jack mackerel, saury, sunfish, and non-dogfish sharks) mostly similar to those identified in the present study. Water transparency was not consistently measured in most prior studies but was a significant cross-shelf predictor when data were obtained (e.g. Secchi depth, Brodeur et al. 2005), and the importance of chlorophyll-a concentration as a predictor of nekton structure was not consistent among surveys. Jacobson et al. (2012(b)) used a novel approach to examine spatial patterns and habitat use among several common pelagic fishes, including Chinook and coho salmon. Within certain host species, they found that fish carried different communities of parasites inshore vs. offshore of the shelf break (200m isobath), but found no difference in parasite community (hence no difference in trophic history of the host species) due to the local oceanographic effects of Cape Blanco or inside vs. outside of two biological hotspots in the NCC previously identified by Reese and Brodeur (2006).

In their original hotspot study, Reese and Brodeur (2006) found gradients of change in community structure to be stronger across the shelf than alongshore. In a subsequent reanalysis of data from the same surveys, Reese and Brodeur (2015) looked more closely at species associations and included four common species of large medusae in their revised catch matrix. They found jellyfish species spatially clustered and strongly correlated, and as a group jellyfish inhabited colder, saltier, newly-upwelled water close to shore in the company of market squid, whitebait and surf smelt, juvenile Chinook salmon, juvenile wolf-eel, and other nearshore-typical nekton. These associations of jellyfish, fish, and squid are similar to those we observed, in particular within the nearshore GF community, although water properties in the GF differed from the NCC hotspots. In the most comprehensive study to date on jellyfish abundance in the NCC, Suchman et al. (2012) found much higher densities of sea nettles close to shore in colder water, crystal jellies more evenly distributed across the shelf and usually in warmer water, and moon jellies intermediate for these covariates. In the present study all large jellyfish species were more abundant close to shore, but associations with water temperature differed from previous work conducted in the NCC, with sea nettles in our survey favoring warmer water than crystal jellies—a result of the higher mean temperature in the Gulf of the Farallones where sea nettle density was consistently highest.

Properties of the Gulf of the Farallones:

The physical and biotic properties of the GF set it apart from other coastal habitat in the central and northern CCS, making it a unique biological zone (Karl et al. 2001). Using an indicator-species analysis, Harding et al. (2011) found a suite of fish representative of the GF summer assemblage that included herring, anchovy, sardine, and medusafish, and a measurably different community along the north coast to Point Arena represented by juvenile and subadult Chinook salmon, jacksmelt, and jack mackerel. During upwelling relaxation periods, distinctive gulf water spills north (poleward) around Pt. Reyes (Send et al. 1987, Wing et al. 1998, Kaplan and Largier 2006), presumably carrying with it many plankton and nekton species, especially those with little ability to swim against currents (e.g. jellyfish). This intermittent poleward current appears to extend the biological signature of the GF into adjacent coastal waters to the north, at least as far as the TB line sampled in the present study.

The GF is an unusual mixing zone in the CCS with complex circulation patterns and seasonally variable input from several different water masses, each with its own characteristic properties (Schwing et al. 1991, Steger et al 2000, Kaplan and Largier 2006). Mixed upwelled water in the northern gulf is regularly retained in slow circulation near the coast in the lee of Pt. Reyes (Wing et al. 1998, Largier 2004, Vander Woude et al. 2006, Dorman et al. 2015) and warmed by solar heating, forming conditions similar to the strong upwelling shadow in nearby Monterey Bay described in Graham and Largier (1997) but not as well organized. Retentive circulation of aging upwelled water promotes the development of phytoplankton blooms in the GF (Vander Woude et al. 2006) and supports further enhancement along the food chain to zooplankton, fish, and mammals. The additional influence of freshwater discharge from the SFB further complicates and distinguishes the GF environment. In wet years when SFB outflow is high, a freshwater plume reduces the salinity of nearshore Gulf water (Wilkerson et al. 2002). Several prior studies found GF water to be generally warmer with lower salinity than coastal water north of Pt. Reyes where upwelling is more intense (Send et al. 1987, Kaplan and Largier 2006, Harding et al. 2011), however nearshore mixed water in the gulf may also be warm with variable or high salinity in years with low SFB discharge (Wing et al. 1998). 2010–2015 was a notably dry period in California, with 5 of 6 water years rated at below normal, dry, or critical (California Dept. Water Resources website: http://cdec.water.ca.gov/reportapp/javareports?name=WSIHIST). Only water year 2011 was rated “wet”. The high salinity conditions in the GF reported in the present study are likely the result of the severe drought experienced by California from 2010 to 2015 and the unusually low SFB summer discharge during those years, with the exception of the single wet year 2011 when we observed a low-salinity plume exiting the bay and anomalously high numbers of juvenile Chinook were captured in plume water on the southernmost lines PP and PI that year, suggesting they were transported south and offshore by this feature when they exited the bay.

Salmonid spatial patterns:

Off Oregon and Washington, the highest “center of mass” of juvenile salmon catch consistently occurs in a narrow zone between appx. 46.5°N and 47.5°N latitude in June surveys, rather than more uniformly along the entire coast (Peterson et al. 2010). This regional concentration of fish was similar to our finding of highest salmon CPUE in a narrow latitude zone north of Cape Mendocino. Juvenile salmon were also found very close to shore off OR-WA in June, with 80% of Chinook taken at stations in 30–83m water depth, 80% of coho in 30–124m depth, and highest abundance of both species in cold, shallow, high-chlorophyll water with high biomass of boreal copepods (Peterson et al. 2010). In a separate Oregon survey, preferred habitat for

juvenile Chinook was identified as high chlorophyll water close to shore, and for juvenile coho as slightly fresher, more northerly water further from shore and with high abundance of larval decapods (Pool et al. 2012). Using data from the first three years of the present study (2010–12), Hassrick et al. (2016) found young Chinook salmon abundance was negatively correlated to distance from their natal river and positively correlated with chlorophyll concentration, but unrelated to krill density. Our analysis of juvenile Chinook CPUE suggests that transmissivity was the best predictor among the environmental covariates in this study, after accounting for spatial, temporal, and depth effects. Due to the negative correlation between chlorophyll and transmissivity, substituting chlorophyll for transmissivity in the best-fit model resulted in a minor reduction in predictive performance of the model. In California waters, average juvenile Chinook CPUE was highest just south of the California-Oregon border. The best-fit model in our analysis identifies a significant reduction in juvenile Chinook CPUE north of the California-Oregon border, although the magnitude of this change varies by year. Similar to Hassrick et al. (2016), we found that the available data did not strongly support a single best model, and that model predictions were highly variable despite evidence for changes in CPUE with transmissivity, depth, latitude and year. Unlike Hassrick et al., we found that a simpler negative binomial regression model adequately reproduced the observed proportion of zero observations in the data, without resorting to zero-inflated or hurdle models that require additional parameters.

Interannual variation in the California Current System:

Change over time in pelagic communities is often described in relation to some periodic marine climate event such as El Niño or La Niña that occurs unpredictably every few years. El Niño Southern Oscillation (ENSO) events typically affect water temperature, winds and currents, upwelling, productivity, and other properties in the CCS to varying degrees through processes linking the equatorial and northeastern Pacific Ocean (Fiedler 2002, Schwing et al. 2010). Surveys that span many years are more likely to encounter significant ENSO events and other anomalies, presenting unplanned opportunities to study the local consequences of large-scale climate variability and test predictions about the response of marine communities to climate change. For example, the biological effects of historically strong El Niños in 1982–83, 1997–98, and other less dramatic episodes were documented by long-running ocean surveys initiated before the onset of these events, and thus well positioned to describe the evolution of change in CCS pelagic communities associated with them (Pearcy et al. 1996, Peterson et al. 2002, Bograd et al. 2003, Koslow et al. 2013, McClatchie 2014, Fisher et al. 2015). One of these surveys, the Rockfish Recruitment and Ecosystem Assessment Study (RREAS), was started in 1983 to monitor juvenile groundfish abundance and now maintains an extensive record of the forage community throughout California shelf waters (Ralston et al. 2013, 2015, Santora et al. 2017). RREAS is currently the only annual community-level survey of pelagic micronekton and midwater forage in the central CCS, and the most similar in geographical coverage to the SWFSC salmon survey.

Beginning around June 2010 and just prior to our July survey, the CCS transitioned from mild El Niño conditions to a strong La Niña with increased upwelling, high productivity, and record cold SST by summer (Bjorkstedt et al. 2011). In May 2010 when El Niño conditions still prevailed, anomalously high diversity and abundance of larval fishes were reported off Oregon, but by the following summer an almost complete disappearance of several taxa had occurred at the same locations and abundance declined coast-wide following the rapid reversal of conditions (Auth et al. 2015). In our study, 2010 was the most dissimilar year in a community-level classification analysis. The rapid reversal of environmental conditions just prior to our cruise may have

contributed to the greater dissimilarity of community structure we observed that year, relative to the period that followed.

Continuing in 2011, cool productive conditions prevailed in the northern and central CCS under a waning La Niña. Spring upwelling began late but was stronger than average in northern California during our July 2011 survey, and high variability at local event scales was reported, especially in the north (Bjorkstedt et al. 2012). Conditions in the CCS in 2012 were similar to 2011 and other recent cool years with strong southward transport, strong local upwelling in the central region and mostly cold, productive conditions dominating, but with very low primary productivity throughout northern and central California in spring (March–May). Summer mean chlorophyll on the Newport Hydrographic (NH) line in central Oregon (44.65°N) was at a 12-year low near the coast in 2012, and record low surface chlorophyll levels were recorded in Monterey Bay in June 2012 (Wells et al. 2013). 2013 remained cold with negative ENSO values, strong upwelling, high transport, near average spring chlorophyll levels, and productive conditions in July (Leising et al. 2014).

In contrast to the conditions that prevailed through most of 2010–13, an unusual and extreme event did occur during the final two years of the present study. The 2014–16 marine heat wave was the most notable large anomalous oceanographic event to affect the CCS since the strong 1997–98 El Niño, and coincided with the first change in North Pacific climate indices in several years. This historic event started as a pool of unusually warm surface water nicknamed the Blob in the Gulf of Alaska in late 2013, and continued into 2014 as the warm feature intensified and expanded through the Northeastern Pacific (Bond et al. 2015, Di Lorenzo and Mantua 2016). Values of the Multivariate ENSO Index, a metric used to characterize the strength of an ENSO event (Wolter and Timlin 1993), turned positive in April 2014 as the Pacific Ocean entered an El Niño phase, although upwelling in the central CCS was near the long-term average in 2014 with a strong pulse in June and July between 36°–42°N coinciding with our 2014 survey. This upwelling pulse produced localized phytoplankton blooms and elevated chlorophyll levels that peaked in June 2014 and were measured by survey teams working on the Trinidad Line and at the M1 mooring in Monterey Bay (36.8°N) (Leising et al. 2015). Water temperature remained extremely warm throughout the CCS in 2015, although strong upwelling-favorable winds in winter and spring once again kept coastal SST cool in the central region at the time of our June survey. Upwelling was positive and strong from April to June 2015 at 39°–45°N, even though June 2015 MEI was the highest recorded since the 1997–98 El Niño (McClatchie et al. 2016). During the May–June 2015 RREAS, water temperature at 30m was cooler than average near Point Arena, but unusually warm in the southern California bight (Sakuma et al. 2016, Fig. 3). June 2014 and 2015 water temperature in the upper 20m was also below the long-term average at stations off Oregon and Washington (Peterson et al. 2017, Morgan et al. 2019). Despite the ongoing marine heat wave, these reports are consistent with the cool to average water temperatures we encountered during the summer in 2014 and 2015.

Biological anomalies during the marine heat wave:

Coastal surveys during the warm period saw changes in abundance of some taxa and shifts in gross community structure across a range of functional groups including copepods, larval fish, epipelagic fish and invertebrates, and pelagic micronekton (Leising et al. 2015, Peterson et al. 2017). Anomalous biotic patterns were generally stronger in 2015 than 2014. For example, the RREAS recorded anomalous catches in spring 2015, including record numbers of unusual warm-water species in the south (considered El Niño signature species) in combination with average or record numbers of normally cold-water associated species such as YOY rockfish

and sanddab, market squid, and krill, resulting in anomalously high diversity (Sakuma et al. 2016, Santora et al. 2017). In the NCC off Oregon and Washington in 2015, the abundance of several prominent invertebrate species (market squid, crystal jellies, fried-egg jellies) was notably higher than the 20-year average but much lower for sea nettle jellyfish, which virtually disappeared from the NCC in 2015 (Morgan et al. 2019). Sea nettles were also seen at near-record low numbers in 2015 by the RREAS team (Leising et al. 2015), consistent with our observations. Prior to their disappearance in 2015, sea nettles were the second most abundant organism in our trawl catch, after market squid. Larval anchovy and sardine appeared early and in unprecedented numbers in 2015 on the NH line in central Oregon (Auth et al. 2018), and the RREAS observed record high abundance of larval anchovy and sardine in their core and north central regions in May–June 2015 (Sakuma et al. 2016), consistent with our highest recorded catch of anchovy larvae in June 2015 (we did not record sardine larvae). In contrast to these anomalous patterns, juvenile Chinook and coho salmon abundance off Oregon and Washington in June 2014 and 2015 were very close to 20-year mean values for both species (Morgan et al. 2019), and our salmon catch during the warm event was not obviously different from prior years in our shorter time series.

Ocean sunfish are one of the El Niño signature species associated with anomalous nearshore warming in the California Current. These large, migratory oceanic fish are sometimes observed close to shore in the central and northern CCS, especially during unusual warm events such as the 1997–98 El Niño (Pearcy 2002). At other times fisheries surveys in this region typically encounter them only in high temperature and high salinity water far from shore, often in association with fish that typify warmer oceanic habitat such as blue shark, Pacific saury, and jack mackerel (Brodeur et al. 2005). In 2014 we caught a total of 13 ocean sunfish, all taken on the four southern lines within the advancing warm front that year. Had we not been using the MED, it is likely the sunfish catch would have been even higher. None were taken by us in any other summer survey 2010–15. Sunfish were reported in surveys as far north as the Gulf of Alaska in summer 2015 (Cavole et al. 2016).

Ordinations depicting 18 and 27 years of continuous annual sampling by the JSOES and RREAS programs, respectively, showed a clear change in gross community structure coinciding roughly with the 2014–16 marine heat wave (McClatchie et al. 2016). For JSOES, 2015 and 2016 stood apart as different from all previous years in their time series, including previous warm years. For the RREAS core area, a coherent shift in community structure was first detected in May 2013, a full year before SST anomalies appeared in the central CCS and two years before the JSOES community signal changed in Oregon. In a PCA filtered to include just nine key taxonomic groups of common forage organisms, 2013–16 separated “dramatically” from all previous years in the RREAS time series, including previous warm years, productive and unproductive years, and the 1997–98 El Niño period (McClatchie et al. 2016). These results are in contrast to our study. With the exception of a few individual species (sea nettles, fried-egg jellyfish, larval anchovies, ocean sunfish) in a few locations, anomalous community structure was not observed in our trawl catch in 2014 or 2015 during the marine heat wave, and we did not consistently encounter unusual numbers of southern or offshore taxa in those years.

The absence of a strong Blob signal in our 2014–15 data was probably related to the timing and location of our survey and the cooling effects of strong coastal upwelling that coincided with our cruise. As of early July 2014, nearshore ocean temperatures were near or below long-term averages from Point Conception north to central Oregon. However, by late July when our survey vessel was sampling southern stations, a very warm water mass that originated off Southern California was spreading rapidly north and onshore following the abrupt cessation of coastal upwelling (NASA JPL news item:

https://podaac.jpl.nasa.gov/OceanEvents/2014_09_04_CaliforniaCoast_warming). We briefly encountered this advancing warm front near Point Reyes and in the GF (Fig. S1). Hydrographic and species anomalies were mostly not seen off northern California and Oregon until later that summer and fall when the large northern warm pool also advanced rapidly onshore following the relaxation of upwelling favorable winds. For example, strong temperature, salinity, and copepod anomalies off Newport first appeared in late September 2014 (Peterson et al. 2017), about 3 months after the June JSOES and 2 months after our July survey. The separate northern and southern warm features ultimately merged in October 2014 to form a single continuous warm pool affecting the entire CCS from Vancouver Island to Baja California, Mexico that persisted and intensified through the following winter (Leising et al. 2015, Gentemann et al. 2017). Stronger than average upwelling-favorable winds again developed in winter and spring 2015, injecting cool water along the coast in the central and northern CCS in May and June (McClatchie et al. 2016, Gentemann et al. 2017) and pushing the warm pool off the shelf just before and during our 2015 survey. As a result, the sampling time frame was once again out of sync with the maximum warm water intrusion.

The observed differences in the strength and timing of community-level change in CCS pelagic organisms during the marine heat wave may also be partly explained by operational differences among the various surveys and differences in the species and life-stages targeted. RREAS sampled the midwater mesopelagic community at night, using a smaller trawl with a finer mesh towed deeper and at slower speed than JSOES and the present study, and their annual survey takes place earlier in spring than either of the two salmon-centric projects. Geographic range also varies. JSOES covers Oregon and Washington, our study covers northern and central California, and RREAS covers the entire California coast but focuses heavily on a core area in the GF and Monterey Bay. Length of time series also matters. JSOES and especially RREAS had a much longer span of data prior to the marine heat wave, and therefore a more accurate measure of “average” community structure than the present study and greater power to detect deviation from the prior norm. The effect of survey longevity can be seen in a comparison of long (26 year) vs short (12 year) time series PCA phase plots depicting change in annual community structure in the RREAS core area (Sakuma et al. 2016, Fig. 11). In their analysis, the years 2013–15 appear more anomalous in the longer time series.

The importance of jellyfish in the CCS:

Popular and scientific reports have noted an apparent increase in the frequency of jellyfish blooms in coastal waters worldwide in recent decades (Mills 2001, Brotz et al. 2012, but see Sanz-Martín et al. 2016), possibly as an unintended consequence of human industrial and agricultural activities (Purcell 2012), and potentially resulting in new, simplified, and less desirable ecosystem states (Richardson et al. 2009). Whether or not blooms are increasing in frequency, jellyfish biomass can at times reach impressive levels. The total biomass of sea nettles in our catch from 2010–14 easily exceeded the combined mass of all other organisms taken aboard, and would have been even higher had we not deliberately shortened or canceled tows at locations with visibly dense aggregations. Our largest sea nettle hauls contained 3,000–6,000 individual medusae with estimated mass of 7,000–15,000 Kg, and one attempted haul (survey FR1101, station PI01) was estimated to contained 8,700 jellyfish and weigh 25,000 Kg., and could not be taken aboard. Suchman and Brodeur (2005) reported similar maximum counts of sea nettles in the NCC off Oregon in June of 2000 and 2002, and an astonishing record haul equivalent to 76,800 individuals per $10^6 m^3$ in August 2000.

Medusae feed on zooplankton and the early life stages of fish, and have the potential to alter trophic pathways and pelagic food webs (Robinson et al. 2014). Sea nettles in the NCC consumed on average one-third of the daily standing stock of euphausiid eggs in nearshore locations were sea nettles were most abundant (Suchman et al. 2008). Morgan et al. (2019) also saw a significant increase in all stages of euphausiids in years when sea nettles were least abundant. The euphausiid *Thysanoessa spinifera* is one of several important prey items for salmon. In the central CCS high *T. spinifera* abundance was positively correlated to improved juvenile Chinook salmon body condition and the number of 2-year adults returning to the Sacramento River to spawn the following year (Wells et al. 2012). Large jellyfish are believed to compete with juvenile salmon to the extent that salmon production was reduced in years with high densities of sea nettles (Ruzicka et al. 2016). Due to their position in the food web, annual life cycles, fast growth, seasonal abundance, opportunism and rapid response to physical forcing (e.g. local upwelling), jellyfish are thought to be one of the most sensitive ecosystem indicators available (Suchman et al. 2012). Jellyfish actually outperformed most other functional and taxonomic groups as consistent indicators of model ecosystem attributes used to support ecosystem-based fishery management (Samhouri et al. 2009). We observed a change in abundance of two large jellyfish species in the final year of the present study (decrease in sea nettles, increase in fried-egg jellies) coinciding with an unusual marine climate event. Although our time series was too short to ascribe these changes to anything more than interannual variability, even a single year of anomalous jellyfish abundance is a noteworthy event with potential significance for trophic pathways including those affecting salmon populations.

Small organisms, vertical migrators, and net efficiency:

Our choice to be broadly inclusive of species in the community analysis draws the criticism that, because of their small size relative to the mesh of the codend liner, it is not possible to accurately sample larval fish with the NRT and standard liner. Undeniably, pelagic trawls catch different taxa with different efficiency (Mais 1974). For example, salmon and other actively swimming fish that detect the net may be herded toward the center by passage of the large forward meshes or may maneuver to avoid capture, while jellyfish, salps, larval fish, and other weak swimmers simply drift through the passing forward meshes and are lost from the catch. In effect, larger mobile nekton experience a much larger net than drifting organisms and larval fish. Small things may also escape through the liner, and we recognize that the equipment we used was not optimized to sample larval fish. However, net efficiency alone should not affect differences in the *relative* abundance of the same taxa among sites or years. So long as the gear, methods and effort remain the same, underestimates of the true density of some species should have little effect on the resulting community patterns. In 2016 we modified the survey plan to include back-to-back comparisons of trawl catch using a standard-mesh (6x10 mm) liner vs. a fine-mesh (3x3 mm) liner intended to retain more larval fish and small invertebrates. Improved retention of small taxa would allow more accurate sampling of the prey field of juvenile Chinook and coho salmon. Results of that comparison are forthcoming, and will help us determine the extent to which larval taxa may have been under-sampled previously.

Even with this limitation we did consistently catch larval and postlarval fishes, most notably rockfish and flatfish. These were among the most abundant and frequently occurring taxa sampled, and we believe their inclusion in the community analysis is both justified and revealing. Larval fish are important prey items for juvenile Chinook and coho salmon at sea. Their inclusion along with salmon and other mid-trophic predators in a community-level study is important because fish larvae have a direct trophic link to salmon and the co-occurrence of predators and prey at various scales is ecologically revealing.

We fished during daylight hours with flotation added to the trawl headrope because previous studies comparing depth and diel timing found juvenile Chinook and coho salmon catch was highest in surface water (upper 12m) and during the daytime (Emmett et al. 2004, Krutzikowsky and Emmett 2005). Because sampling occurred during daylight, the CPUE of diel vertically migrating fish can be misleading, especially if they are consistently absent from samples. Even general trends in abundance may be misreported by sampling the correct habitat at the wrong time of the day. Night trawling would certainly have caught more of the diel migrating species (e.g. anchovy, herring, sardine, whitebait smelt, Pacific hake, and mackerels) that disperse and move closer to the surface after dark (Mais 1974, Krutzikowsky and Emmett 2005). But as with larval fish, we do not present CPUE of diel migrators as measures of absolute abundance. More simply, when we did catch these species at the surface during daylight they were part of the community of interest as we defined it and therefore included in community-level statistical tests. Ideally we would also like to have night-time samples to build a more complete picture of salmon marine habitat, but resources did not allow regular around-the-clock trawling operations. On two separate occasions when we were able to conduct multiple repeated trawls during both daylight and darkness at a single location, the night catch of anchovy and herring was much higher than the day catch, and Chinook salmon catch was lower at night (FED, unpublished data).

Alternate survey designs are available to obtain more accurate abundance estimates of schooling diel migrators such as anchovy and sardine. In addition to simply trawling at night and/or deeper in the water column, acoustic-trawl methods (ATM) use a hybrid approach combining information from echosounders and nets (Zwolinski et al. 2012, 2014, 2019). In ATM, acoustic data are gathered continuously along preselected transects during daylight while trawls are made the following night at stations distributed along the track line, either at predetermined locations or adaptively set on acoustic targets of interest (e.g. schools of fish). Fish abundance and distribution are determined from acoustic signal strength, and trawl catch is used to estimate species composition and length distributions. Concurrent and spatially overlapping data from ATM surveys would be a useful compliment to the present study and to our JSOES partners, allowing us to assess whether we can accurately track patterns of abundance for these coastal pelagic species using our current methods alone. ATM has not yet been used to measure salmon abundance or distribution, although improving echosounder technology may eventually make this possible.

CONCLUSION

This study presents a portion of the data collected during a 6-year annual time series of ship-based coastal ocean observation with mostly consistent timing, sampling methodology and spatial coverage. Including this report, the SWFSC FED ocean salmon survey has published quantitative observations of coastal pelagic fish communities with species-level resolution in the central CCS spanning 16 years and including two uninterrupted 6-year periods. We improved the sampling design for the second period (2010–15) in several ways, for example by increasing cross-shelf coverage and by enumerating medusae and other large invertebrates in the bycatch. Although we referred to our program as a cruise or survey and not an ocean observing program per se, we have nonetheless conducted systematic ocean observing and obtained a valuable community-level ecological time series, albeit a short one. Systematic survey data such as these are necessary for detecting trends in abundance and shifts in distribution, often functioning as a launch pad for more focused process studies with testable hypotheses. The need for improved and sustained ecological ocean monitoring is critical, especially as the

world's oceans face a plethora of anthropogenic stressors whose full effect on marine ecosystems remains unknown and mostly unmeasured (Koslow and Couture 2015).

ACKNOWLEDGEMENTS

We thank V. Sridharan and M. Sabal for assistance with map figures, M. O'Farrell for insight on Klamath salmon populations, and E. Sturm, D. Chastagner, and S. Bertolino for logistic support. K. Johnson provided invaluable assistance with manuscript formatting and 508 compliance. We thank the Captains and crew of the R/V Ocean Starr, F/V Frosti, and NOAA ship Bell Shimada. Special thanks to Bud and Armando. Forty-one scientists and volunteers participated in sea duty for this project, which would not have been possible without their commitment and hard work. Support was provided by the Ernest F. Hollings Undergraduate Scholarship Program and the NOAA Sea Grant program. This paper is dedicated to Dr. Umihiko "Umi" Hoshijima, a promising young biologist and polymath who sailed with us and enriched our lives.

REFERENCES

Anderson, M.J., Gorley, R.N., Clarke, K.R., 2008. PERMANOVA+ for PRIMER: Guide to software and statistical methods. Primer-E, Ltd., Plymouth, UK.

Auth, T.D., 2008. Distribution and community structure of ichthyoplankton from the northern and central California Current in May 200406. Fisheries Oceanography 17, 316–331. https://doi.org/10.1111/j.1365-2419.2008.00481.x

Auth, T.D., Brodeur, R.D., Peterson, J.O., 2015. Anomalous ichthyoplankton distributions and concentrations in the northern California Current during the 2010 El Niño and La Niña events. Progress in Oceanography 137, 103–120. https://doi.org/10.1016/j.pocean.2015.05.025

Auth, T.D., Daly, E.A., Brodeur, R.D., Fisher, J.L., 2018. Phenological and distributional shifts in ichthyoplankton associated with recent warming in the northeast Pacific Ocean. Glob. Change Biol. 24, 259–272. https://doi.org/10.1111/gcb.13872

Bjorkstedt, E., Rosenfeld, L., Grantham, B., Shkedy, Y., Roughgarden, J., 2002. Distributions of larval rockfishes Sebastes spp. across nearshore fronts in a coastal upwelling region. Mar. Ecol. Prog. Ser. 242, 215–228. https://doi.org/10.3354/meps242215

Bjorkstedt, E.P., Goericke, R., McClatchie, S., and others. 2012. State of the California Current 2011-2012: Ecosystems respond to local forcing as La Niña wavers and wanes. CalCOFI Rep. 53, 41–76.

Bjorkstedt, E.P., Goericke, R., McClatchie, S., and others. 2011. State of the California Current 2010-2011: Regionally variable responses to a strong (but fleeting?) La Niña. CalCOFI Rep. 52, 36–68.

Bograd, S.J., Checkley, D.A., Wooster, W.S., 2003. CalCOFI: a half century of physical, chemical, and biological research in the California Current System. Deep Sea Research Part II: Topical Studies in Oceanography 50, 2349–2353. https://doi.org/10.1016/S0967-0645(03)00122-X

Bond, N.A., Cronin, M.F., Freeland, H., Mantua, N., 2015. Causes and impacts of the 2014 warm anomaly in the NE Pacific. Geophys. Res. Lett. 42, 3414–3420. https://doi.org/10.1002/2015GL063306

Brodeur, R., Fisher, J., Emmett, R., Morgan, C., Casillas, E., 2005. Species composition and community structure of pelagic nekton off Oregon and Washington under variable oceanographic conditions. Mar. Ecol. Prog. Ser. 298, 41–57. https://doi.org/10.3354/meps298041

Brodeur, R.D., Fisher, J.P., Teel, D.J., Emmett, R.L., Casillas, E., Miller, T.W., 2004. Juvenile salmonid distribution, growth, condition, origin, and environmental and species associations in the Northern California Current. Fish. Bull. 102, 25–46.

Brodeur, R.D., Pearcy, W.G., 1990. Trophic Relations of Juvenile Pacific Salmon off the Oregon and Washington Coast. Fish. Bull. 88, 617–636.

Brotz, L., Cheung, W.W.L., Kleisner, K., Pakhomov, E., Pauly, D., 2012. Increasing jellyfish populations: trends in Large Marine Ecosystems. Hydrobiologia 690, 3–20. https://doi.org/10.1007/s10750-012-1039-7

Cavole, L.M., Demko, A.M., Diner, R.E., Giddings, A., Koester, I., Pagniello, C.M.L.S., Paulsen, M.-L., Ramirez-Valdez, A., Schwenck, S.M., Yen, N.K., Zill, M.E., Franks, P.J.S., 2016. Biological Impacts of the 2013–2015 Warm-Water Anomaly in the Northeast Pacific. Oceanography 29, 273–285.

Checkley, D.M., Barth, J.A., 2009. Patterns and processes in the California Current System. Progress in Oceanography 83, 49–64. https://doi.org/10.1016/j.pocean.2009.07.028

Clarke, K.R., Warwick, R.M., 2001. Change in marine communities: An approach to statistical analysis and interpretation, 2nd ed. Primer-E, Ltd., Plymouth, UK.

Daly, E.A., Brodeur, R.D., Weitkamp, L.A., 2009. Ontogenetic Shifts in Diets of Juvenile and Subadult Coho and Chinook Salmon in Coastal Marine Waters: Important for Marine Survival? Transactions of the American Fisheries Society 138, 1420–1438. https://doi.org/10.1577/T08-226.1

Di Lorenzo, E., Mantua, N., 2016. Multi-year persistence of the 2014/15 North Pacific marine heatwave. Nature Climate Change 6, 1042.

Dorman, J., Sydeman, W., García-Reyes, M., Zeno, R., Santora, J., 2015. Modeling krill aggregations in the central-northern California Current. Mar. Ecol. Prog. Ser. 528, 87–99. https://doi.org/10.3354/meps11253

Ebert, T.A., Russell, M.P., 1988. Latitudinal variation in size structure of the west coast purple sea urchin: A correlation with headlands. Limnol. Oceanogr. 33, 286–294. https://doi.org/10.4319/lo.1988.33.2.0286

Emmett, R.L., Brodeur, R.D., Orton, P.M., 2004. The vertical distribution of juvenile salmon (Oncorhynchus spp.) and associated fishes in the Columbia River plume. Fisheries Oceanography 13, 392–402.

Emmett, R.L., Krutzikowsky, G.K., Bentley, P., 2006. Abundance and distribution of pelagic piscivorous fishes in the Columbia River plume during spring/early summer 1998–2003: Relationship to oceanographic conditions, forage fishes, and juvenile salmonids. Progress in Oceanography 68, 1–26. https://doi.org/10.1016/j.pocean.2005.08.001

Fiedler, P., 2002. Environmental change in the eastern tropical Pacific Ocean: review of ENSO and decadal variability. Mar. Ecol. Prog. Ser. 244, 265–283. https://doi.org/10.3354/meps244265

Fisher, J.L., Peterson, W.T., Rykaczewski, R.R., 2015. The impact of El Niño events on the pelagic food chain in the northern California Current. Glob. Change Biol. 21, 4401–4414. https://doi.org/10.1111/gcb.13054

Fluharty, D., Cyr, N., 2001. Implementing ecosystem-based management of fisheries in the context of U.S. regional fisheries management: recommendations of the NMFS ecosystem principles advisory panel. CalCOFI Rep. 42, 66–73.

Francis, R.C., Hixon, M.A., Clarke, M.E., Murawski, S.A., Ralston, S., 2007. Ten Commandments for Ecosystem-Based Fisheries Scientists. Fisheries 32, 217–233. https://doi.org/10.1577/1548-8446(2007)32[217:TCFBFS]2.0.CO;2

Gentemann, C.L., Fewings, M.R., García-Reyes, M., 2017. Satellite sea surface temperatures along the West Coast of the United States during the 2014-2016 northeast Pacific marine heat wave: Coastal SSTs During “the Blob.” Geophys. Res. Lett. 44, 312–319. https://doi.org/10.1002/2016GL071039

Goodrich, B., Gabry, J., Ali, I., Brilleman, S., 2018. rstanarm: Bayesian applied regression modeling via Stan. R package version 2.17.4.

Graham, W.M., Field, J.G., Potts, D.C., 1992. Persistent “upwelling shadows” and their influence on zooplankton distributions. Marine Biology 114, 561–570. https://doi.org/10.1007/BF00357253

Graham, W.M., Largier, J.L., 1997. Upwelling shadows as nearshore retention sites: the example of northern Monterey Bay. Continental Shelf Research 17, 509–532. https://doi.org/10.1016/S0278-4343(96)00045-3

Harding, J.A., Ammann, A.J., MacFarlane, R.B., 2011. Regional and seasonal patterns of epipelagic fish assemblages from the central California Current. Fish. Bull. 109, 261–281.

Hassrick, J.L., Henderson, M.J., Huff, D.D., Sydeman, W.J., Sabal, M.C., Harding, J.A., Ammann, A.J., Crandall, E.D., Bjorkstedt, E.P., Garza, J.C., Hayes, S.A., 2016. Early ocean distribution of juvenile Chinook salmon in an upwelling ecosystem. Fish. Oceanogr. 25, 133–146. https://doi.org/10.1111/fog.12141

Hayward, T.L., Mantyla, A.W., 1990. Physical, chemical and biological structure of a coastal eddy near Cape Mendocino. J. Mar. Res. 48, 825–850. https://doi.org/10.1357/002224090784988683

Hertz, E., Trudel, M., Brodeur, R., Daly, E., Eisner, L., Farley Jr, E., Harding, J., MacFarlane, R., Mazumder, S., Moss, J., Murphy, J., Mazumder, A., 2015. Continental-scale variability in the feeding ecology of juvenile Chinook salmon along the coastal Northeast Pacific Ocean. Mar. Ecol. Prog. Ser. 537, 247–263. https://doi.org/10.3354/meps11440

Hickey, Barbara, 1998. Coastal oceanography of western North America from the tip of Baja California to Vancouver Island, in: Robinson, A., Brink, K. (Eds.), The Global Coastal Ocean: Regional Studies and Syntheses, The Sea: Ideas and Observations in the Study of the Seas. Wiley & Sons, pp. 345–393.

Huyer, A., 1983. Coastal upwelling in the California current system. Progress in Oceanography 12, 259–284. https://doi.org/10.1016/0079-6611(83)90010-1

Jacobson, K., Peterson, B., Trudel, M., Ferguson, J., Morgan, C., Welch, D., Baptista, A., Beckman, B., Brodeur, R., Casillas, E., Emmett, R., Miller, J., Teel, D., Wainwright, T., Weitkamp, L., Zamon, J., Fresh, K., 2012(a). The Marine Ecology of Juvenile Columbia River Basin Salmonids: A Synthesis of Research 1998-2011.

Jacobson, K., Baldwin, R., Reese, D., 2012(b). Parasite communities indicate effects of cross-shelf distributions, but not mesoscale oceanographic features on northern California Current mid-trophic food web. Mar. Ecol. Prog. Ser. 454, 19–36. https://doi.org/10.3354/meps09654

Kaplan, D.M., Largier, J., 2006. HF radar-derived origin and destination of surface waters off Bodega Bay, California. Deep Sea Research Part II: Topical Studies in Oceanography 53, 2906–2930. https://doi.org/10.1016/j.dsr2.2006.07.012

Karl, H.A., Chin, J.L., Ueber, E., Stauffer, P.H., Hendley II, J.W. (Eds.), 2001. Beyond the Golden Gate — Oceanography, Geology, Biology, and Environmental Issues in the Gulf of the Farallones. U.S. Department of the Interior, U.S. Geological Survey.

Keister, J.E., Cowles, T.J., Peterson, W.T., Morgan, C.A., 2009. Do upwelling filaments result in predictable biological distributions in coastal upwelling ecosystems? Progress in Oceanography 83, 303–313. https://doi.org/10.1016/j.pocean.2009.07.042

Kelly, K.A., 1985. The influence of winds and topography on the sea surface temperature patterns over the northern California slope. J. Geophys. Res. 90, 11783. https://doi.org/10.1029/JC090iC06p11783

Koslow, J.A., Couture, J., 2015. Pacific Ocean observation programs: Gaps in ecological time series. Marine Policy 51, 408–414. https://doi.org/10.1016/j.marpol.2014.09.003

Koslow, J.A., Goericke, R., Watson, W., 2013. Fish assemblages in the Southern California Current: relationships with climate, 1951-2008. Fish. Oceanogr. 22, 207–219. https://doi.org/10.1111/fog.12018

Krutzikowsky, G.K., Emmett, R.L., 2005. Diel differences in surface trawl fish catches off Oregon and Washington. Fisheries Research 71, 365–371. https://doi.org/10.1016/j.fishres.2004.08.037

Largier, J., 2004. The importance of retention zones in the dispersal of larvae. American Fisheries Society Symposium 42, 105–122.

Leising, A.W., Schroeder, I.D., Bograd, S.J., and others. 2015. State of the California Current 2014-15: Impacts of the warm-water “blob.” CalCOFI Rep. 56, 31–68.

Leising, A.W., Schroeder, I.D., Bograd, S.J., and others. 2014. State of the California Current 2013-2014: El Niño looming. CalCOFI Rep. 55, 51–87.

Litz, M.N.C., Emmett, R.L., Bentley, P.J., Claiborne, A.M., Barceló, C., 2014. Biotic and abiotic factors influencing forage fish and pelagic nekton community in the Columbia River plume (USA) throughout the upwelling season 1999–2009. ICES Journal of Marine Science 71, 5–18. https://doi.org/10.1093/icesjms/fst082

Mace, A., Morgan, S., 2006. Larval accumulation in the lee of a small headland: implications for the design of marine reserves. Mar. Ecol. Prog. Ser. 318, 19–29. https://doi.org/10.3354/meps318019

MacFarlane, R.B., 2010. Energy dynamics and growth of Chinook salmon (Oncorhynchus tshawytscha) from the Central Valley of California during the estuarine phase and first ocean year. Can. J. Fish. Aquat. Sci. 67, 1549–1565. https://doi.org/10.1139/F10-080

MacFarlane, R.B., Norton, E.C., 2002. Physiological ecology of juvenile chinook salmon (Oncorhynchus tshawytscha) at the southern end of their distribution, the San Francisco Estuary and Gulf of the Farallones, California. Fish. Bull. 100, 244–257.

MacFarlane, R.B., Ralston, S., Royer, C., Norton, E.C., 2005. Juvenile chinook salmon (Oncorhynchus tshawytscha) growth on the central California coast during the 1998 El Niño and 1999 La Niña. Fisheries Oceanogr. 14, 321–332. https://doi.org/10.1111/j.1365-2419.2005.00338.x

Mackas, D.L., Beaugrand, G., 2010. Comparisons of zooplankton time series. Journal of Marine Systems 79, 286–304. https://doi.org/10.1016/j.jmarsys.2008.11.030

Mais, K.F., 1974. Pelagic fish surveys in the California Current. Fish Bulletin, California Dept Fish and Game, Fish Bulletin 162, 79 pp.

McClatchie, S., 2014. Regional Fisheries Oceanography of the California Current System. Springer Netherlands, Dordrecht. https://doi.org/10.1007/978-94-007-7223-6

McClatchie, S., Goericke, R., Leising, A., and others. 2016. State of the California Current 2015-16: Comparisons with the 1997-98 El Niño. CalCOFI Rep. 57, 5–61.

Mills, C.E., 2001. Jellyfish blooms: are populations increasing globally in response to changing ocean conditions? Hydrobiologia 451, 55–68. https://doi.org/10.1023/A:1011888006302

Morgan, C., Peterson, W., Emmett, R., 2003. Onshore-offshore variations in copepod community structure off the Oregon coast during the summer upwelling season. Mar. Ecol. Prog. Ser. 249, 223–236. https://doi.org/10.3354/meps249223

Morgan, C.A., Beckman, B.R., Weitkamp, L.A., Fresh, K.L., 2019. Recent Ecosystem Disturbance in the Northern California Current. Fisheries 44, 465–474. https://doi.org/10.1002/fsh.10273

Morgan, C.A., Zamon, J.E., Bucher, C.A., 2015. Cruise Report 15-02. https://www.cbfish.org/Document.mvc/Viewer/P147258

National Research Council, Committee on Endangered and Threatened Fishes in the Klamath River Basin, 2004. Endangered and threatened fishes in the Klamath River Basin. The National Academies Press, Washington, DC.

Nelson, C., 1977. Wind stress and wind stress curl over the California Current. NOAA Technical Report NMFS SSRF-714.

Pacific Fishery Management Council, 2006. Preseason Report III: Analysis of Council Adopted Management Measures for 2006 Ocean Salmon Fisheries.

Paduan, J.D., Rosenfeld, L.K., 1996. Remotely sensed surface currents in Monterey Bay from shore-based HF radar (Coastal Ocean Dynamics Application Radar). J. Geophys. Res. 101, 20669–20686. https://doi.org/10.1029/96JC01663

Papastephanou, K.M., Bollens, S.M., Slaughter, A.M., 2006. Cross-shelf distribution of copepods and the role of event-scale winds in a northern California upwelling zone. Deep Sea Research Part II: Topical Studies in Oceanography 53, 3078–3098. https://doi.org/10.1016/j.dsr2.2006.07.014

Pearcy, W.G., 2002. Marine nekton off Oregon and the 1997–98 El Niño. Progress in Oceanography 54, 399–403. https://doi.org/10.1016/S0079-6611(02)00060-5

Pearcy, W.G., Fisher, J.P., Anma, G., Meguro, T., 1996. Species associations of epipelagic nekton of the North Pacific Ocean, 1978–1993. Fisheries Oceanogr. 5, 1–20. https://doi.org/10.1111/j.1365-2419.1996.tb00013.x

Pearcy, W.G., McKinnell, S.M., 2007. The ocean ecology of salmon in the Northeast Pacific Ocean: An abridged history. American Fisheries Society Symposium 57, 7–30.

Peterson, W.T., Fisher, J.L., Strub, P.T., Du, X., Risien, C., Peterson, J., Shaw, C.T., 2017. The pelagic ecosystem in the Northern California Current off Oregon during the 2014-2016 warm anomalies within the context of the past 20 years. J. Geophys. Res. Oceans 122, 7267–7290. https://doi.org/10.1002/2017JC012952

Peterson, W.T., Keister, J.E., 2002. The effect of a large cape on distribution patterns of coastal and oceanic copepods off Oregon and northern California during the 1998–1999 El Niño–La Niña. Progress in Oceanography 53, 389–411. https://doi.org/10.1016/S0079-6611(02)00038-1

Peterson, W.T., Keister, J.E., Feinberg, L.R., 2002. The effects of the 1997–99 El Niño/La Niña events on hydrography and zooplankton off the central Oregon coast. Progress in Oceanography 54, 381–398. https://doi.org/10.1016/S0079-6611(02)00059-9

Peterson, W.T., Miller, C.B., 1977. Seasonal cycle of zooplankton abundance and species composition along the central Oregon coast. Fish. Bull. 75.

Peterson, W.T., Morgan, C.A., Fisher, J.P., Casillas, E., 2010. Ocean distribution and habitat associations of yearling coho (Oncorhynchus kisutch) and Chinook (O. tshawytscha) salmon in the northern California Current: Ocean distribution of juvenile salmonids. Fisheries Oceanography 19, 508–525. https://doi.org/10.1111/j.1365-2419.2010.00560.x

Phillips, A.J., Brodeur, R.D., Suntsov, A.V., 2009. Micronekton community structure in the epipelagic zone of the northern California Current upwelling system. Progress in Oceanography 80, 74–92. https://doi.org/10.1016/j.pocean.2008.12.001

Pool, S.S., Reese, D.C., Brodeur, R.D., 2012. Defining marine habitat of juvenile Chinook salmon, Oncorhynchus tshawytscha, and coho salmon, O. kisutch, in the northern California Current System. Env. Biol. Fish 93, 233–243. https://doi.org/10.1007/s10641-011-9909-9

Purcell, J.E., 2012. Jellyfish and Ctenophore Blooms Coincide with Human Proliferations and Environmental Perturbations. Ann. Rev. Mar. Sci. 4, 209–235. https://doi.org/10.1146/annurev-marine-120709-142751

Ralston, S., Field, J.C., Sakuma, K.M., 2015. Long-term variation in a central California pelagic forage assemblage. Journal of Marine Systems 146, 26–37. https://doi.org/10.1016/j.jmarsys.2014.06.013

Ralston, S., Sakuma, K.M., Field, J.C., 2013. Interannual variation in pelagic juvenile rockfish (Sebastes spp.) abundance - going with the flow. Fish. Oceanogr. 22, 288–308. https://doi.org/10.1111/fog.12022

Reese, D.C., Brodeur, R.D., 2015. Species associations and redundancy in relation to biological hotspots within the northern California Current ecosystem. Journal of Marine Systems 146, 3–16. https://doi.org/10.1016/j.jmarsys.2014.10.009

Reese, D.C., Brodeur, R.D., 2006. Identifying and characterizing biological hotspots in the northern California Current. Deep Sea Research Part II: Topical Studies in Oceanography 53, 291–314. https://doi.org/10.1016/j.dsr2.2006.01.014

Reese, D.C., Miller, T.W., Brodeur, R.D., 2005. Community structure of near-surface zooplankton in the northern California Current in relation to oceanographic conditions. Deep Sea Research Part II: Topical Studies in Oceanography 52, 29–50. https://doi.org/10.1016/j.dsr2.2004.09.027

Richardson, A.J., Bakun, A., Hays, G.C., Gibbons, M.J., 2009. The jellyfish joyride: causes, consequences and management responses to a more gelatinous future. Trends in Ecology & Evolution 24, 312–322. https://doi.org/10.1016/j.tree.2009.01.010

Robinson, K., Ruzicka, J., Decker, M.B., Brodeur, R., Hernandez, F., Quiñones, J., Acha, M., Uye, S., Mianzan, H., Graham, W., 2014. Jellyfish, Forage Fish, and the World's Major Fisheries. Oceanography 27, 104–115. https://doi.org/10.5670/oceanog.2014.90

Ruzicka, J.J., Daly, E.A., Brodeur, R.D., 2016. Evidence that summer jellyfish blooms impact Pacific Northwest salmon production. Ecosphere 7, e01324. https://doi.org/10.1002/ecs2.1324

Sakuma, K.M., Field, J.C., Mantua, N.J., Ralston, S., Marinovic, B.B., Carrion, C.N., 2016. Anomalous epipelagic micronekton assemblage patterns in the neritic waters of the California Current in spring 2015 during a period of extreme ocean conditions. CalCOFI Rep. 57, 163–183.

Samhouri, J.F., Levin, P.S., Harvey, C.J., 2009. Quantitative Evaluation of Marine Ecosystem Indicator Performance Using Food Web Models. Ecosystems 12, 1283–1298. https://doi.org/10.1007/s10021-009-9286-9

Santora, J., Hazen, E., Schroeder, I., Bograd, S., Sakuma, K., Field, J., 2017. Impacts of ocean climate variability on biodiversity of pelagic forage species in an upwelling ecosystem. Mar. Ecol. Prog. Ser. 580, 205–220. https://doi.org/10.3354/meps12278

Sanz-Martín, M., Pitt, K.A., Condon, R.H., Lucas, C.H., Novaes de Santana, C., Duarte, C.M., 2016. Flawed citation practices facilitate the unsubstantiated perception of a global trend toward increased jellyfish blooms: Flawed citation practices in jellyfish population trends. Global Ecol. Biogeogr. 25, 1039–1049. https://doi.org/10.1111/geb.12474

Schwing, F.B., Husby, D.M., Garfield, N., Tracy, D.E., 1991. Mesoscale oceanic response to wind events off central California during spring 1989: CTD surveys and AVHRR imagery. CalCOFI Rep. 32, 47–62.

Schwing, F.B., Mendelssohn, R., Bograd, S.J., Overland, J.E., Wang, M., Ito, S., 2010. Climate change, teleconnection patterns, and regional processes forcing marine populations in the Pacific. Journal of Marine Systems 79, 245–257. https://doi.org/10.1016/j.jmarsys.2008.11.027

Send, U., Beardsley, R.C., Winant, C.D., 1987. Relaxation from upwelling in the Coastal Ocean Dynamics Experiment. J. Geophys. Res. 92, 1683. https://doi.org/10.1029/JC092iC02p01683

Steger, J.M., Schwing, F.B., Collins, C.A., Rosenfeld, L.K., Garfield, N., Gezgin, E., 2000. The circulation and water masses in the Gulf of the Farallones. Deep Sea Research Part II: Topical Studies in Oceanography 47, 907–946. https://doi.org/10.1016/S0967-0645(99)00131-9

Suchman, C., Daly, E., Keister, J., Peterson, W., Brodeur, R., 2008. Feeding patterns and predation potential of scyphomedusae in a highly productive upwelling region. Mar. Ecol. Prog. Ser. 358, 161–172. https://doi.org/10.3354/meps07313

Suchman, C.L., Brodeur, R.D., 2005. Abundance and distribution of large medusae in surface waters of the northern California Current. Deep Sea Research Part II: Topical Studies in Oceanography 52, 51–72. https://doi.org/10.1016/j.dsr2.2004.09.017

Suchman, C.L., Brodeur, R.D., Daly, E.A., Emmett, R.L., 2012. Large medusae in surface waters of the Northern California Current: variability in relation to environmental conditions, in: Purcell, J., Mianzan, H., Frost, J.R. (Eds.), Jellyfish Blooms IV. Springer Netherlands, Dordrecht, pp. 113–125. https://doi.org/10.1007/978-94-007-5316-7_9

Thompson, A., Auth, T., Brodeur, R., Bowlin, N., Watson, W., 2014. Dynamics of larval fish assemblages in the California Current System: a comparative study between Oregon and southern California. Mar. Ecol. Prog. Ser. 506, 193–212. https://doi.org/10.3354/meps10801

Vander Woude, A.J., Largier, J.L., Kudela, R.M., 2006. Nearshore retention of upwelled waters north and south of Point Reyes (northern California)—Patterns of surface temperature and chlorophyll observed in CoOP WEST. Deep Sea Research Part II: Topical Studies in Oceanography 53, 2985–2998. https://doi.org/10.1016/j.dsr2.2006.07.003

Vehtari, A., Gelman, A., Gabry, J., 2017. Practical Bayesian model evaluation using leave-one-out cross-validation and WAIC. Stat. Comput. 27, 1413–1432. https://doi.org/10.1007/s11222-016-9696-4

Wainwright, T.C., Emmett, R.L., Weitkamp, L.A., Hayes, S.A., Bentley, P.J., Harding, J.A., 2019. Effect of a Mammal Excluder Device on Trawl Catches of Salmon and Other Pelagic Animals. Mar. Coast. Fish. 11, 17–31. https://doi.org/10.1002/mcf2.10057

Wells, B., Santora, J., Field, J., MacFarlane, R., Marinovic, B., Sydeman, W., 2012. Population dynamics of Chinook salmon Oncorhynchus tshawytscha relative to prey availability in the central California coastal region. Mar. Ecol. Prog. Ser. 457, 125–137. https://doi.org/10.3354/meps09727

Wells, B.K., Schroeder, I.D., Santora, J.A., and others. 2013. State of the California Current 2012-13: No such thing as an “average” year. CalCOFI Rep. 54, 37–71.

Wilkerson, F.P., Dugdale, R.C., Marchi, A., Collins, C.A., 2002. Hydrography, nutrients and chlorophyll during El Niño and La Niña 1997–99 winters in the Gulf of the Farallones, California. Progress in Oceanography 54, 293–310. https://doi.org/10.1016/S0079-6611(02)00055-1

Wing, S.R., Botsford, L.W., Ralston, S.V., Largier, J.L., 1998. Meroplanktonic distribution and circulation in a coastal retention zone of the northern California upwelling system. Limnol. Oceanogr. 43, 1710–1721. https://doi.org/10.4319/lo.1998.43.7.1710

Wolter, K., Timlin, M.S., 1993. Monitoring ENSO in COADS with a seasonally adjusted principal component index. Proceedings of the 17th Climate Diagnostics Workshop, Norman, OK 52–57.

Zwolinski, J., Demer, D., Cutter, G., Stierhoff, K., Macewicz, B., 2014. Building on Fisheries Acoustics for Marine Ecosystem Surveys. Oceanography 27, 68–79. https://doi.org/10.5670/oceanog.2014.87

Zwolinski, J.P., Demer, D.A., Byers, K.A., Cutter, G.R., Renfree, J.S., Sessions, T.S., Macewicz, B.J., 2012. Distributions and abundances of Pacific sardine (Sardinops sagax) and other pelagic fishes in the California Current Ecosystem during spring 2006, 2008, and 2010, estimated from acoustic–trawl surveys. Fish. Bull. 110, 110–122.

Zwolinski, J.P., Stierhoff, K.L., Demer, D.A., 2019. Distribution, biomass, and demography of coastal pelagic fishes in the California Current Ecosystem during summer 2017 based on acoustic-trawl sampling. NOAA Technical Memorandum NMFS NOAA-TM-NMFS-SWFSC-610, 74. https://doi.org/10.25923/Y0YF-9156

Table 1. Summary of operations showing date range of survey and number of samples obtained during FED summer and fall salmon surveys 2010-15.

cruise	ship	start date	end date	lines	stations	NRT	CTD	bongo	vertical	birds
summer										
FR1001	F/V Frosti	7/1/10	7/13/10	13	61	60	62	62	62	13
FR1101	F/V Frosti	6/30/11	7/15/11	16	78	68	78	77	77	16
OS1201	R/V Ocean Starr	6/11/12	6/25/12	15	59	53	57	48	47	13
OS1301	R/V Ocean Starr	7/9/13	7/23/13	14	57	54	57	56	57	12
OS1401	R/V Ocean Starr	7/6/14	7/22/14	15	70	68	69	68	68	13
OS1501	R/V Ocean Starr	6/18/15	7/2/15	14	39	63	51	37	39	6
fall										
FR1102	F/V Frosti	9/7/11	9/16/11	11	53	34	54	54	54	9
BS1301	R/V Bell Shimada	9/11/13	9/15/13	5	23	23	23	0	23	0
OS1503	R/V Ocean Starr	8/30/15	9/14/15	10	19	39	28	0	19	0

Table 2. Transect lines and sampling stations for FED summer salmon surveys 2010-15. Operations at each station usually included deployment of a CTD, surface rope trawl, bongo net, and vertical net. Completed trawls are indicated by a number in the column under sample year (numbers >1 indicate replicate trawl samples obtained), and blank cells indicate no trawl completed (although other sample types may have been obtained).

Line	Station	Shelf Pos'n	LAT DEG	LAT D-MIN	LON DEG	LON D-MIN	Chart Depth (m)	Offshore (km)	2010	2011	2012	2013	2014	2015
Heceta Head (HH)	HH01	1	44	00.00	124	10.25	30	2.6	1	1	1	1	1	1
	HH02	2	44	00.00	124	12.70	55	5.9	1	1	1	1	1	1
	HH03	3	44	00.00	124	16.50	80	10.9	1	1	1	1	1	3
	HH04	4	44	00.00	124	23.40	117	20.2	1	1	1	1	1	
	HH05	5	44	00.00	124	30.40	133	29.4	1	1				
Five Mile (FM)	FM01	1	43	13.00	124	26.00	30	3.0	1	1	1	1	1	3
	FM02	2	43	13.00	124	28.40	55	6.1	1	1	1	1	1	1
	FM03	3	43	13.00	124	33.80	73	13.3	1	1	1	1	1	1
	FM04	4	43	13.00	124	39.30	137	20.7	1	1	1	1		
	FM05	5	43	13.00	124	46.20	340	30.0	1	1	1			
Rogue River (RR)	RR01	1	42	30.00	124	29.50	32	5.6	1	1	1			1
	RR02	2	42	30.00	124	32.50	57	9.6	1	1	1			1
	RR03	3	42	30.00	124	36.00	82	14.4	1	1	1			
	RR04	4	42	30.00	124	41.80	118	22.4	1	1				
	RR05	5	42	30.00	124	48.60	600	31.7	1	1				
Smith River (SR)	SR01	1	41	54.00	124	16.30	30	5.4	1	1	1	1	1	1
	SR02	2	41	54.00	124	21.25	55	12.2	1	1	1	1	1	1
	SR03	3	41	54.00	124	26.70	91	19.6	1	1	1	1	1	3
	SR04	4	41	54.00	124	33.40	400	28.9		1		1	1	
	SR05	5	41	54.00	124	40.10	680	38.1		1			1	
Klamath River (KR)	KR01	1	41	35.00	124	09.50	30	5.0	1	1	1	1	1	1
	KR02	2	41	35.00	124	15.20	51	13.0	1	1	1	1	1	1
	KR03	3	41	35.00	124	20.60	82	20.4		1	1	1	1	3
	KR04	4	41	35.00	124	26.50	137	28.5		1		1	1	
	KR05	5	41	35.00	124	33.20	647	37.8					1	
Mussel Point (MP)	MP01	1	41	21.00	124	08.50	30	5.4		1	1	1	1	1
	MP02	2	41	21.00	124	12.00	55	10.2		1	1	1	1	3
	MP03	3	41	21.00	124	16.60	83	16.5		1	1	1	1	1
	MP04	4	41	21.00	124	21.90	110	23.9		1		1	1	
	MP05	5	41	21.00	124	28.60	250	33.1				1	1	
Trinidad Head (TD)	TD01	1	41	03.50	124	11.40	32	3.1	1	1	1	1	1	3
	TD02	2	41	03.50	124	14.10	52	6.9	1	1	1	1	1	1
	TD03	3	41	03.50	124	16.70	87	10.6	1	1	1	1	1	1
	TD04	4	41	03.50	124	23.30	260	19.8	1	1	1	1	1	
	TD05	5	41	03.50	124	29.90	650	29.1	1				1	
Eel River (ER)	ER01	1	40	38.00	124	23.60	30	6.3	1	1	1	1	1	3
	ER02	2	40	38.00	124	26.80	55	10.7	1	1	1	1	1	1
	ER03	3	40	38.00	124	30.80	700	16.3	1	1	1	1	1	1
	ER04	4	40	38.00	124	37.40	700	25.6	1	1	1		1	
	ER05	5	40	38.00	124	44.00	1000	34.8	1	1	1			
Big Flat (BF)	PG01	1	40	13.90	124	21.20	30	2.4						1
	PG02	2	40	13.45	124	22.75	56	5.0						3
	BF01	1	40	08.00	124	12.90	30	2.0				1	1	
	BF02	2	40	08.00	124	14.00	55	3.5			1	1	1	
	BF03	3	40	08.00	124	15.20	91	5.2				1	1	
	BF04	4	40	08.00	124	21.70	400	14.4				1	1	
	BF05	5	40	08.00	124	28.25	600	23.7				1	1	
	PD01	1	40	02.00	124	06.50	31	2.4	1	1	1			
	PD02	2	40	02.00	124	07.70	54	4.1	1	1				
	PD03	3	40	02.00	124	11.60	540	9.6	1	1				
	PD04	4	40	02.00	124	18.00	540	18.7	1					
	PD05	5	40	02.00	124	24.40	810	27.8	1					
Albion River (AR)	AR01	1	39	15.00	123	48.20	59	1.5	1	1		1	1	3
	AR02	2	39	15.00	123	49.75	92	3.7	1	1		1	1	1
	AR03	3	39	15.00	123	53.60	130	9.3	1	1		1	1	1
	AR04	4	39	15.00	124	00.00	420	18.5	1	1		1	1	
	AR05	5	39	15.00	124	06.50	720	27.8	1				1	
Gualala Point (GP)	GP01	1	38	45.00	123	32.70	35	1.7	1	1	1	1	1	1
	GP02	2	38	45.00	123	34.10	55	3.7	1	1	1	1	1	3
	GP03	3	38	45.00	123	37.30	87	8.3	1	1	1		1	1
	GP04	4	38	45.00	123	43.70	126	17.6	1	1	1		1	
	GP05	5	38	45.00	123	50.10	300	26.9	1	1	1		1	

Line	Station	Shelf Pos'n	LAT DEG	LAT D-MIN	LON DEG	LON D-MIN	Chart Depth (m)	Offshore (km)	2010	2011	2012	2013	2014	2015
Fort Ross (FR)	FR01	1	38	30.00	123	14.80	39	2.2	1	1	1	1	1	1
	FR02	2	38	30.00	123	15.60	55	3.3	1	1	1	1	1	3
	FR03	3	38	30.00	123	18.50	81	7.6	1	1	1	1	1	1
	FR04	4	38	30.00	123	24.90	112	16.9	1	1	1	1	1	
	FR05	5	38	30.00	123	33.80	164	29.8	1	1	1		1	
Tomales Bay (TB)	TB01	1	38	08.00	122	58.30	30	1.5				1		1
	TB02	2	38	08.00	123	00.40	58	4.6				1	1	3
	TB03	3	38	08.00	123	06.75	76	13.9		1		1	1	1
	TB04	4	38	08.00	123	13.20	108	23.1		1		1	1	
	TB05	5	38	08.00	123	19.60	141	32.4		1			1	
Gulf Farallones (GF)	GF01	1	37	50.50	122	41.70	28	12.2	1	1	1	1	1	1
	GF02	2	37	50.50	122	48.00	46	21.5	1	1	1	1	1	1
	GF03	3	37	50.50	123	01.50	80	41.1	1	1	1	1	1	
	GF04	4	37	50.50	123	11.60	85	55.9	1	1	1	1	1	
	GF05	5	37	50.50	123	23.00	190	72.6	1	1				
Pillar Point (PP)	PP01	1	37	30.00	122	31.60	32	2.2	1					
	PP02	2	37	30.00	122	36.40	56	9.3	1		1		1	
	PP03	3	37	30.00	122	45.50	80	22.6	1		1	1	1	
	PP04	4	37	30.00	122	54.30	110	35.6	1	1	1	1	1	
	PP05	5	37	30.00	123	00.60	400	44.8	1	1	1	1	1	
Pigeon Point (PI)	PI01	1	37	10.00	122	24.20	34	3.7			1		1	
	PI02	2	37	10.00	122	26.15	55	6.5		1	1		1	
	PI03	3	37	10.00	122	30.00	83	12.2		1	1		1	
	PI04	4	37	10.00	122	38.30	107	24.4		1			1	
	PI05	5	37	10.00	122	44.60	200	33.7		1			1	

Table 3: Water property variables measured in association with trawl samples on summer surveys 2010-15. BucTemp and Secchi were measured directly at the water surface, and the remaining variables were measured by instruments on the CTD package with values averaged for all reading between 3-20m of water depth.

Variable	*Abbreviation*	*Units*	*Sample Location*
Bucket Temperature	BucTemp	degrees Celsius, ^{o}C	surface
CTD Temperature	Temp	degrees Celsius, ^{o}C	3-20m average
Salinity	Sal	psu	3-20m average
Secchi disk depth	Secchi	meters, m	surface
Transmissivity	Trans	% transmission	3-20m average
Chlorophyll-a	Chl	mg/m^3	3-20m average
Photosynthetically Active Radiation	PAR	µE/m^2	3-20m average

Table 4. Sequential test result of distance-based linear model (DISTLM) to measure the effect of four space-time variables (predictor set) on a group of six water property variables (response set) measured at 358 CTD casts during the period 2010-15. Year was coded as binary data and treated as a categorical variable. Variables are shown in order of decreasing proportion of total variance explained by the model (*Prop.var.*); all variables significant at p=0.001.

Group	*Adj R^2*	*Pseudo-F*	*Prop.var.*	*P*
+ Year	0.234	22.83	0.245	0.001
+ Latitude	0.313	41.38	0.080	0.001
+ Bottom Dep	0.368	31.51	0.056	0.001
+ Distance	0.379	7.26	0.013	0.001

Table 5. Summary of fish and invertebrate species or broader taxa captured by surface trawl during FED summer salmon surveys 2010-15. CPUE is the number of individuals per $10^6 m^3$ trawled; ΣCPUE is the sum of all CPUE values for each taxa for an entire cruise. Frequency of occurrence, FO, is the number of hauls in which one or more individuals of each species or taxa was observed; %FO is the percentage of that number among all hauls conducted. Forty-two fish and 15 invertebrate species/taxa were observed in >1 haul and shown here.

		2010		2011		2012		2013		2014		2015		total	*grand*
common name	***Genus species***	**ΣCPUE**	***%FO***	**ΣCPUE**	***%FO***	**ΣCPUE**	***%FO***	**ΣCPUE**	***%FO***	**ΣCPUE**	***%FO***	**ΣCPUE**	***%FO***	**CPUE**	***avg %FO***
fish															
Chinook salmon, jv	*Oncorhynchus tshawytscha*	419	*31.7*	621	*33.8*	122	*24.5*	466	*50.0*	152	*30.9*	299	*64.1*	**2079**	***37.4***
Chinook salmon, ad	*Oncorhynchus tshawytscha*	36	*13.3*	521	*52.9*	378	*60.4*	235	*44.4*	37	*20.6*	29	*33.3*	**1236**	***37.1***
rockfish YOY	*Sebastes sp.*	19122	*68.3*	411	*32.4*	3898	*34.0*	642	*18.5*	1.9	*2.9*	73	*53.8*	**24149**	***33.3***
flatfish larvae	flatfish unidentified	396	*28.3*	130	*19.1*	317	*52.8*	27	*18.5*	19	*17.6*	248	*76.9*	**1136**	***32.2***
wolf-eel	*Anarrhichthys ocellatus*	31	*33.3*	10	*17.6*	26	*30.2*	47	*31.5*	18	*19.1*	20	*46.2*	**153**	***28.1***
coho salmon, ad	*Oncorhynchus kisutch*	15	*15.0*	55	*29.4*	18	*15.1*	33	*24.1*	47	*25.0*	8.6	*23.1*	**177**	***22.2***
coho salmon, jv	*Oncorhynchus kisutch*	15	*15.0*	66	*23.5*	82	*11.3*	48	*16.7*	22	*14.7*	28	*30.8*	**262**	***18.1***
medusafish	*Icichthys lockingtoni*	25	*13.3*	16	*7.4*	6.4	*1.9*	12	*18.5*	22	*16.2*	9.9	*25.6*	**92**	***13.2***
lingcod YOY	*Ophiodon elongatus*	456	*18.3*	203	*19.1*	67	*20.8*	0	*0*	0	*0*	7.9	*20.5*	**733**	***12.6***
osmerid larvae	osmerid unidentified	46	*11.7*	1840	*8.8*	189	*28.3*	239	*13.0*	0.9	*1.5*	4.5	*2.6*	**2319**	***10.8***
surf smelt	*Hypomesus pretiosus*	280	*15.0*	406	*7.4*	391	*11.3*	0.9	*1.9*	73	*4.4*	70	*25.6*	**1222**	***9.9***
steelhead, ad	*Oncorhynchus mykiss*	0.8	*1.7*	32	*16.2*	11	*7.5*	44	*18.5*	7.2	*7.4*	3.0	*7.7*	**98**	***9.9***
Pacific herring	*Clupea pallasii*	27	*10.0*	30	*5.9*	138	*9.4*	1350	*11.1*	47	*8.8*	28	*15.4*	**1619**	***9.6***
king-of-the-salmon	*Trachipterus altivelis*	66	*25.0*	8.6	*7.4*	0	*0*	0	*0*	4.1	*7.4*	7.5	*17.9*	**86**	***9.4***
Pacific butterfish	*Peprilus simillimus*	0	*0*	1.5	*2.9*	23	*3.8*	1323	*18.5*	335	*19.1*	2.3	*7.7*	**1685**	***8.8***
jacksmelt	*Atherinopsis californiensis*	15	*3.3*	689	*11.8*	70	*5.7*	139	*11.1*	489	*11.8*	462	*5.1*	**1865**	***8.5***
jack mackerel	*Trachurus symmetricus*	7.6	*3.3*	78	*20.6*	0.9	*1.9*	34	*9.3*	3.5	*4.4*	0.3	*2.6*	**125**	***7.6***
whitebait smelt	*Allosmerus elongatus*	7702	*5.0*	174	*13.2*	111	*5.7*	750	*3.7*	0	*0*	16	*15.4*	**8754**	***6.7***
steelhead, jv	*Oncorhynchus mykiss*	0	*0*	27	*13.2*	22	*11.3*	4.2	*7.4*	0.8	*1.5*	1.0	*2.6*	**55**	***6.1***
anchovy larvae	*Engraulis mordax*	15	*3.3*	0	*0*	0	*0*	0	*0*	0	*0*	297	*33.3*	**312**	***4.4***
sablefish	*Anoplopoma fimbria*	48	*11.7*	3.0	*4.4*	0	*0*	4.6	*3.7*	19	*4.4*	0	*0*	**74**	***4.4***
cabezon YOY	*Scorpaenichthys marmoratus*	8.7	*5.0*	2.9	*5.9*	0	*0*	0	*0*	0	*0*	21	*12.8*	**33**	***3.5***
starry flounder	*Platichthys stellatus*	3.3	*3.3*	5.8	*7.4*	3.5	*5.7*	0	*0*	0	*0*	0.4	*2.6*	**13**	***3.2***
ocean sunfish	*Mola mola*	0	*0*	0	*0*	0	*0*	0	*0*	14	*14.7*	0	*0*	**14**	***2.9***
Pacific tomcod	*Microgadus proximus*	0	*0*	6.5	*2.9*	0.9	*1.9*	10	*5.6*	3.4	*4.4*	0	*0*	**21**	***2.6***
Pacific hake	*Merluccius productus*	6.2	*6.7*	0.7	*1.5*	0.9	*1.9*	0	*0*	2.4	*1.5*	0	*0*	**10**	***2.0***
Pacific electric ray	*Torpedo californica*	0.8	*1.7*	0.8	*1.5*	1.8	*3.8*	1.8	*3.7*	1.4	*1.5*	0	*0*	**6.5**	***2.0***
pink salmon, ad	*Oncorhynchus gorbuscha*	0	*0*	5.1	*8.8*	0	*0*	1.0	*1.9*	0	*0*	0	*0*	**6.1**	***2.0***
northern anchovy	*Engraulis mordax*	14	*6.7*	0	*0*	0	*0*	0	*0*	0	*0*	1.1	*5.1*	**15**	***1.8***
American shad	*Alosa sapidissima*	0.8	*1.7*	8.1	*2.9*	0.9	*1.9*	1.8	*1.9*	0	*0*	3.2	*2.6*	**15**	***1.8***
barracudina	*Lestidium ringens*	21	*6.7*	25	*1.5*	0	*0*	0	*0*	0	*0*	0	*0*	**46**	***1.5***
poacher	family Agonidae	2.3	*3.3*	0.7	*1.5*	0	*0*	1.9	*3.7*	0	*0*	0	*0*	**4.9**	***1.5***

		2010		2011		2012		2013		2014		2015		total	*grand*
common name	***Genus species***	**ΣCPUE**	***%FO***	**ΣCPUE**	***%FO***	**ΣCPUE**	***%FO***	**ΣCPUE**	***%FO***	**ΣCPUE**	***%FO***	**ΣCPUE**	***%FO***	**CPUE**	***avg %FO***
Pacific sardine	*Sardinops sagax*	2.8	*1.7*	83	*1.5*	0	*0*	18	*3.7*	0	*0*	0	*0*	**104**	***1.2***
pipefish	syngnathid unidentified	0	*0*	0	*0*	0	*0*	0	*0*	7.6	*5.9*	0	*0*	**7.6**	***1.2***
Pacific saury	*Cololabis saira*	552	*3.3*	0.7	*1.5*	0	*0*	0	*0*	0	*0*	0	*0*	**552**	***0.9***
chum salmon, jv	*Oncorhynchus keta*	0.8	*1.7*	0	*0*	2.3	*1.9*	0	*0*	0	*0*	13	*2.6*	**16**	***0.9***
white seabass	*Atractoscion nobilis*	0	*0*	0.7	*1.5*	0.8	*1.9*	0	*0*	0	*0*	1.0	*2.6*	**2.5**	***0.9***
Pacific sanddab	*Citharichthys sordidus*	77	*1.7*	0.7	*1.5*	0	*0*	0	*0*	0	*0*	0	*0*	**77**	***0.6***
spiny dogfish shark	*Squalus acanthias*	0	*0*	6.3	*1.5*	0	*0*	20	*1.9*	0	*0*	0	*0*	**27**	***0.6***
Pacific mackerel	*Scomber japonicus*	0	*0*	1.4	*1.5*	0	*0*	0	*0*	0.8	*1.5*	0	*0*	**2.2**	***0.6***
yellowtail rockfish	*Sebastes flavidus*	0	*0*	0	*0*	0	*0*	0	*0*	0.9	*1.5*	0.8	*2.6*	**1.7**	***0.6***
staghorn sculpin	*Leptocottus armatus*	0	*0*	1.5	*2.9*	0	*0*	0	*0*	0	*0*	0	*0*	**1.5**	***0.6***
invertebrates															
market squid	*Doryteuthis opalescens*	38684	*61.7*	125168	*44.1*	206561	*64.2*	73738	*85.2*	118487	*83.8*	107533	*87.2*	**670171**	***69.6***
crystal jellyfish	*Aequorea sp*	36	*3.3*	125	*8.8*	5856	*47.2*	667	*51.9*	5248	*47.1*	16495	*89.7*	**28427**	***37.4***
sea nettle jellyfish	*Chrysaora fuscescens*	15511	*56.7*	7905	*29.4*	16002	*17.0*	5176	*44.4*	5227	*44.1*	1.5	*7.7*	**49821**	***35.1***
moon jellyfish	*Aurelia labiata*	301	*55.0*	35	*11.8*	31	*9.4*	101	*48.1*	90	*36.8*	64	*48.7*	**621**	***33.9***
fried-egg jellyfish	*Phacellophora camtschatica*	1.6	*3.3*	2.6	*4.4*	8.0	*5.7*	25	*25.9*	306	*60.3*	701	*89.7*	**1044**	***28.7***
twin-sailed (bunny) salp	*Thetys vagina*	16	*10.0*	0	*0*	113	*18.9*	1217	*57.4*	52	*23.5*	41	*46.2*	**1439**	***23.7***
glassy nautilus	*Carinaria cristata*	65	*25.0*	14	*7.4*	3.6	*1.9*	9.9	*13.0*	55	*11.8*	1.3	*5.1*	**148**	***11.1***
bell jellyfish	*Scrippsia/Polyorchis sp*	5.4	*5.0*	26	*7.4*	3.4	*1.9*	5.2	*3.7*	5.7	*4.4*	93	*12.8*	**138**	***5.6***
Pegea salp	*Pegea confoederata*	0	*0*	29	*2.9*	6.2	*1.9*	11	*7.4*	19	*7.4*	0	*0*	**66**	***3.5***
salp, unid	salp unidentified	2.3	*5.0*	0	*0*	29	*9.4*	20	*3.7*	0	*0*	0	*0*	**52**	***2.9***
comb jellyfish	*Beroe sp*	0	*0*	0	*0*	15	*7.5*	92	*9.3*	0	*0*	0	*0*	**107**	***2.6***
octopus, unid		0	*0*	0	*0*	0.9	*1.9*	0.9	*1.9*	6.3	*4.4*	0	*0*	**8.0**	***1.5***
pyrosome	*Pyrosoma atlanticum*	0	*0*	0	*0*	0	*0*	0	*0*	19	*4.4*	0.7	*2.6*	**19**	***1.2***
lion's mane jellyfish	*Cyanea capillata*	2.8	*1.7*	0	*0*	0	*0*	1.9	*3.7*	0	*0*	0.3	*2.6*	**5.0**	***1.2***
purple-striped jellyfish	*Pelagia colorata*	0.8	*1.7*	0	*0*	0	*0*	0	*0*	3.9	*2.9*	0	*0*	**4.7**	***0.9***

Table 6. Sample size (number of tows) by year and 1-degree latitude bin.

N. Latitude	2010	2011	2012	2013	2014	2015	Total
43-44	10	10	9	8	7	6	50
42-43	5	5	3	0	0	2	15
41-42	10	17	11	17	20	12	87
40-41	10	8	6	8	8	5	45
39-40	5	4	0	4	5	3	21
38-39	10	13	10	10	14	9	66
37-38	5	5	4	4	4	2	24
Total	55	62	43	51	58	39	308

Table 7. Model selection results for alternative linear predictors ('Formula') in the negative binomial regression for juvenile Chinook CPUE. Pairwise differences in the expected log pointwise predictive densities (elpd_diff) are relative to the best-fit model (row 1, elpd_diff = 0). Standard errors of the pairwise differences (se_diff) and the ratio of each difference to its standard error (elpd_diff / se_diff) are included to characterize uncertainty in measures of predictive performance. Models with ratios having an absolute value less than 2 are considered to have predictive performance similar to the best-fit model.

Model Number	Formula	elpd_diff	se_diff	elpd_diff / se_diff
1	Lat + Dep + Trans + (1 | Year:Lat)	0	0	--
2	Lat + Dep + Trans + Temp + (1 | Year:Lat)	-1.2	1.5	-0.80
3	Lat + Dep + Trans + Temp + Sal + (1 | Year:Lat)	-1.4	1.5	-0.93
4	Lat + Dep + Chl + (1 | Year:Lat)	-5.1	5.0	-1.02
5	Lat + Dep + Temp + (1 | Year:Lat)	-11.9	7.2	-1.65
6	Lat + Trans + (1 | Year:Lat)	-13.0	5.6	-2.32
7	Lat + Dep + (1 | Year:Lat)	-13.9	8.2	-1.70
8	Lat + Dep + Sal + (1 | Year:Lat)	-14.0	8.0	-1.75
9	Lat + Dep + Trans + Dep:Trans	-15.8	8.0	-1.98
10	Lat + (1 | Year) + Dep + Trans	-17.7	7.5	-2.36
11	Lat + Dep + Trans + Lat:Trans	-18.3	5.9	-3.10
12	(1 | Lat) + (1 | Year) + Dep + Trans	-21.3	6.9	-3.09
13	Lat + Dep + Trans	-23.7	8.2	-2.89
14	Lat + Dep + Trans + Temp + Sal	-23.8	8.3	-2.87
15	Lat + Dep + Trans + Temp	-24.7	8.4	-2.94
16	Lat + Dep + Trans + Lat:Dep	-25.1	9.3	-2.70
17	(1 | Lat) + Dep + Trans	-27.4	8.1	-3.38
18	Lat + (1 | Year:Lat)	-27.6	7.9	-3.49
19	(1 | Year:Lat)	-29.7	8.1	-3.67
20	Lat + Dep + Temp + Lat:Temp	-29.8	9.4	-3.17
21	Dep + Trans	-34.3	9.1	-3.77
22	Lat + Trans	-34.5	8.5	-4.06
23	Dep + Trans + Temp	-35.5	9.2	-3.86
24	Lat + Year	-39.8	8.3	-4.80
25	Lat + Dep + Chl	-40.4	11.2	-3.61
26	Lat + Dep + Temp	-43.6	13.3	-3.28
27	Trans	-44.0	8.6	-5.12
28	Lat	-44.3	9.1	-4.87
29	Lat + Dep	-45.5	13.2	-3.45
30	Lat + Dep + Sal	-47.0	13.8	-3.41
31	Lat + Dep + Sal + Lat:Sal	-50.4	12.7	-3.97
32	Dep	-57.8	16.2	-3.57

Table 8. Result of linear regression of diversity measures along a latitudinal gradient, taking the north-to-south sequential order of 15 transect lines as the independent variable and four univariate measures of community structure as the dependent variable in separate tests. Diversity measures were first calculated for each haul, then averaged by transect line. They include species richness, S; total abundance of individuals, N; the Shannon diversity index, H', and Pielou's index of evenness, J'. One transect line (BF) was excluded from latitudinal analysis due to inconsistencies in its location from year to year, leaving 330 hauls included in the analysis.

Independent variable	*Dependent variable*	*Transform*	*Sample size*	*R-squared*	*F*	*P*
Line order (1-15)	Richness (S)	square root	330	0.0051	2.655	0.104
	Abundance (N)	$\log_{10}$	330	0.0967	36.226	<0.001
	Evenness (J')	square root	330	0.0293	10.940	0.001
	Diversity (H')	square root	330	0.0170	6.702	0.01

Table 9. Result of one-way ANOVA tests for differences among shelf positions (upper 4 rows) and years (lower 4 rows) for each of the four diversity measures (8 separate tests). Samples from all 16 transect lines and 6 survey years (351 hauls) were included for tests of shelf position. For interannual differences, survey year 2015 was excluded due to the absence of samples from shelf positions 4 and 5 in that year alone, leaving 288 hauls.

Independent variable	*Dependent variable*	*Transform*	*Sample size*	*F*	*P*
Shelf pos'n (1-5)	Richness (S)	square root	351	6.694	<0.001
	Abundance (N)	$\log_{10}$	351	5.399	<0.001
	Evenness (J')	square root	351	0.943	0.439
	Diversity (H')	square root	351	0.407	0.803
Year (2010-14)	Richness (S)	square root	288	3.166	0.014
	Abundance (N)	$\log_{10}$	288	2.312	0.058
	Evenness (J')	square root	288	3.927	0.004
	Diversity (H')	square root	288	5.154	<0.001

Table 10. Result of BIO-ENV test to assess the correlation between matching biotic and environmental samples, taking 9 candidate variables for water properties and location in the ENV matrix and 62 trawl + CTD stations in the analysis. The top-10 selections and their Spearman correlation (rho) to the biotic matrix are shown in rank order, along with the full 9-variable comparison.

Rank	Corr (rho)	Variable Selection
1	0.578	Dep, Temp, Trans
2	0.573	Lat, Dep, Temp, Trans
3	0.572	Lat, Dep, Temp, PAR, Trans
4	0.564	Dep, Temp, PAR, Trans
5	0.563	Lat, Dep, Secchi, Temp, PAR, Trans
6	0.563	Dep, Temp, Sal, Trans
7	0.560	Dep, Temp, Sal, PAR, Trans
8	0.556	Lat, Dep, Secchi, Temp, Trans
9	0.556	Dep, Secchi, Temp, Sal, PAR, Trans
10	0.554	Lat, Dis, Dep, Temp, PAR, Trans
⋮	⋮	
38	0.538	Lat, Dis, Dep, Secchi, Temp, Sal, PAR, Chl, Trans

Figure 1. (a) Map of study area and ship's track from a representative survey, in this case 2014, showing transect lines and sampling stations. Black circles indicate stations with trawls completed in 2014; red circles indicate stations where trawling was not completed that year. The ship's track is shown in green, starting in Newport, Oregon (top) and ending in San Francisco, California. (b) Sea surface temperature (C°) measured at one-minute time intervals along the ship's track by thermosalinometer in 2014.

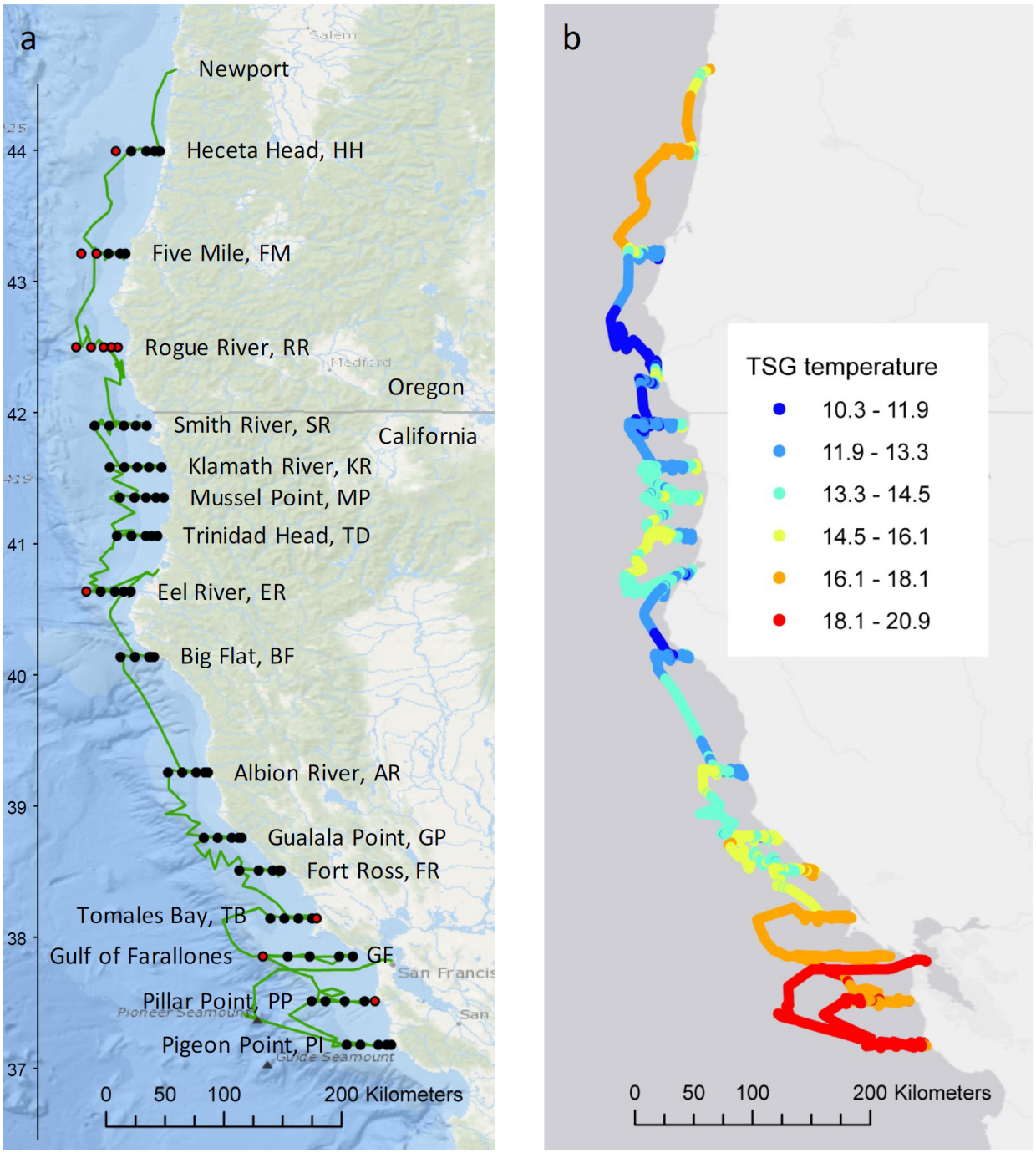

Figure 2. Pairwise plots of environmental variables measured at stations occupied on summer surveys 2010-15. Each point represents one station in one year. Variables Temp, Sal, PAR, Chl, and Trans were measured by instruments on the CTD package and are reported here as mean values from 3-20m in the water column. BucTemp and Secchi were measured at the water surface. Numbers in each plot are Pearson product-moment correlations (r); * denotes P<0.05.

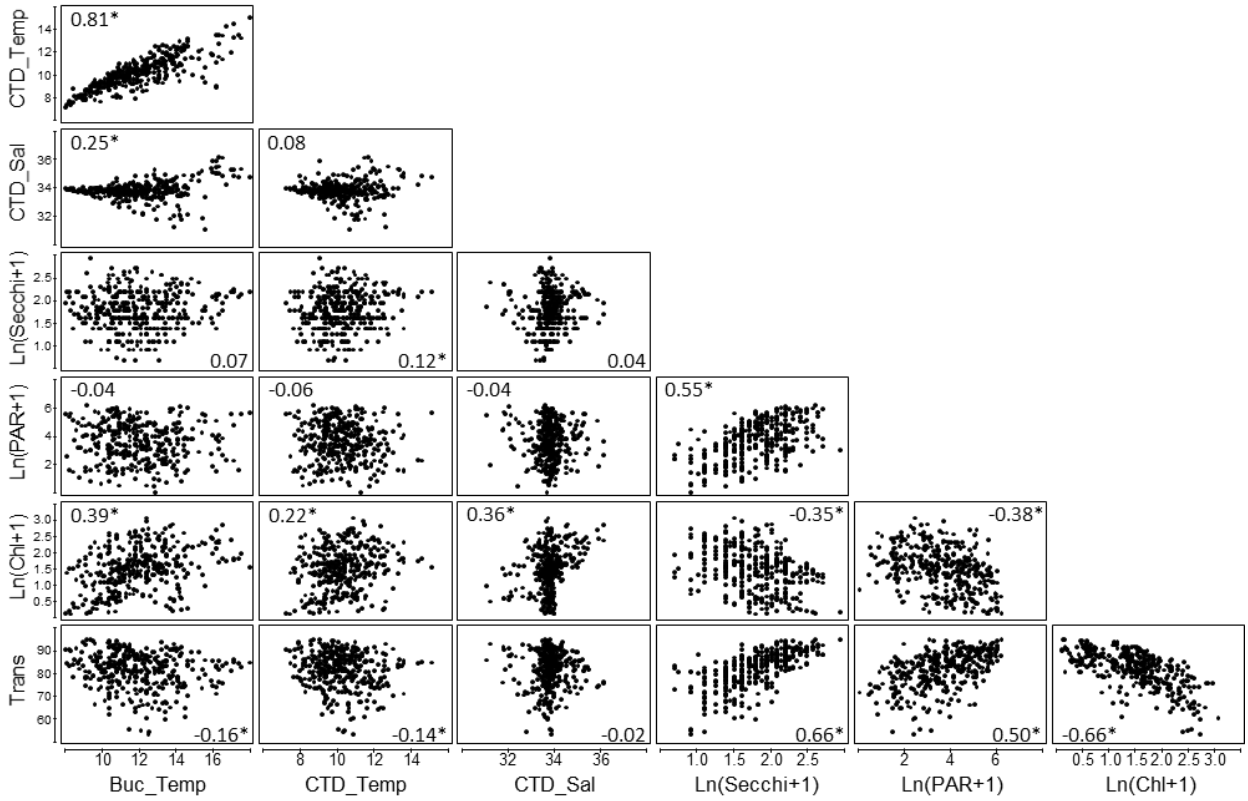

Figure 3. Plot of temperature and salinity from CTD casts at stations occupied on summer surveys 2010-15. Each point represents one station in one year. Data are mean values for the upper 3-20m of the water column.

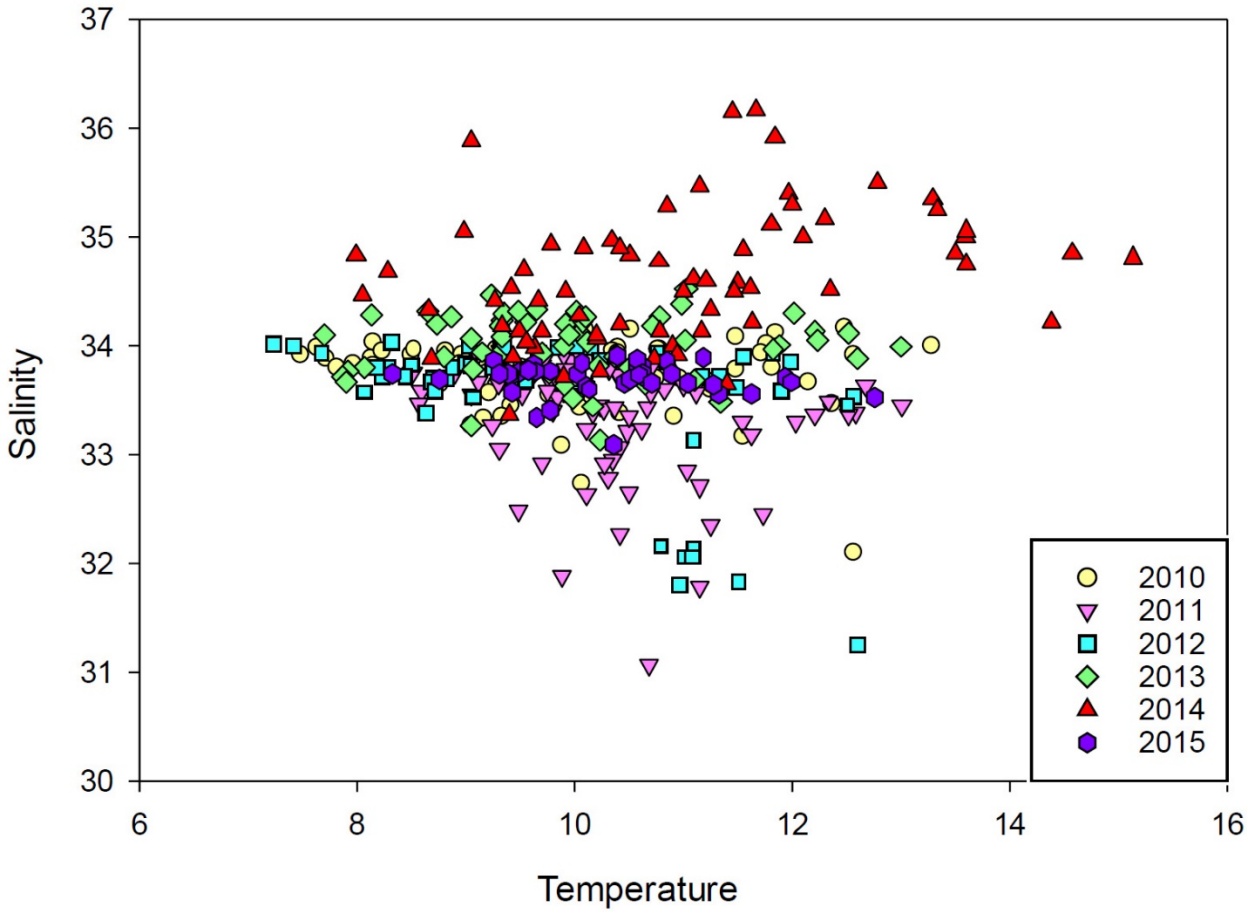

Figure 4. Distribution of salmon catch among 16 transect lines on summer surveys 2010-2015. Abundance is expressed as percent of total cumulative CPUE for each species and size class over the six-year period. JV ≤ 250mm FL, AD > 250mm FL.

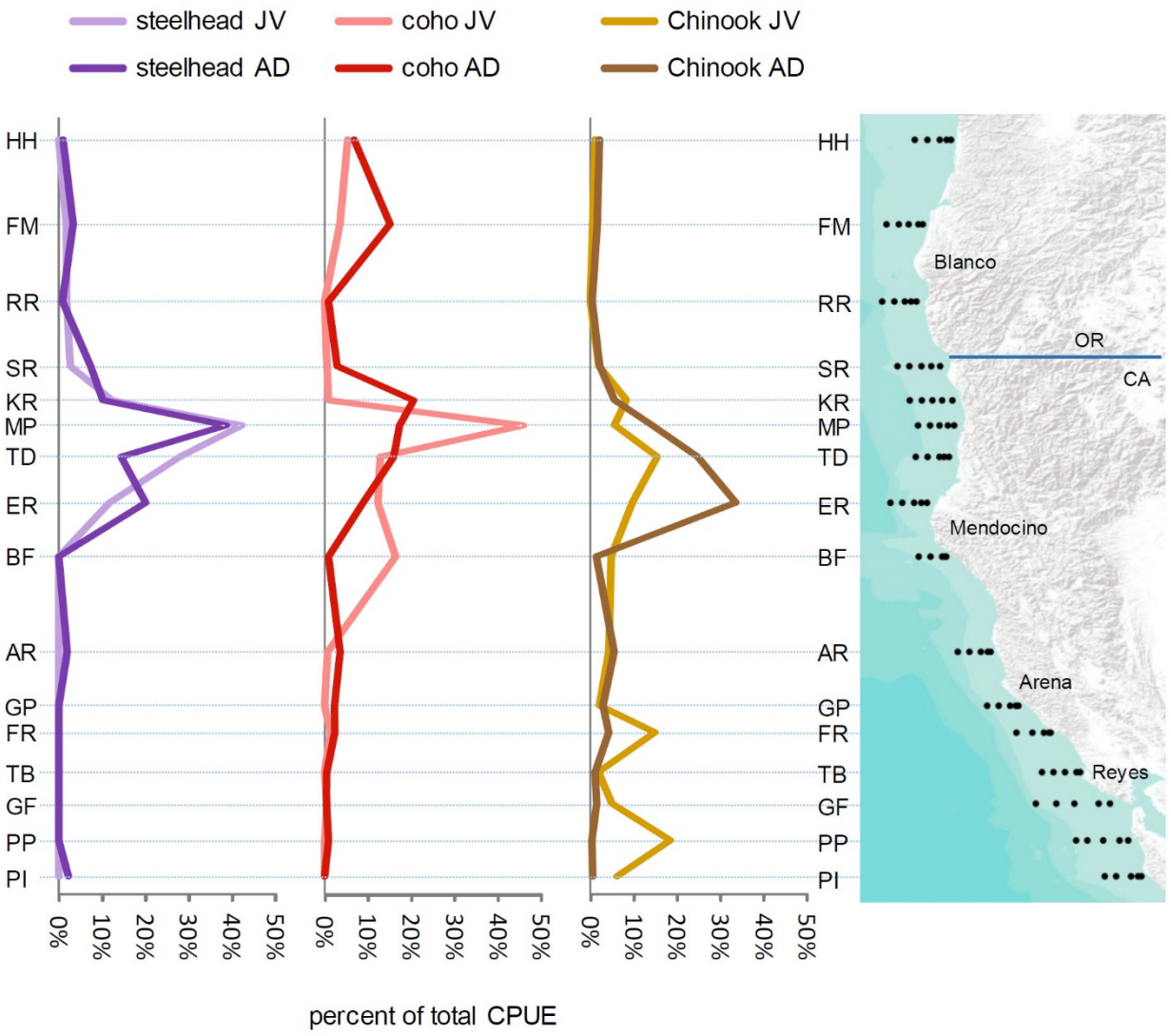

Figure 5. Probability of catching one or more salmon per haul at each of the five shelf positions during summer surveys 2010-2015. Position 1 is closest to shore (~30m bottom depth), position 5 is furthest from shore (>180m bottom depth). JV ≤ 250mm FL, AD > 250mm FL. Note different scales.

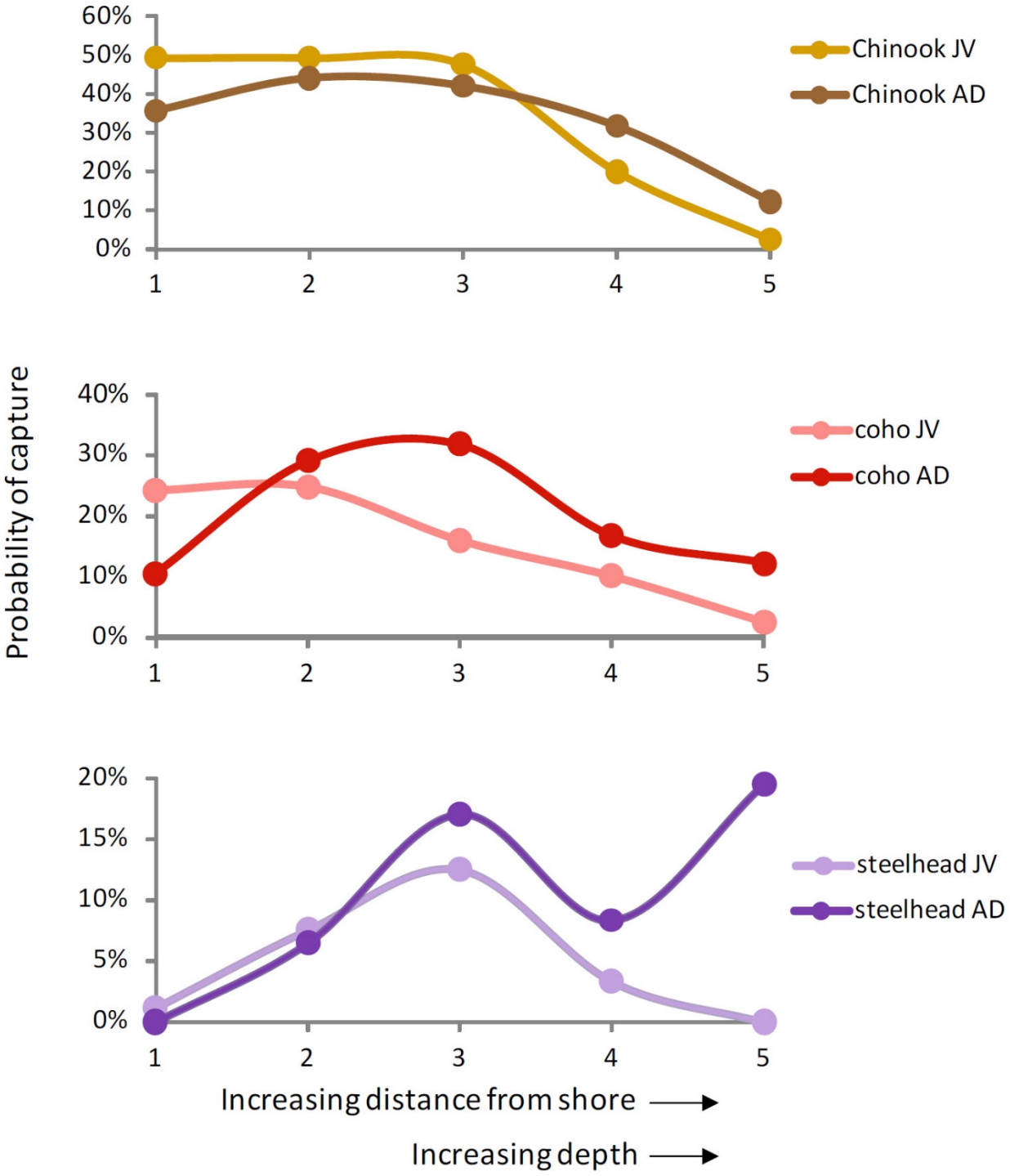

Figure 6. Mean annual salmon CPUE (fish/$10^6 m^3$) on summer surveys 2010-2015. Error bars are ±1 standard error of the mean. JV ≤250mm FL, AD >250mm FL. Scales of abundance differ among graphs.

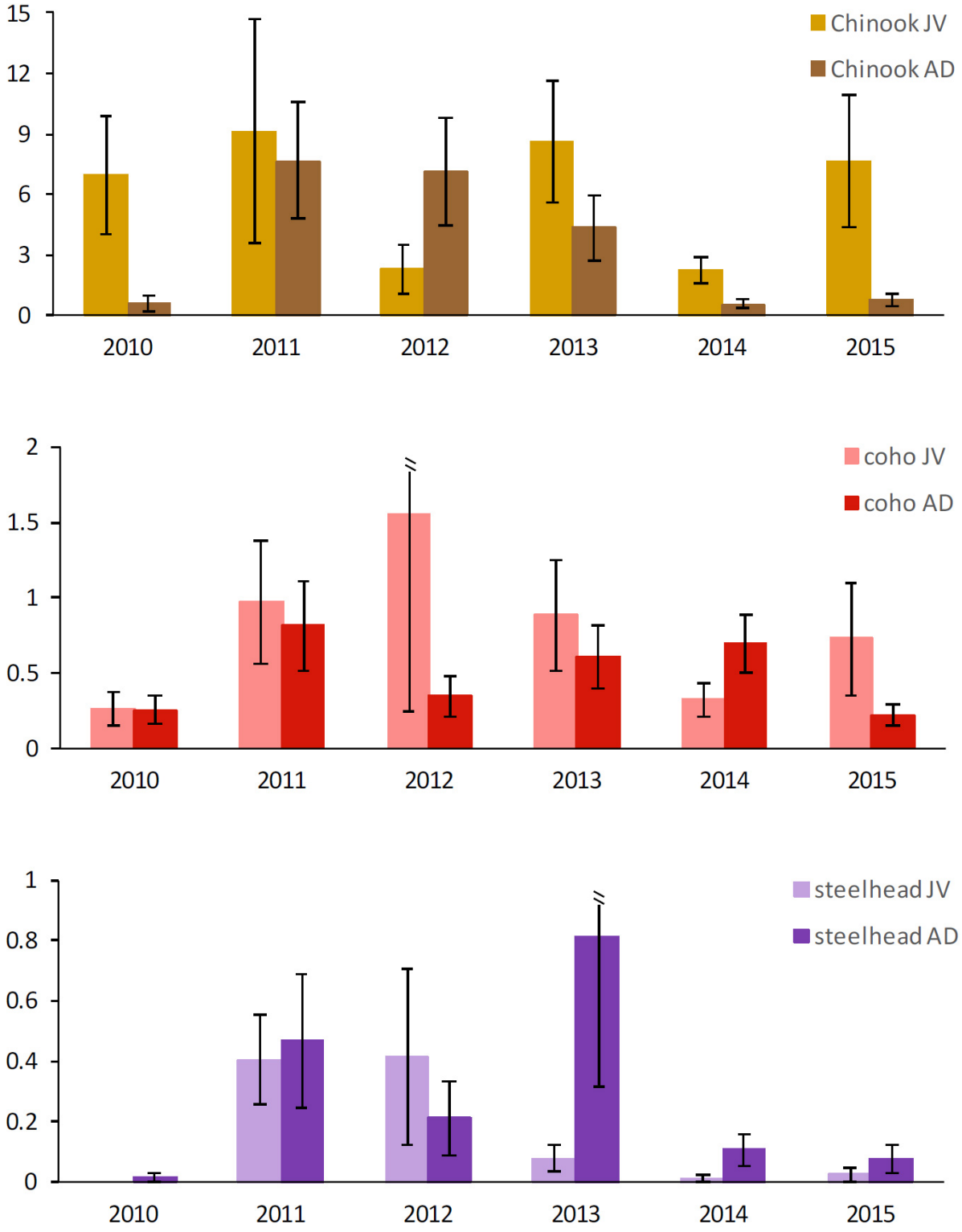

Figure 7. Posterior distributions from the best-fit negative binomial regression model for juvenile Chinook abundance: (a) CPUE as a function of depth in meters (posterior median, solid line) with posterior percentiles (2.5% and 97.5%, dashed lines) and distribution of observations ('rug' on upper edge); (b) boxplots of posterior CPUE by 1-degree latitude bin (boxes span the interquartile range of the posterior, with medians indicated by the thick horizontal line), and the California-Oregon border indicated by the dashed vertical line; (c) CPUE as a function of transmissivity (% transmission); (d) proportion of zeros in replicate data sets generated by the best-fit model (grey histogram) relative to the observed proportion (solid vertical line).

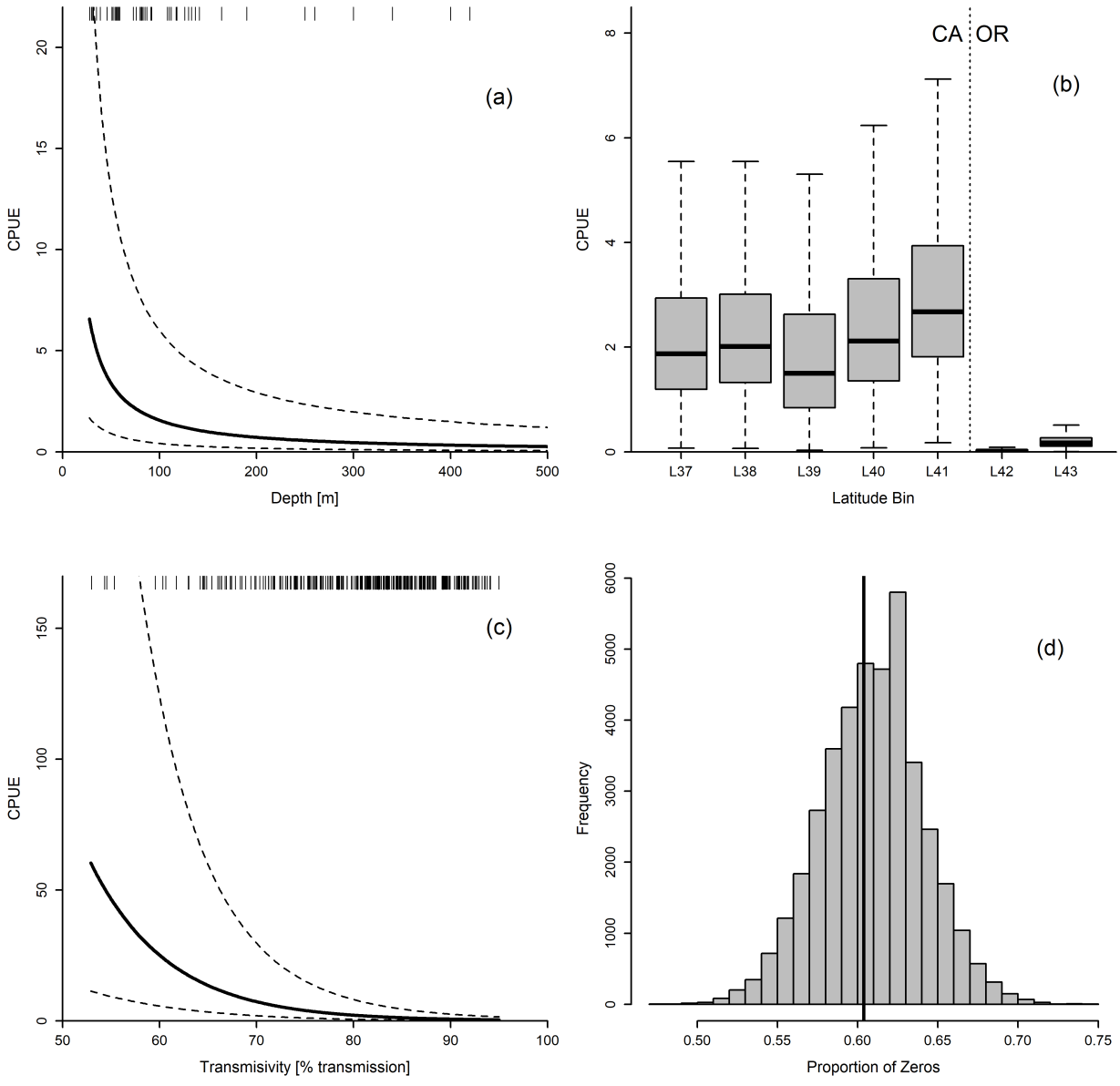

Figure 8. Mean annual CPUE (fish/$10^6 m^3$; blue bars) and frequency of occurrence, FO (red circles) of selected invertebrates and non-salmonid fish on summer surveys 2010-2015. Scales of abundance and occurrence differ among graphs.

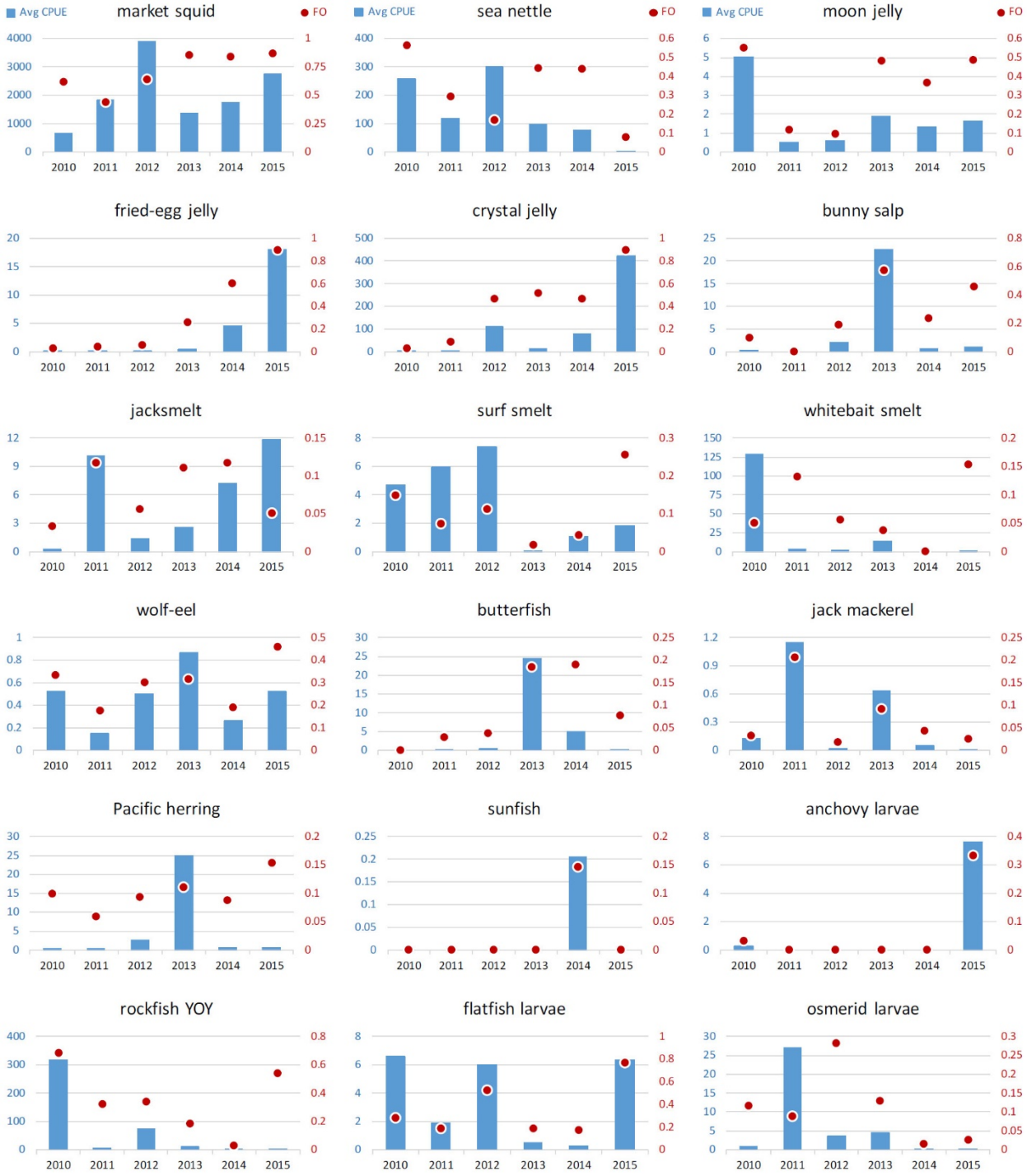

Figure 9. Taxonomic richness, abundance and diversity measures of organisms captured in surface trawls during summer salmon surveys, plotted by transect line order from central Oregon (northernmost line HH) to the Gulf of the Farallones in California (southernmost line PI). One transect line (BF) was excluded because of inconsistencies in its location from year to year. Hauls with zero or one species were also excluded. These filters resulted in 330 hauls with at least two taxa, for which all four diversity statistics could be obtained. (a) species richness, S; (b) total abundance of individuals, N; (c) Pielou's evenness index, J'; (d) Shannon diversity index, H'. Points show mean values and 95% confidence intervals.

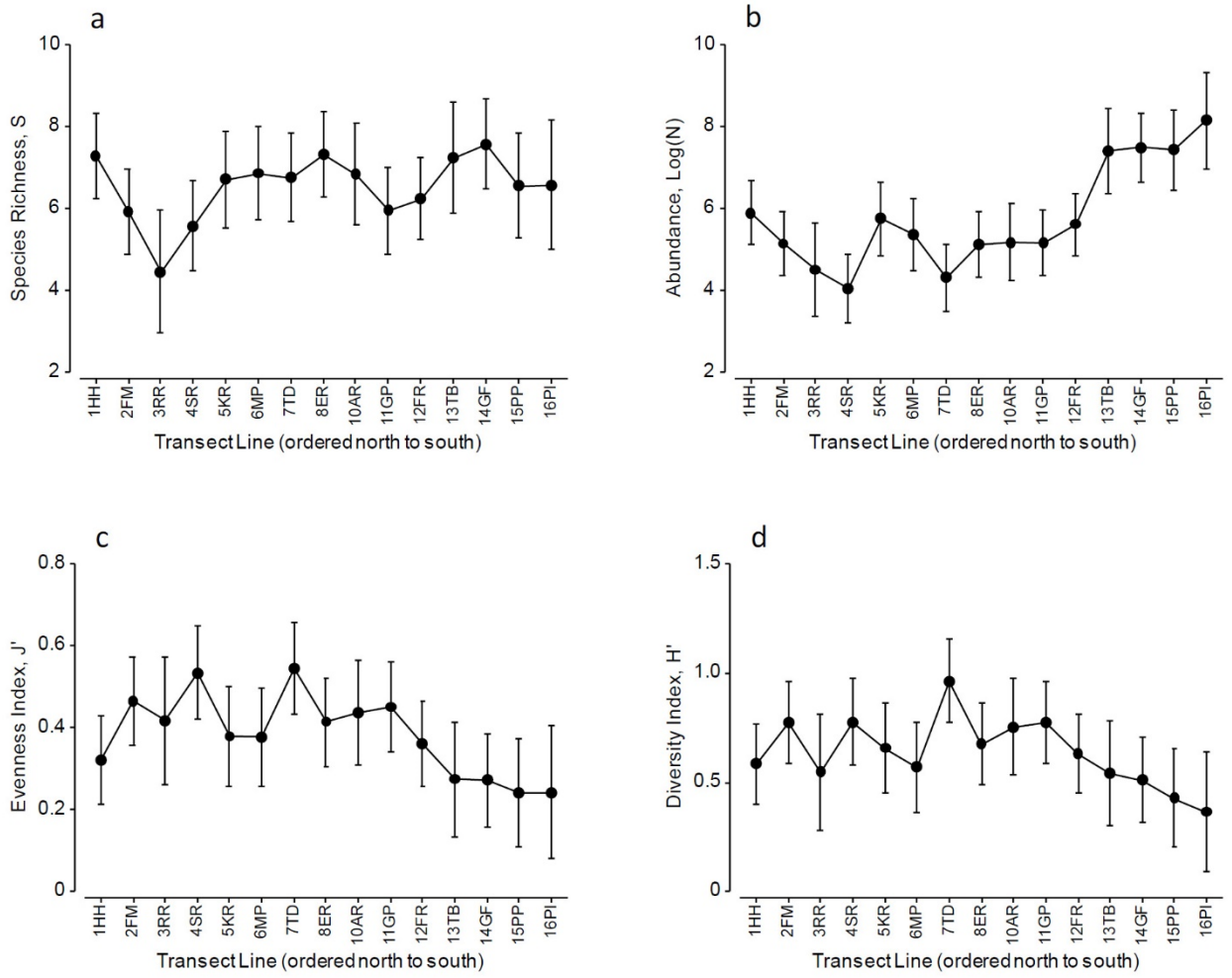

Figure 10. nMDS plot of the full community sampled by surface trawl, with CPUE of each species averaged across all five shelf positions and six survey years, separately for each transect line. Thus, each point here represents the average catch on one transect line during the period 2010-2015. The line connecting the points on the graph shows their spatial order along the coast from HH (north) to PI (south). Points are color coded by their location relative to major headlands: NoBl = North of Blanco; BlMe = Blanco to Mendocino; MeAr = Mendocino to Arena; ArRe = Arena to Reyes; SoRe = South of Reyes. One transect line (BF) was excluded because of inconsistency in location from year to year, leaving 15 lines and 342 hauls included in the analysis.

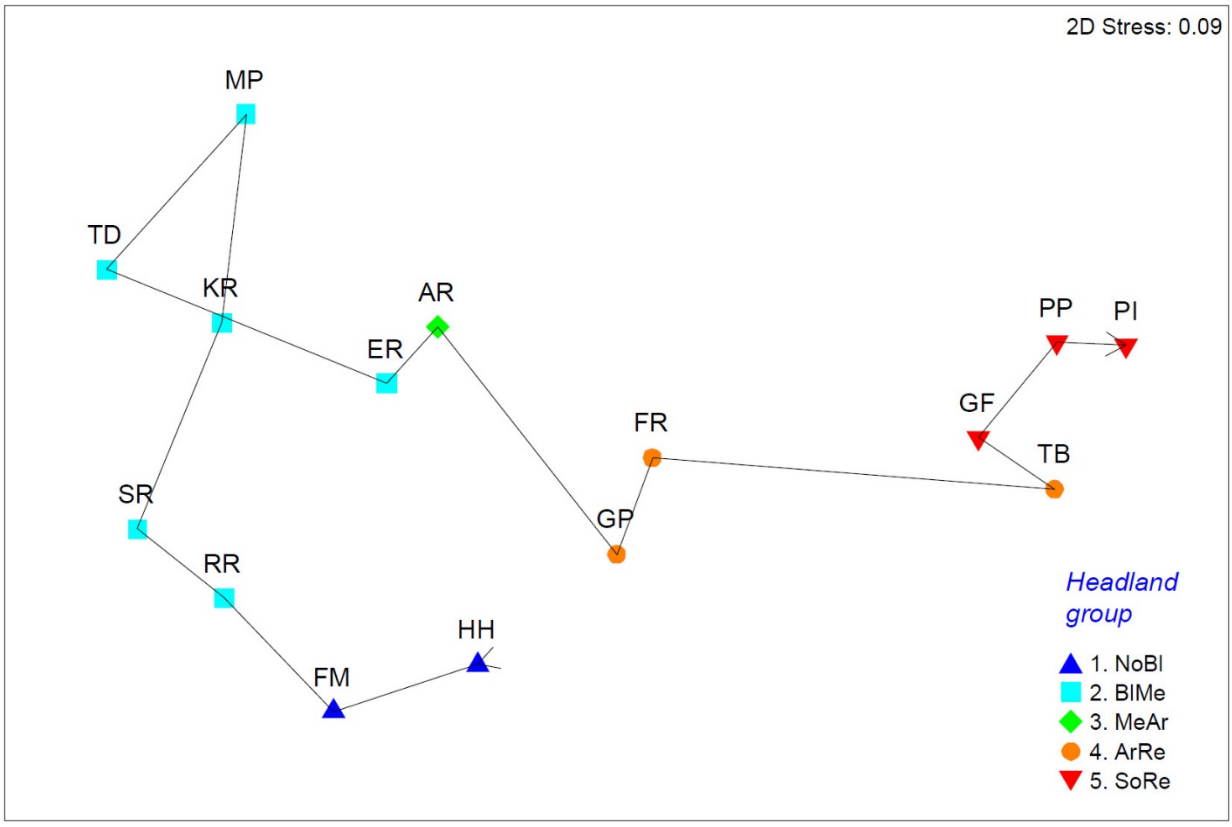

Figure 11. Taxonomic richness, abundance and diversity measures of organisms captured in surface trawls during summer salmon surveys, plotted by shelf position from 1 (shallowest and closest to shore) to 5 (deepest and furthest from shore). Hauls with zero or one species were excluded, leaving 351 hauls. (a) species richness, S; (b) total abundance of individuals, N; (c) Pielou's evenness index, J'; (d) Shannon diversity index, H'. Points show mean values and 95% confidence intervals.

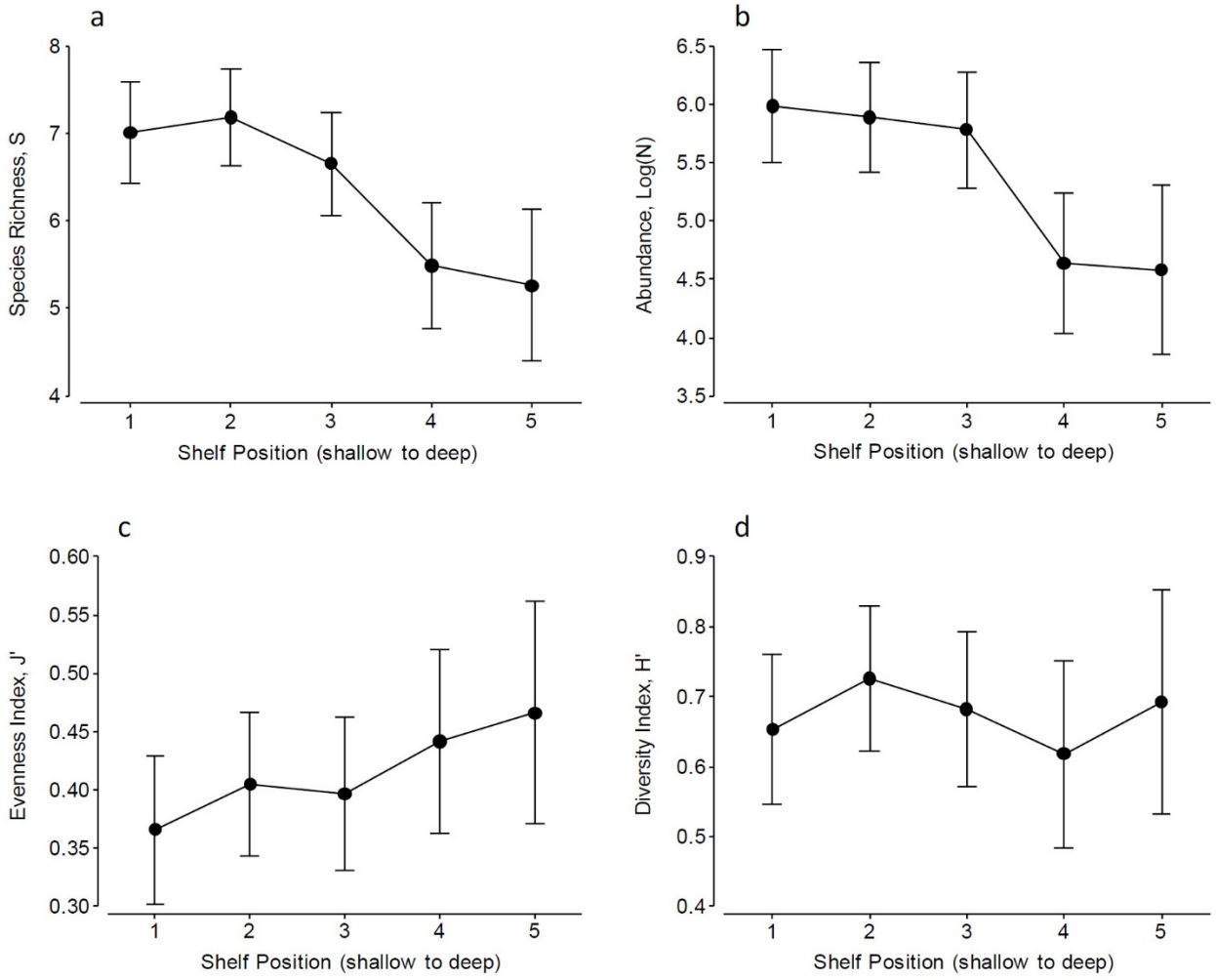

Figure 12. Taxonomic richness, abundance and diversity measures of organisms captured in surface trawls during summer salmon surveys, plotted by year. The 2015 survey was excluded due to the absence of samples from shelf positions 4 and 5 in that year. Hauls with zero or one species were also excluded, resulting in 288 remaining hauls. (a) species richness, S; (b) total abundance of individuals, N; (c) Pielou's evenness index, J'; (d) Shannon diversity index, H'. Points show mean values and 95% confidence intervals.

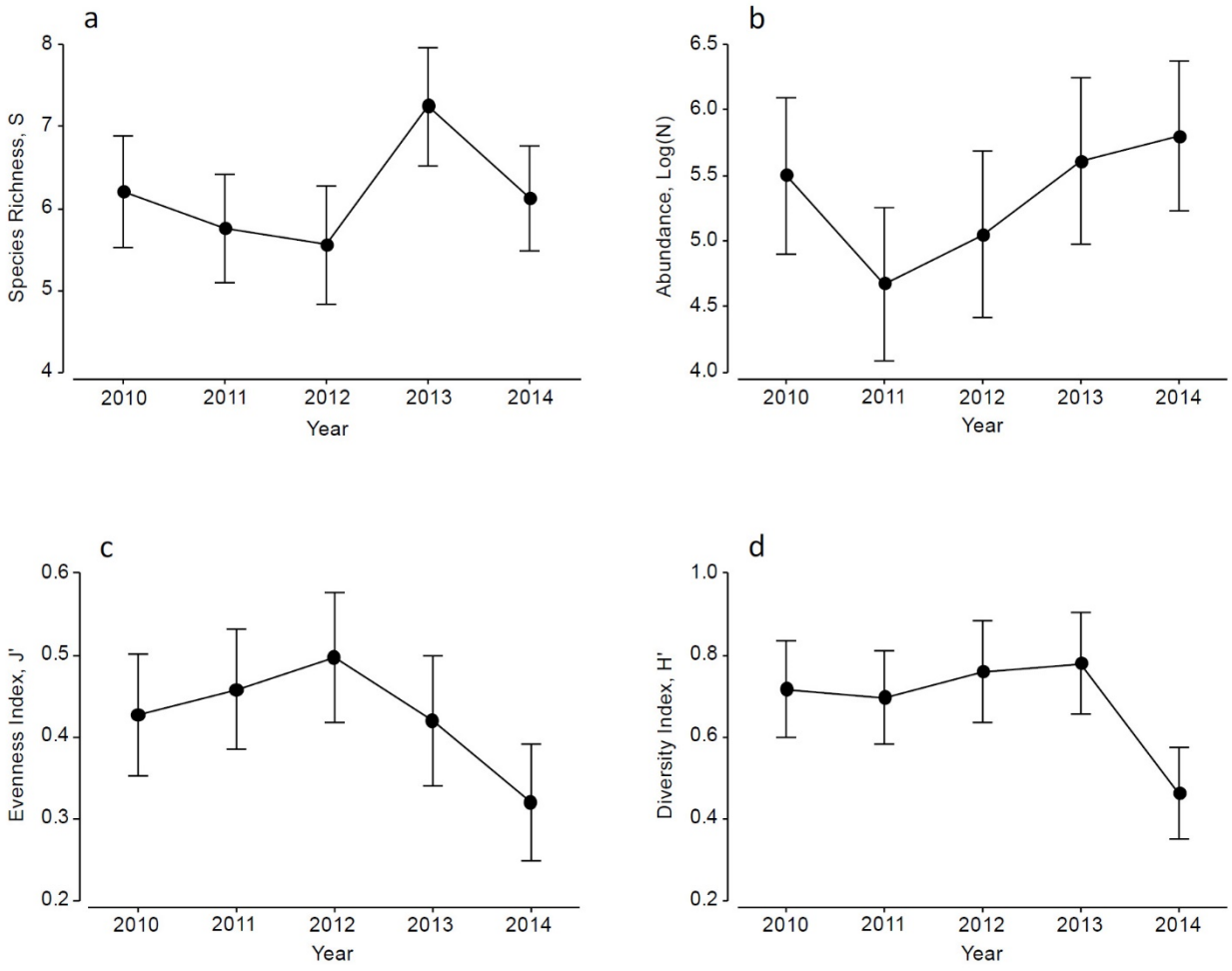

Figure 13. nMDS plot of the full community sampled by surface trawl, with CPUE of each species averaged across all sixteen transect lines, separately for each shelf position and year. Thus, each point here represents the average trawl catch at each of the five shelf positions in each of the five years 2010-2014. The 2015 survey was excluded due to the absence of samples from shelf positions 4 and 5 in that year, leaving 303 hauls included in the analysis. Points are color coded by sample year and labeled by shelf position. The lines connecting the points are visual aids to show the order of the five shelf positions from deepest/farthest offshore (5) to shallowest/closest to shore (1).

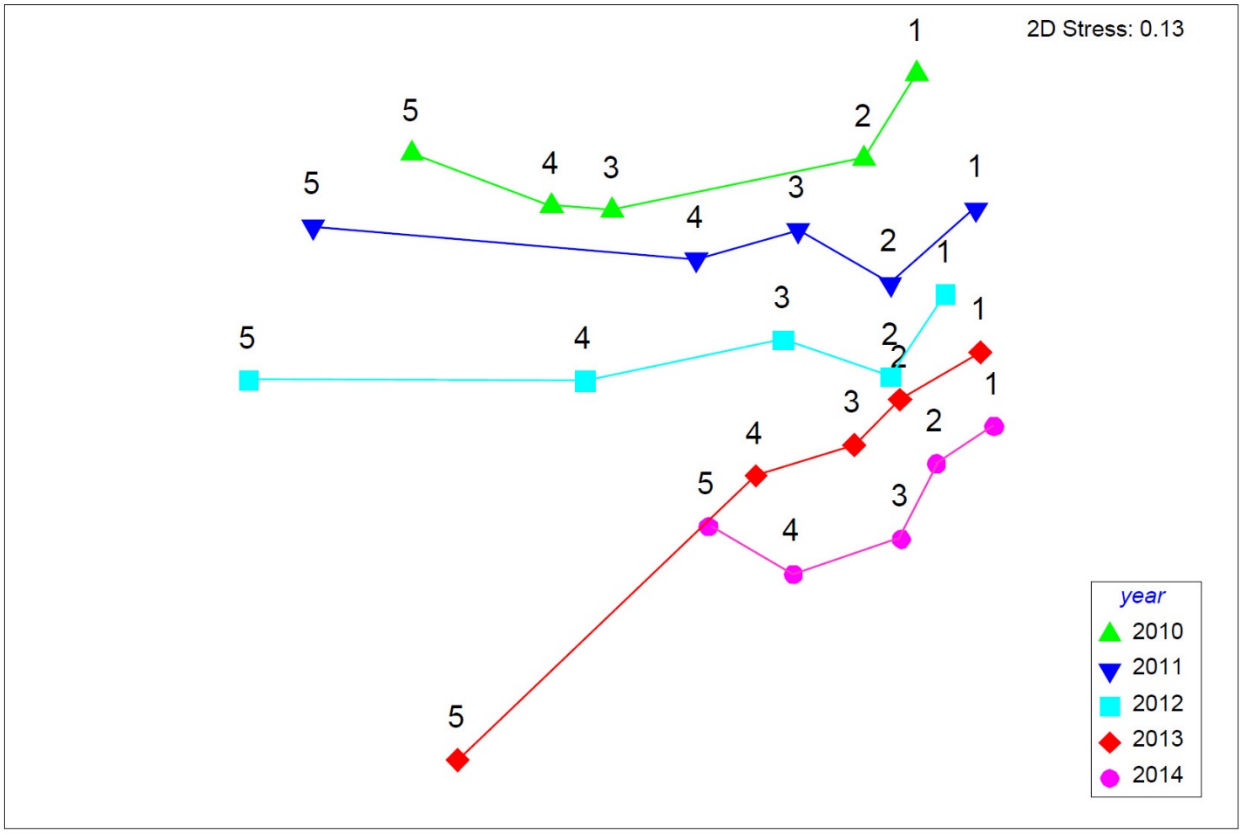

Figure 14. Single linkage cluster plot of the full community sampled by surface trawl, with CPUE of each species averaged across all inshore stations (shelf positions 1-3), separately for each year. Each endpoint represents the average inshore trawl catch for one cruise. In order to include 2015 in this comparison, offshore samples (shelf positions 4-5) from the other five years were excluded.

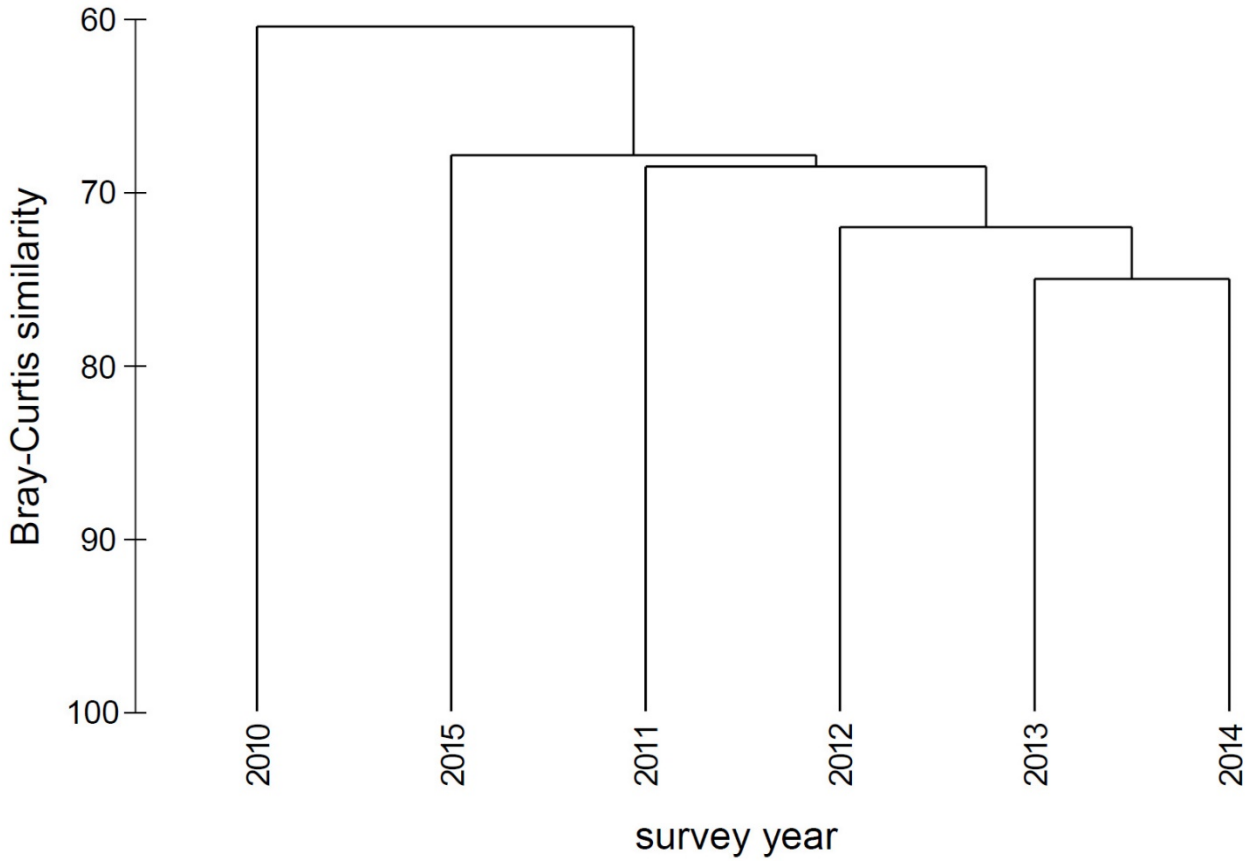

Figure 15. (a) PCO plot of the full community sampled by surface trawl, with CPUE of each species averaged by station across years. Each point represents the average catch at one station over the six-year period 2010-2015. Data were filtered as described in text, leaving 62 stations plotted. Orange group = GOF region; blue group = central and northern region. (b-d) Vectors showing plotted Spearman rank correlations of each variable with PCO axes for environmental variables, fish, and invertebrates, respectively. Species selection was based on a cutoff of FO>6%. The point of vector origin is arbitrary, and the circle has a radius of 1.0 relative to vector length, representing the maximum possible correlation (+/-).

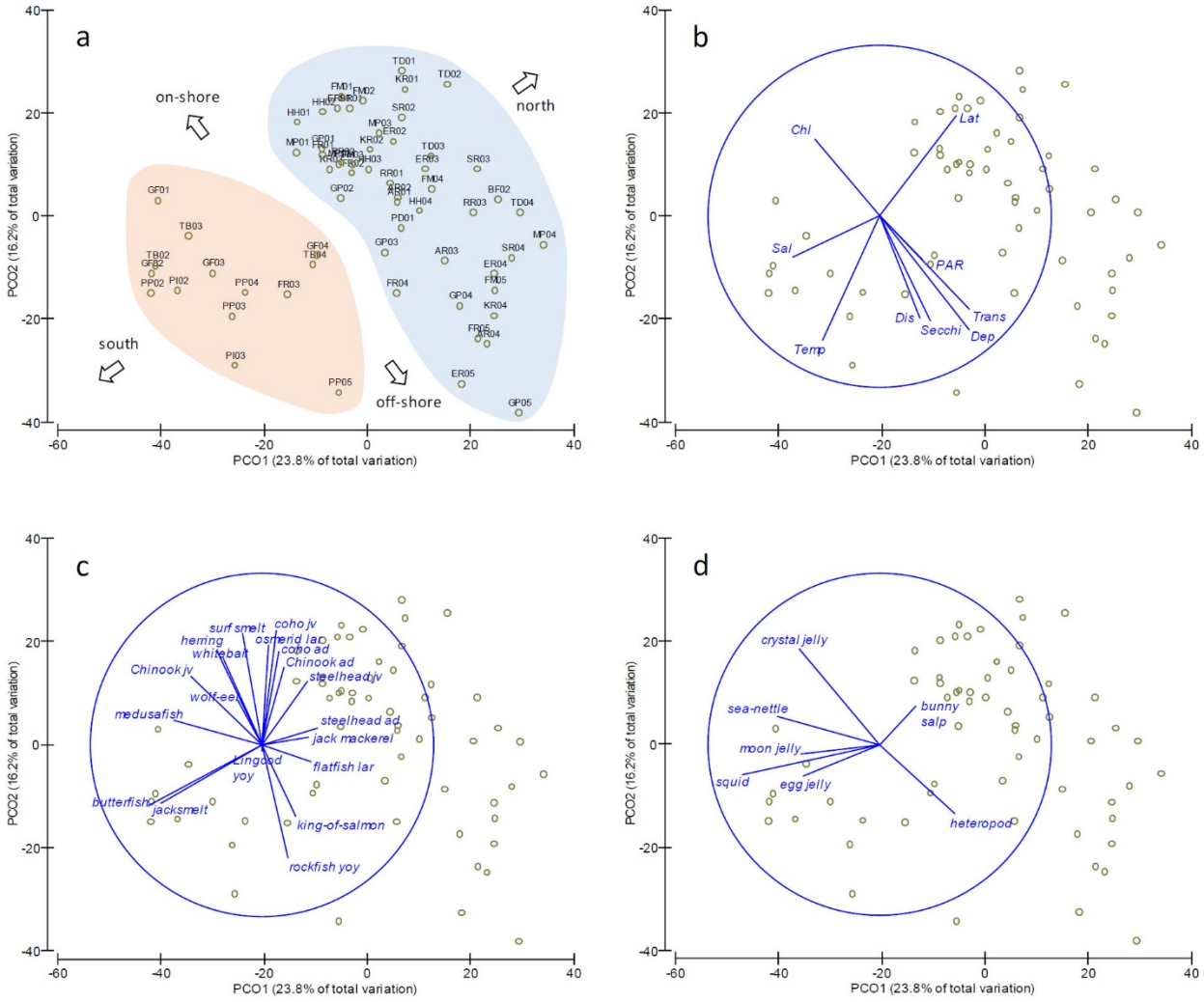

Figure S1. Maps showing annual and 6-year average values of selected environmental variables derived from ship-based sampling at stations occupied on summer surveys 2010-15. Variables were measured by instruments on the CTD package and maps are based on mean values from 3-20m in the water column.

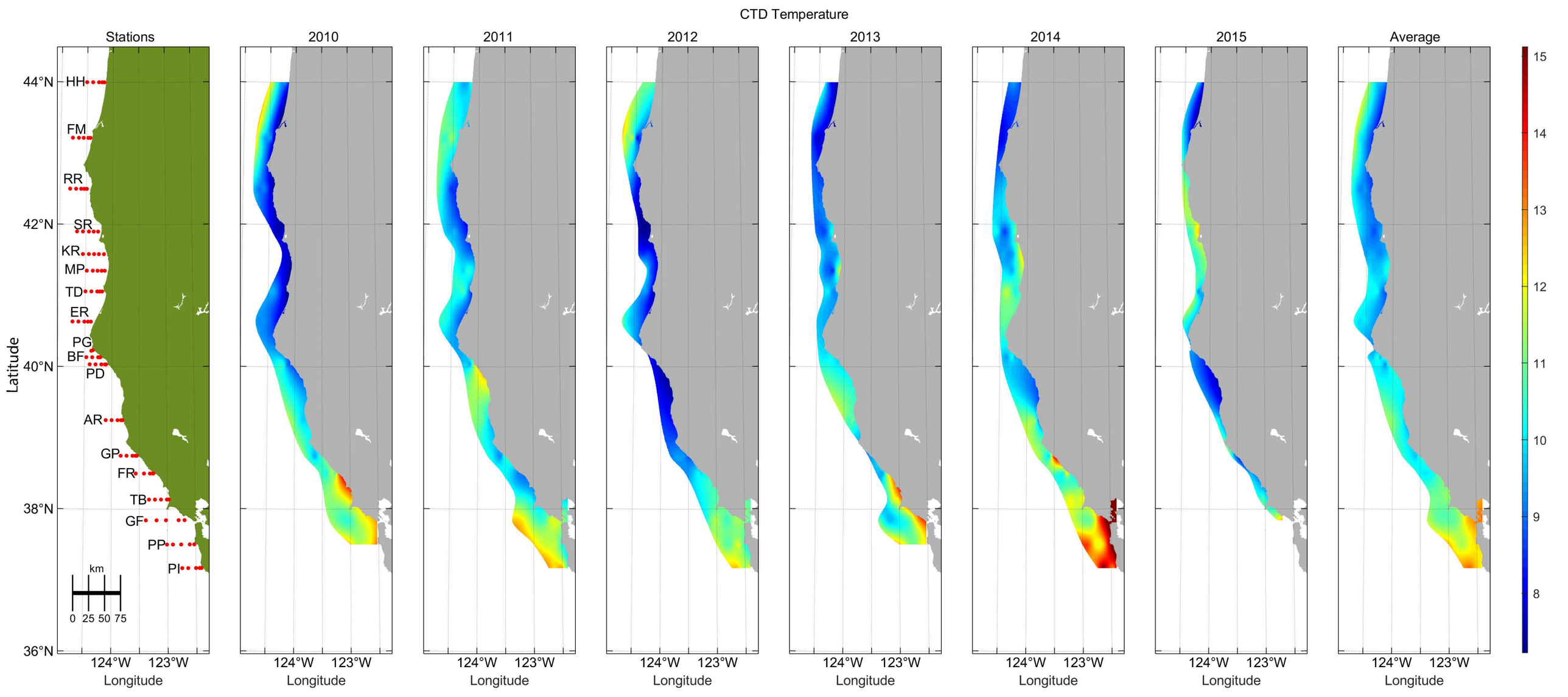
CTD Temperature
Stations
2010
2011
2012
2013
2014
2015
Average
Latitude
Longitude
44°N
42°N
40°N
38°N
36°N
124°W
123°W
HH
FM
RR
SR
KR
MP
TD
ER
PG
BF
PD
AR
GP
FR
TB
GF
PP
PI
km
0 25 50 75
15
14
13
12
11
10
9
8

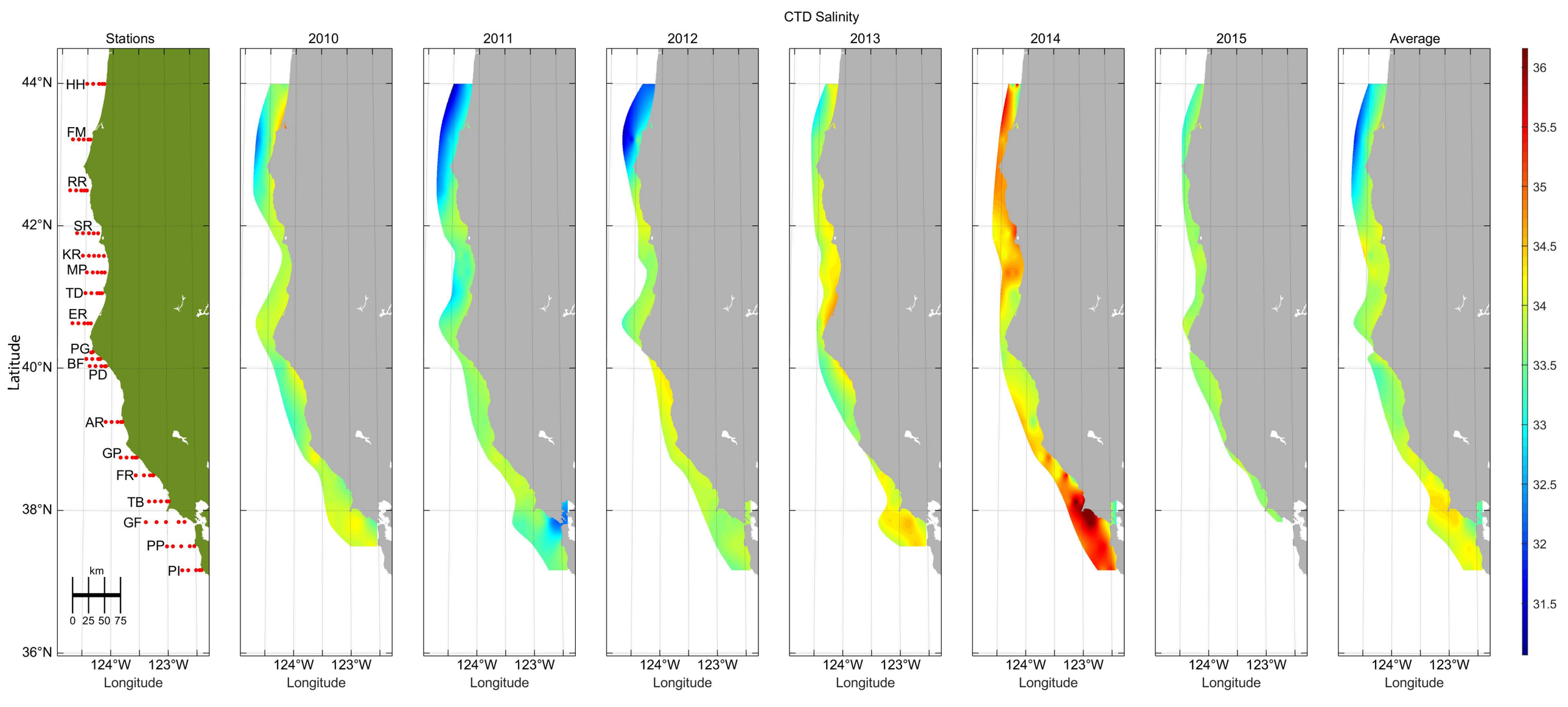
CTD Salinity
Stations
2010
2011
2012
2013
2014
2015
Average
HH
FM
RR
SR
KR
MP
TD
ER
PG
BF
PD
AR
GP
FR
TB
GF
PP
PI
km
0 25 50 75
44°N
42°N
40°N
38°N
36°N
Latitude
124°W
123°W
Longitude
36
35.5
35
34.5
34
33.5
33
32.5
32
31.5

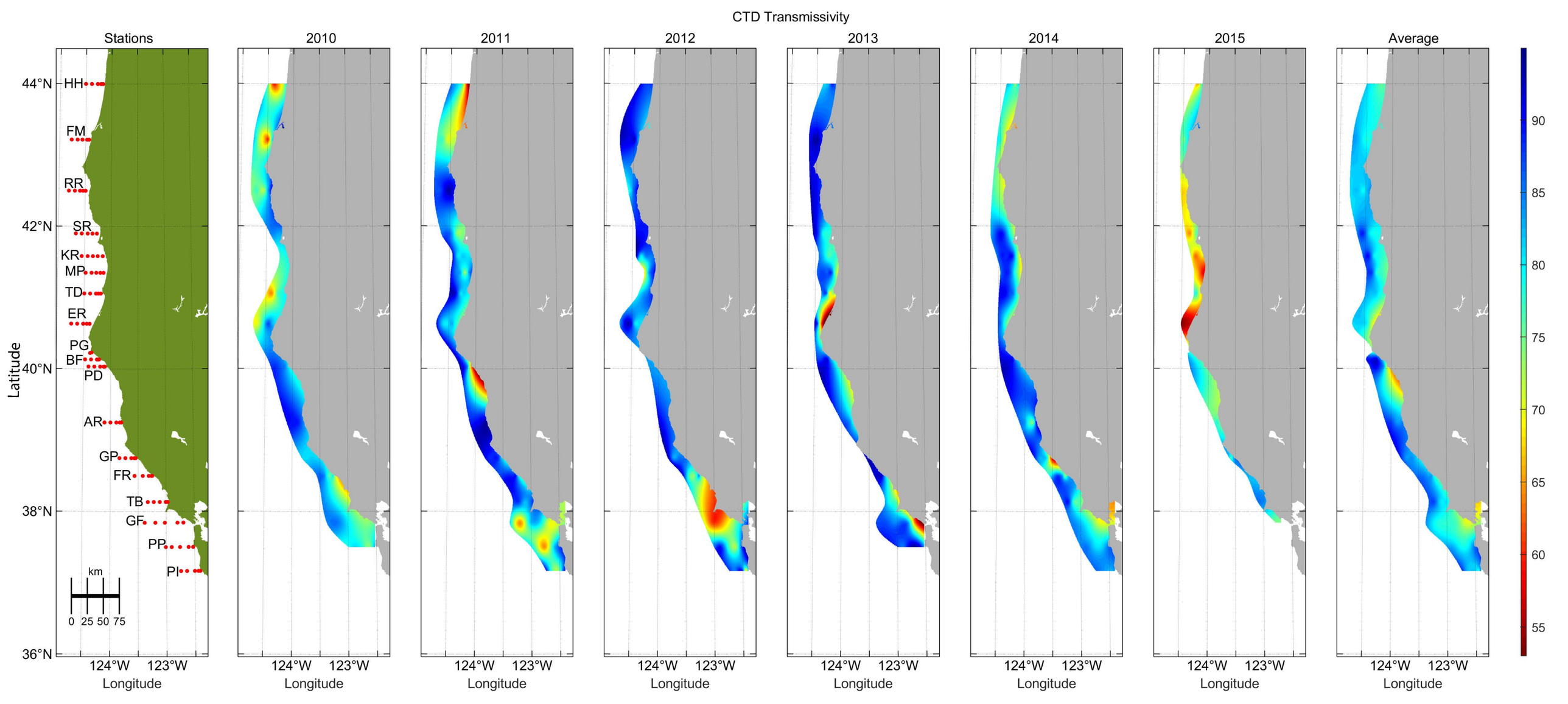
CTD Transmissivity
Stations
2010
2011
2012
2013
2014
2015
Average
Latitude
Longitude
44°N
42°N
40°N
38°N
36°N
124°W
123°W
HH
FM
RR
SR
KR
MP
TD
ER
PG
BF
PD
AR
GP
FR
TB
GF
PP
PI
km
0 25 50 75
90
85
80
75
70
65
60
55

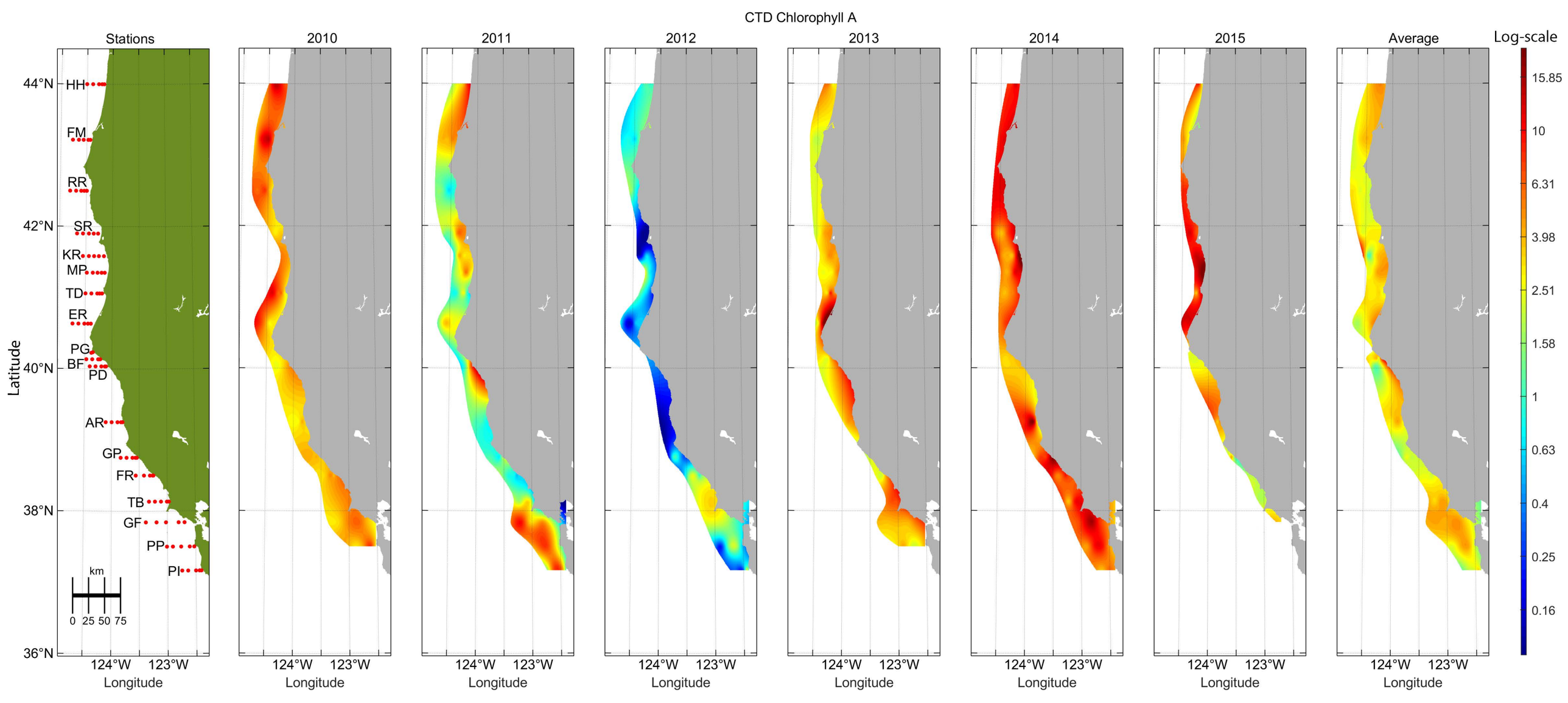
CTD Chlorophyll A
Stations
2010
2011
2012
2013
2014
2015
Average
Log-scale
15.85
10
6.31
3.98
2.51
1.58
1
0.63
0.4
0.25
0.16
Latitude
44°N
42°N
40°N
38°N
36°N
HH
FM
RR
SR
KR
MP
TD
ER
PG
BF
PD
AR
GP
FR
TB
GF
PP
PI
km
0 25 50 75
124°W
123°W
Longitude

Figure S2. Temperature-Salinity plots from summer surveys 2010-15 showing scaled CPUE of selected individual species in trawl catch. Yellow bubbles indicate positive catch; black dots indicate no catch or no trawl conducted. Bubble size within each plot is scaled to the maximum CPUE of that species, and does not denote equivalent CPUE among species.

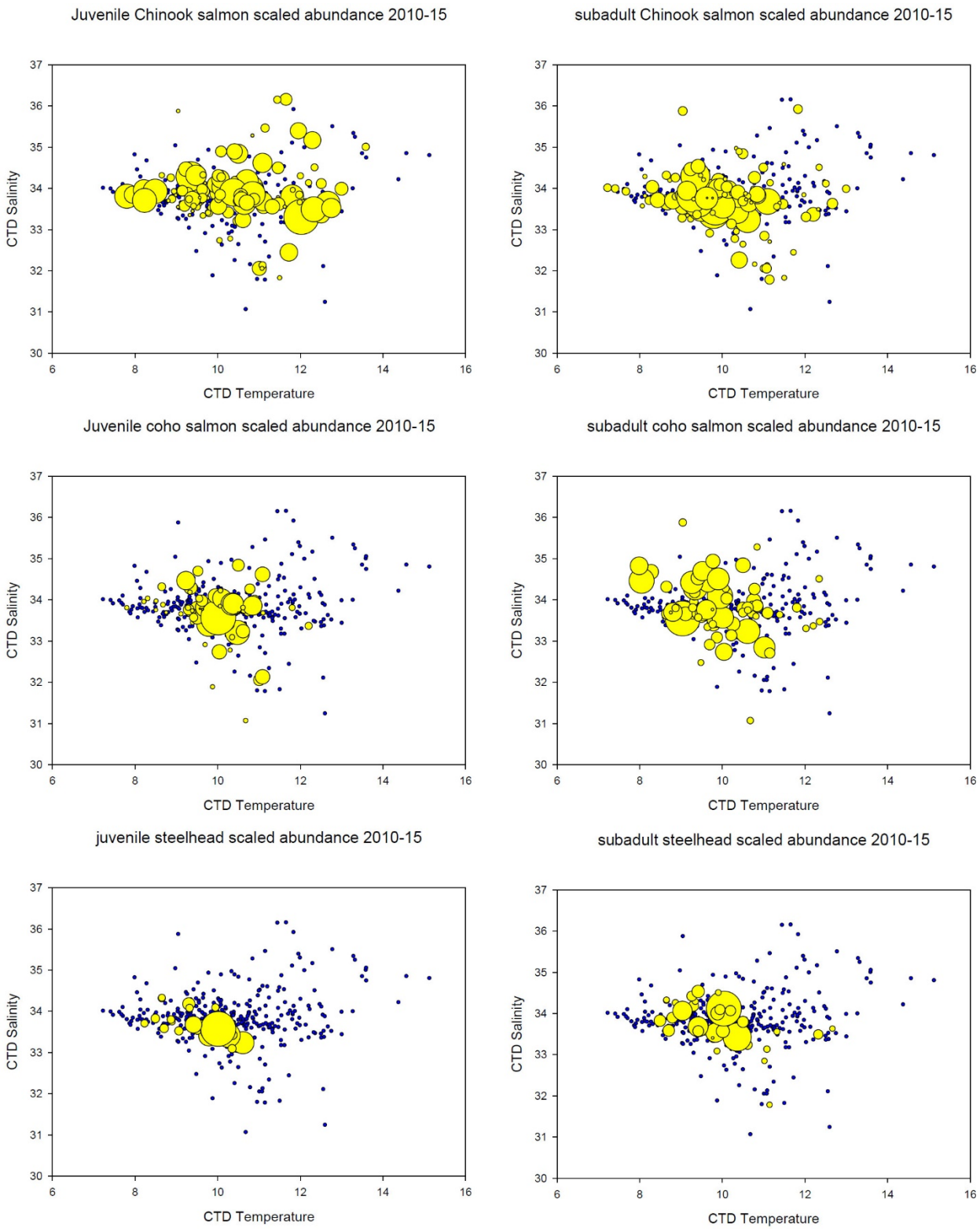

wolf-eel scaled abundance 2010-15

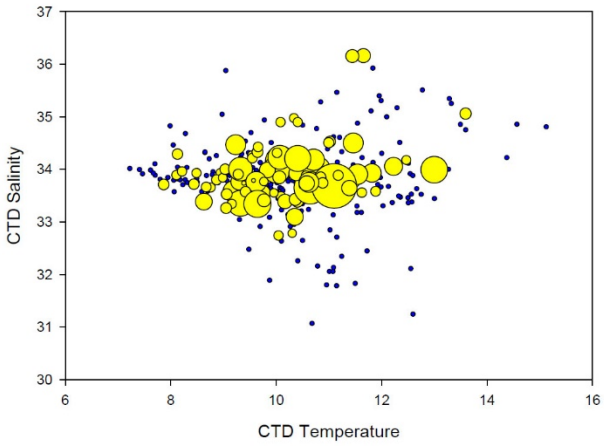

Pacific herring scaled abundance 2010-15

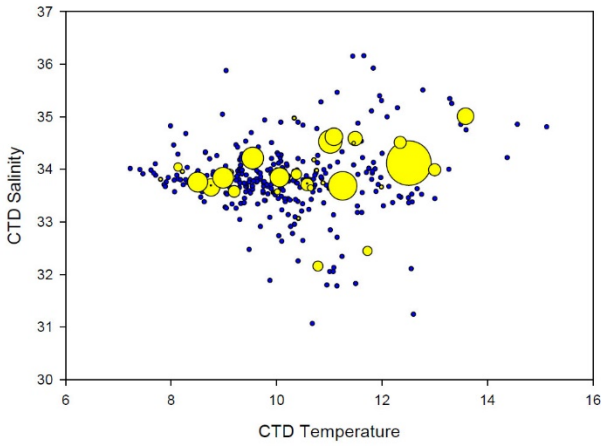

surfsmelt scaled abundance 2010-15

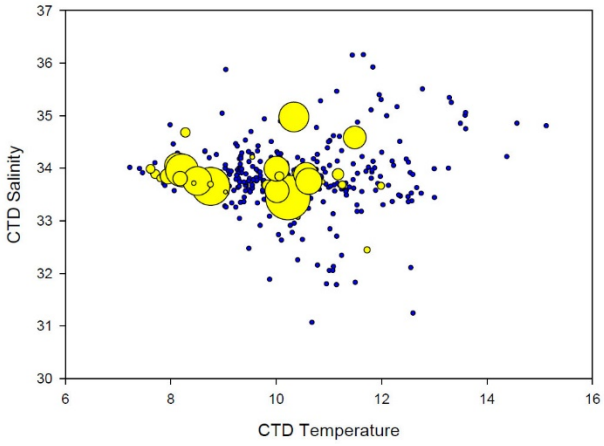

jacksmelt scaled abundance 2010-15

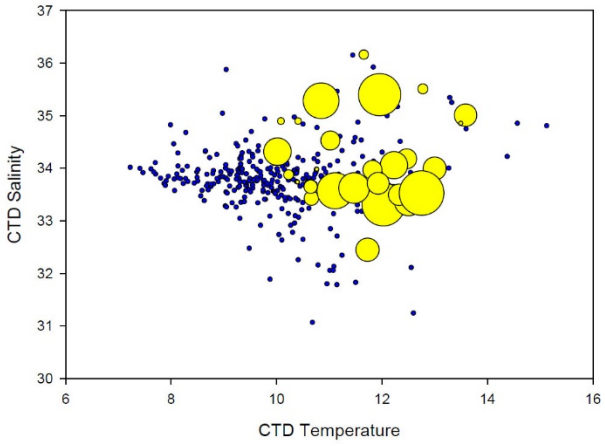

flatfish larvae scaled abundance 2010-15

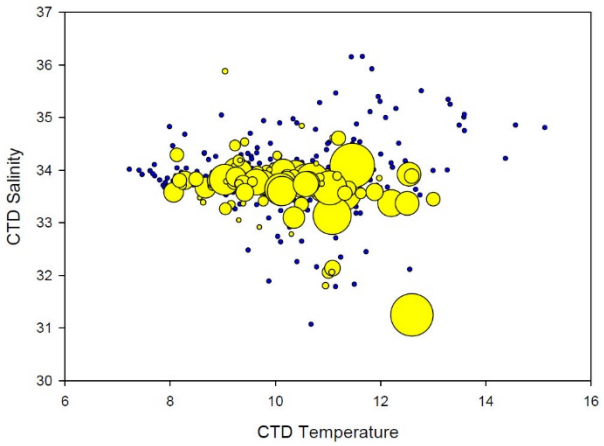

northern anchovy larvae scaled abundance 2010-15

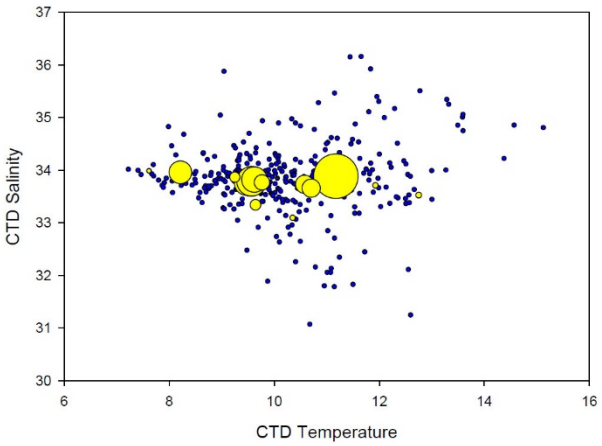

Osmerid larvae scaled abundance 2010-15

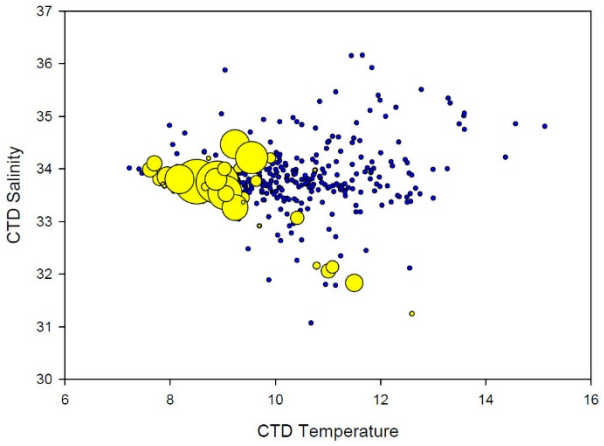

rockfish YOY scaled abundance 2010-15

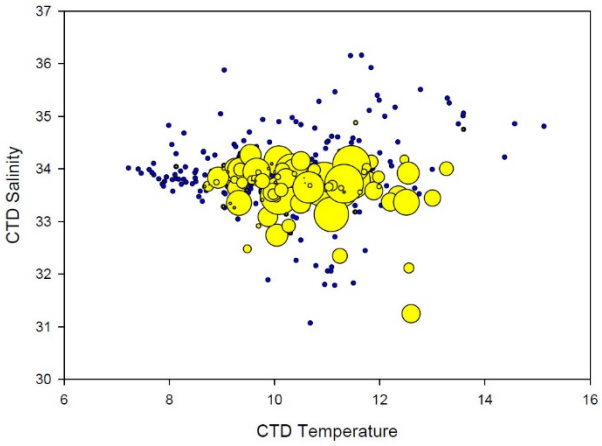

market squid scaled abundance 2010-15

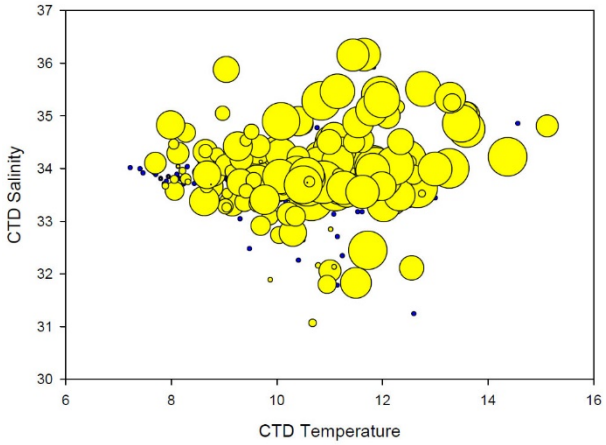

sea nettle jellyfish scaled abundance 2010-15

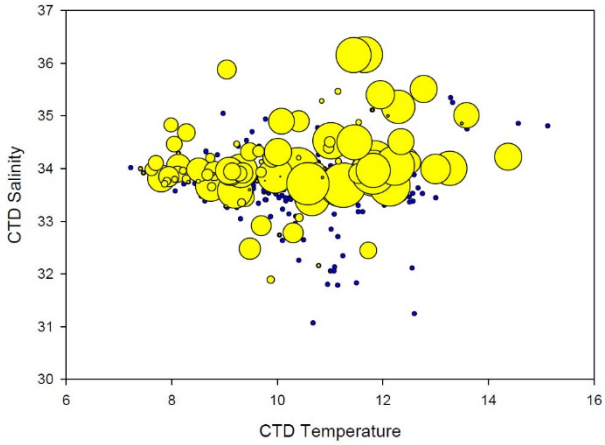

moon jellyfish scaled abundance 2010-15

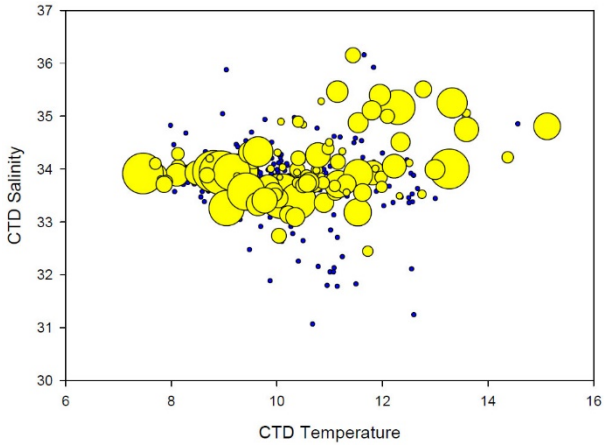

crystal jellyfish scaled abundance 2010-15